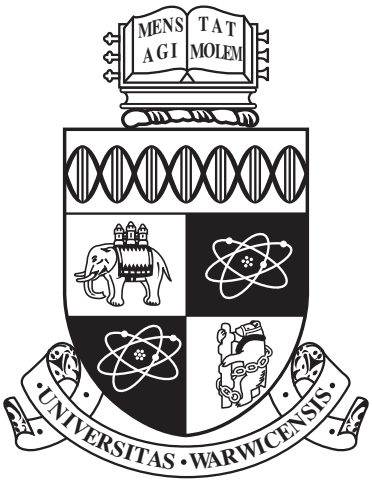

The Design and Performance Analysis of Diffusive Molecular Communication Systems

by

Xiayang Wang

Thesis

Submitted to the University of Warwick

for the degree of

Doctor of Philosophy

School of Engineering

January 2016

THE UNIVERSITY OF
WARWICK

Contents

List of Tables **v**

List of Figures **vi**

Acknowledgments **ix**

Declarations **x**

List of Publications **xi**

Abstract **xii**

Abbreviations **xiii**

Chapter 1 Introduction **1**

1.1 Basic elements for nano-communications systems 2

1.2 Molecular communications systems 3

1.2.1 MC system transportation modes 3

1.2.2 Diffusive MC systems 5

1.2.3 Comparisons between CC systems and diffusive MC systems 8

1.2.4 Recent advancements in diffusive MC systems 9

1.3 The aim and specifically divided tasks of the Ph.D. project 10

1.4 Contributions to drive the entire thesis 13

1.5 The organisation of the thesis 14

Chapter 2 The Design of MC System Model-I and Its Performance Analysis **18**

2.1 Introduction 18

2.2 The diffusion-based MC system model based on the motion of individual molecules 20

2.3 Performance analysis of MC system Model-I . . . 25
2.3.1 Bit Error Rate analysis . . . 26
2.3.2 Capacity analysis . . . 29
2.3.3 A refined design of the decision variable . . . 30
2.4 Numeral results . . . 31
2.4.1 Channel performance when $P_{\text{tx}} = 0.5$ . . . 32
2.4.2 Channel performance with different P_{tx} . . . 36
2.5 Conclusions . . . 37

Chapter 3 An Algorithmic Distance Estimation Scheme Based on System Model-I 38
3.1 Introduction . . . 38
3.2 Diffusion-Based MC System Structure . . . 40
3.3 Distance estimation scheme . . . 43
3.3.1 The Distance Estimation Scheme in Unsynchronised Conditions 44
3.3.2 The Distance Estimation Scheme in Synchronised Conditions 45
3.3.3 Parameter Optimisation Methods . . . 46
3.4 Numeral results . . . 47
3.4.1 Distance Estimation Scheme in Unsynchronised Condition . . . 48
3.4.2 Distance Estimation Scheme in Synchronised Condition . . . 52
3.5 Conclusions . . . 53

Chapter 4 Communication Protocols: SW-ARQ schemes in MC systems 54
4.1 Introduction . . . 54
4.2 System transmission structure . . . 56
4.3 SW-ARQ schemes . . . 58
4.3.1 Scheme 1 . . . 58
4.3.2 Scheme 2 . . . 60
4.3.3 Scheme 3 . . . 61
4.3.4 Scheme 4 . . . 62
4.3.5 Scheme 5 . . . 63
4.4 Numeral results . . . 63
4.4.1 Results for Scheme 1 and 2 . . . 64
4.4.2 Results for Scheme 3 . . . 65
4.4.3 Results for Scheme 4 . . . 66
4.4.4 Results for Scheme 5 . . . 68
4.5 Conclusions . . . 69

Chapter 5 The Design of MC System Model-II and The Performance Analysis **71**
5.1 Introduction . . . 71
5.2 The diffusion-based MC system model based on molecular concentrations . . . 73
5.3 Performance analysis of MC system Model-II . . . 78
5.3.1 Bit Error Rate analysis . . . 79
5.3.2 Capacity analysis . . . 81
5.4 Numeral results . . . 82
5.4.1 The concentration with different emission durations . . . 83
5.4.2 Performance analysis for Model-II at one distance . . . 84
5.4.3 Performance analysis for Model-II at different distances . . . 87
5.5 Conclusions . . . 89

Chapter 6 Distance estimation schemes based on system Model-II **91**
6.1 Introduction . . . 91
6.2 Concentration-Based MC System Structure . . . 93
6.3 Distance estimation schemes . . . 94
6.3.1 Using the peak time to estimate the distance . . . 94
6.3.2 Using the energy to estimate the distance . . . 96
6.3.3 Applying the estimated distance to decode messages . . . 97
6.4 Numeral results . . . 99
6.4.1 Using the peak time to estimate the distance . . . 100
6.4.2 Using the energy to estimate the distance . . . 102
6.4.3 System BER analysis with distance estimation scheme applied 104
6.5 Conclusions . . . 105

Chapter 7 Performance analysis of the relaying MC system based on Model-II **106**
7.1 Introduction . . . 106
7.2 Relaying system structure . . . 108
7.3 Relay channel analysis . . . 110
7.3.1 BER for 'Relay-1' . . . 110
7.3.2 BER for 'Relay-2' . . . 114
7.3.3 An alternative way to obtain the system BER . . . 115
7.4 Numeral results . . . 116
7.5 Conclusions . . . 119

Chapter 8 Conclusions and Future Work **120**
8.1 Conclusions 120
8.2 Future work 125

List of Tables

1.1 Differences between CC and MC 8

2.1 Model-I: error patterns and their probabilities for ISI length $I = 2$. . 28
2.2 Parameters assignment for the analysis of Model-I 32
2.3 The comparison between theoretical and simulated BER with $m = 5 \times 10^3$, and I=20 35

3.1 Parameters for simulating the distance estimation scheme for Model-I 48

4.1 Simulation parameters for the investigation of the SW-ARQ schemes 63
4.2 Time cost and energy consumption for Scheme 4 and Scheme 3 at $d = 3\,\mu m$. 67
4.3 Time cost and energy consumption for Scheme 5 at $d = 3\,\mu m$. . . . 68
4.4 Time cost and energy consumption for all five schemes at $d = 3\,\mu m$. 69

5.1 Model-II: error patterns and their probabilities for ISI length $I = 2$. 81
5.2 Parameter assignment to analyse the performance of Model-II 82

6.1 Parameters to simulate the distance estimation schemes for Model-II. 99

7.1 Simulation parameters for the analysis of the relaying system 116

List of Figures

1.1 The block diagram of nano-communications systems. 2
1.2 Five different MC architectures. 4
1.3 The outline of the MC system incorporating nano-machines. 5
1.4 Three ways to encode messages into molecular signals. 6

2.1 The structure of the MC system. 20
2.2 The number of captured molecules vs time with $m = 10^4$. 23
2.3 BER vs. distances for different I with $m = 5 \times 10^3$. 32
2.4 BER vs. distances for different m with $I = 20$. 33
2.5 Channel capacity vs. distances for different m and I. 33
2.6 BER vs. P_{tx} for different m and d with $I = 20$. 36
2.7 Channel capacity vs. P_{tx} for different m and d with $I = 20$. 37

3.1 The structure of the MC system. 40
3.2 The flow chart illustrating the estimation scheme. 44
3.3 $P_{0,t_1 \to t_1+t_2}$ within $t_2 = 500\,\mu\text{s}$ at $d = 1\,\mu\text{m}$. 47
3.4 Unsynchronised, Dev_d vs d for different I with $m = 5 \times 10^3$ and $D = 5 \times 10^{-3} \mu\text{m}^2\,\mu\text{s}^{-1}$. 49
3.5 Unsynchronised, Dev_d vs d for different m with $I = 9$ and $D = 5 \times 10^{-3} \mu\text{m}^2\,\mu\text{s}^{-1}$. 50
3.6 Unsynchronised, Dev_d vs d for different D with $I = 9$ and $m = 5 \times 10^3$. 51
3.7 Unsynchronised, Time consumption vs d for different I, m and D. . 51
3.8 Synchronised, Dev_d vs d for different m and D. 52
3.9 Synchronised, time consumption vs d for different m and D. 53

4.1 The structure of the MC system. 57
4.2 The structures of the packets and ACKs in the MC system. 57
4.3 The five proposed SW-ARQ transmission schemes. 59

4.4 The time and energy required for a successful duplex transmission using Scheme 1 and Scheme 2 ($\varsigma = 1$ represents the results for Scheme 1) 64
4.5 The time and energy required for a successful duplex transmission using Scheme 3 at $d = 3\,\mu m$ (Note: $\rho = 1$ is also Scheme 1). 65
4.6 The number of copies transmitted χ changes with each transmitted packet for Scheme 4 at $d = 3\,\mu m$. Results only show the fist 1000 packets. 66
4.7 The distribution of the occurrence times for each value of χ for Scheme 4 at $d = 3\,\mu m$. The amount of successively transmitted packets is 10^5. 67
4.8 The distribution of the occurrence times for each value of χ at $d = 3\,\mu m$ for Scheme 5. The amount of successively transmitted packets is 10^5. (Note: $\varsigma = 1$ represents the results for Scheme 4.) 68

5.1 The structure of the MC system. 73
5.2 The changing concentration over time for different T_{em} at $d = 1.5\,\mu m$ with $m = 5 \times 10^3$. 83
5.3 BER vs. m for different T_{em} at $d = 1.5\,\mu m$ with $I = 20$. 84
5.4 Capacity and SNR vs. m for different T_{em} at $d = 1.5\,\mu m$ with $I = 20$. 85
5.5 BER vs. m for different I at $d = 1.5\,\mu m$ with $T_{em} = 1000\,\mu m$. 85
5.6 Capacity and SNR vs. m for different I at $d = 1.5\,\mu m$ with $T_{em} = 1000\,\mu m$. 86
5.7 The corresponding difference of BER, capacity, and SNR for increasing I at $d = 1.5\,\mu m$ with $T_{em} = 1000\,\mu m$. 86
5.8 BER vs. d for different m with $T_{em} = 1000\,\mu m$ and $I = 20$. 88
5.9 Capacity and SNR vs. d for different m with $T_{em} = 1000\,\mu m$ and $I = 20$. 88
5.10 BER vs. SNR for different m, d, I, and T_{em}. 89

6.1 The structure of the MC system. 93
6.2 The peak concentration time illumination at different distances with $T_{em} = 10^3 \mu s$ and $T_{em} = 5 \times 10^3 \mu s$. 95
6.3 Using peak time, Dev_d vs. d for different m with $T_{em} = 1000\,\mu s$. . . 100
6.4 Using peak time, Dev_d vs. d for different A and T_{em} with $m = A \times T_{em} = 5 \times 10^3$. 100
6.5 Using peak time, Dev_d vs. d for original and simplified schemes with $m = A \times T_{em} = 10^4$. 101
6.6 Using energy, Dev_d vs. d for different m with $T_{em} = 1000\,\mu s$. 102

6.7 Using energy, Dev_d vs. d for different A and T_{em} with $m = A \times T_{\mathrm{em}} = 5 \times 10^3$. 103
6.8 Using energy, Dev_d vs. d for original and simplified schemes with $m = A \times T_{\mathrm{em}} = 10^4$. 103
6.9 BER and Dev_d vs. d with $m = 1000$. 104
6.10 BER and Dev_d vs. d with $m = 5000$. 105

7.1 The structure of the MC relay system. 108
7.2 BER and d_{23} vs. d_{12} for $\theta = 20°$. 117
7.3 The optimal BER and corresponding for different angles θ. 118

Acknowledgments

Firstly, I would like to express my sincere gratitude towards my supervisors, Dr Matthew D. Higgins and Dr Mark S. Leeson. It is my greatest fortune and pleasure to have their guidance during my Ph.D. journey.

Secondly, I am grateful to my parents who have shown their full support throughout my education life. Even when I was not sponsored by the scholarship, they spared no effort to strengthen my faith and motivate me to pursue my study. There is no words that could express my love to them.

Thirdly, I would like to thank my friends, especially Hu Yuan. He is such an enthusiastic friend, as well as a mentor in my life. Every time I met with troubles, he would be always standing besides me, calming me down and backing me up. I have learnt quite a lot from him. I really value our friendship established during this tough period.

Last but not the least, my sincere thanks also goes to my examiners Dr Yunfei Chen and Prof John Mitchell, for their constructive feedback.

Declarations

I herewith declare that this thesis contains my own research performed under the supervision of Dr Matthew D. Higgins and Dr Mark S. Leeson, without assistance of third parties, unless stated otherwise. No part of this thesis was previously published or submitted for a degree at any other university.

List of Publications

Journals

- **X. Wang**, M. D. Higgins, and M. S. Leeson, "Relay Analysis in Molecular Communications with Time-Dependent Concentration", *IEEE Commun. Lett.*, vol. 19, pp. 1977-1980, 2015.
- **X. Wang**, M. D. Higgins, and M. S. Leeson, "Distance Estimation Schemes for Diffusion Based Molecular Communication Systems", *IEEE Commun. Lett.*, vol. 19,. pp. 399-402, 2015.
- **X. Wang**, M. D. Higgins, and M. S. Leeson, "Simulating the Performance of SW-ARQ Schemes within Molecular Communications", *Simulation Modelling Practice and Theory (SIMPAT)*, vol. 42, pp. 178-188, 2014.

Conferences

- **X. Wang**, M. D. Higgins, and M. S. Leeson, "An Algorithmic Distance Estimation Scheme for Diffusion Based Molecular Communication Systems", in *Proc. IEEE Int. Commun. Conf. (ICC)*, pp. 2737-2742, 2015.
- **X. Wang**, M. D. Higgins, and M. S. Leeson, "Stop-and-Wait Automatic Repeat reQuest Schemes for Molecular Communications, in *Proc. IEEE Int. Black Sea Conf. on Commun. and Networking*, pp. 84-88, 2013.

Abstract

Molecular Communications (MC) is an increasingly attractive technique to enable the networking of nano-machines by utilising molecules as the information carrier. The molecular diffusion can be described by either the movement of individual molecules or the molecular concentration. Accordingly, two kinds of diffusive MC systems have been modelled in previous literature. On the basis of these studies, the aim of this Ph.D. is to refine these two models, to implement functional transmission techniques and technologies, and to investigate the corresponding system performance. To fulfil this target, the whole Ph.D. is divided into two stages. During each stage, specific tasks have been accomplished, each contributing to the overarching research field of diffusive MC systems.

In the first stage, an MC system model, named as the Model-I, is established and enhanced by focusing on the motion of individual molecules. The performance has been evaluated by both deriving mathematical expressions and implementing MATLAB simulations. Based on the Model-I, a distance estimation scheme has been proposed. Compared with existing methods, this new scheme is more accurate and less time-consuming. Moreover, five Stop-and-Wait Automatic Repeat reQuest (SW-AQR) protocols have been implemented on the Model-I. Results reveal that all these SW-ARQ schemes work well and can be beneficial under different circumstances.

In the second stage, another MC system model, named as the Model-II, is established and refined with information conveyed by the molecular concentration. Both theoretical derivations and MATLAB simulations are provided to analyse the system reliability. Laid on this foundation, two distance measurement methods have been proposed and shown to be suitable for the Model-II. Additionally, to solve the long-range MC problem, relaying schemes have been applied by deploying a relay node between the source and target nano-machines. The performance improvement of each scheme is also illustrated respectively.

Abbreviations

1. Abbreviations in the text

ACK, Acknowledgment
AMT, Active Molecular Transportation
BER, Bit Error Rate
CC, Conventional Communications
CDF, Cumulative Distribution Function
Dev, Estimation bias
DF, Decode-and-Forward
EM, Electromagnetic
ISI, Inter-Symbol Interference
MC, Molecular Communications
MLC, Memory Limited Channel
MSE, Mean Square Error
PMT, Passive Molecular Transportation
RN, Relay Node
Rx, Receiver
SF, Sense-and-Forward
Tx, Transmitter

SW-ARQ, Stop-and-Wait Automatic Repeat reQuest
HOP1, The first hop in a relay system
HOP2, The second hop in a relay system
Model-I, The system model by focusing on the individual molecules movement
Model-II, The system model by focusing on the molecular concentration
Relay-1, The relay system with single kinds of molecules utilised
Relay-2, The relay system with two kinds of molecules utilised

Scheme 1, The SW-ARQ scheme 1
Scheme 2, The SW-ARQ scheme 2
Scheme 3, The SW-ARQ scheme 3
Scheme 4, The SW-ARQ scheme 4
Scheme 5, The SW-ARQ scheme 5

2. Abbreviations in subscripts or superscripts

ac, ACK
ca, Capture
em, Emission
er, Error
es, Escape
in, Index

me, Message
pa, Packet
pd, Period
pk, Peak
proc, Process
s1, Scheme 1
s2, Scheme 2
s3, Scheme 3
s4, Scheme 4
s5, Scheme 5
sa, Sampling
se, Sensing
si, Simplified
sy, Synchronised
(1), Relay-1
(2), Relay-2

3. Symbols denotations

a_{k-i}, The binary value for the $(k-i)^{\text{th}}$ symbol
$\{a_{k-i}\}$, The transmitted messages sequence within the ISI for the k^{th} symbol
$\hat{a}_{k-i}$, The binary value for the estimated $(k-i)^{\text{th}}$ symbol
$\{\hat{a}_{k-i}\}$, The estimated messages sequence within the ISI for the k^{th} symbol
A, The emission rate
B_{me}, The message length in bits
B_{in}, The index length in bits
$c(d,t)$, The molecular concentration after an impulse
d, The distance between a couple of nano-machines
d_{12}, The distance between the Tx and RN
d_{13}, The distance between the Tx and Rx
d_{23}, The distance between the RN and Rx
$\hat{d}$, The estimated distance
$\hat{d}_{\text{si}}$, The estimated distance using simplified scheme
Dev_d, The deviation for distance d
D, The diffusion coefficient
$E(\cdot)$, The expected value
$h(t)$, The impulse response for the diffusion channel
I, The ISI length
j, The Error patten index
k, The k^{th} symbol from the beginning of transmission
l_1, The pre-designed criterion for symbol '1'
l_0, The pre-designed criterion for symbol '0'
L, The judgment condition for the Rx
m, The number of molecules emitted per pulse
$n(t)$, The noise of the concentration

N, The number of molecules captured
N_{ac}, The overall numbers of the released molecules for ACKs
N_{pa}, The overall numbers of the released molecules for packets
P, Probability
P_{ca}, The capture probability
P_{er}, The error probability
P_{es}, The escape probability
P_{s1}, The probability for a complete duplex transmission using Scheme 1
$P_{\mathrm{s2}}(\varsigma)$, The probability for a complete duplex transmission using Scheme 2
$P_{\mathrm{s3}}(\rho)$, The probability for a complete duplex transmission using Scheme 3
$P_{\mathrm{s4}}(\chi)$, The probability for a complete duplex transmission using Scheme 4
$P_{\mathrm{s5}}(\chi, \varsigma)$, The probability for a complete duplex transmission using Scheme 5
$P_{\mathrm{sy}}(d, t_2)$, The capture probability within t_2 for synchronised situations
P_{tx}, The probability of '1' transmitted
Q, Q values ranges from 0 to t_1
$r(d, t)$, The Rx sensed concentration
R_{ca}, The capture range in Model-I
R_{se}, The sensing range in Model-II
$s(t)$, The rectangular wave
t, Time
$\triangle t$, The time interval between each counting process
t_1, The delay between the Tx emission and Rx reception
t_2, The counting duration
T_{em}, The emission duration
T_{out}, The waiting time before re-transmission
T_{over}, The overall time for Rx in Model-I to estimate the distance
T_{pd}, The signal period
T_{pk}, The peak time
T_{proc}, The processing time
T_{sa}, The sampling time
$u(d, t)$, The concentration after a rectangular pulse
$\bar{u}_{i-1}$, The averaged concentration within the Tx for the previous $(i-1)^{\mathrm{th}}$ symbol
W_n, The noise power
W_u, The signal power
$\mathbf{X}$, The binary input vector
$\mathbf{Y}$, The binary output vector
$\mathcal{B}$, Binomial distribution

$\mathcal{N}$, Normal distribution
$\mathcal{I}$, Mutual information
∇^2, Laplacian operator
α, The angle between d_{12} and d_{23}
θ, The angle between d_{12} and d_{13}
ϱ_j, The number of '1's within the ISI length for error patten 'j'
ς, The number of copies of the ACK corresponding to one packet
ψ, The ratio of the length of the packets to the length of the ACKs
ρ, The initial number of copies of the packet and ACK
γ, The fluctuation number for Scheme 4
χ, The adaptive number of copies of packets (or ACKs)
$\Phi(\cdot)$, The CDF of the standard normal distribution
Ω, The concentration energy

4. Symbols used as substitutions

η, ζ, ϖ, ϑ, σ_{0j}, ξ, τ, λ, ε, ω.

Chapter 1

Introduction

The issue of accomplishing the information transmission over a distance has always played a vital role in the process of human civilisations. Historically, engineers and researchers have tried to solve this problem by means of utilising electrical or electromagnetic (EM) forms of communications. However, there still remain many aspects in which these traditional technologies cannot be implemented appropriately. For example, in extremely tiny dimensions, such as in the micrometer or even the nanometre scale, it is almost impossible to deploy the Conventional Communications (CC) techniques due to restrictions like the size, the wave length, and the energy budget [1]. The communications in such dimensions is named as "nano-communications".

To expand the application range of communications, the concept of nano-technology was introduced by the Nobel-laureate physicist Richard Feynman during his famous speech entitled "*There's Plenty of Rooms at the Bottom*" (transcribed in [2]). Since then, attention has been drawn on the extreme miniaturisation and related research activities have been carried out to explore the idea of nano-technology. With the help of the remarkable development in manufacture techniques, the advancement in this field began to accelerate in the early 2000s, which lays the foundation for the establishment of nano-communications. As is illuminated in the Fig.

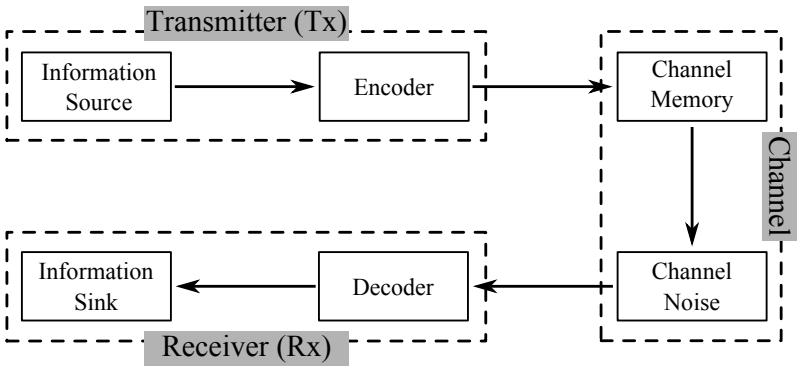

Figure 1.1: The block diagram of nano-communications systems.

1.1, similar to CC systems, a typical nano-communications system is also formed by three functional blocks, namely, the transmitter (Tx), the receiver (Rx), and the channel with the information carrier to achieve message exchange in between.

1.1 Basic elements for nano-communications systems

Within nano-communications systems, nano-machines are implemented to serve as the Tx and Rx. Nano-machines, regarded as the most basic functional units, are defined as the devices that "consist of nano-scaled components (ranging from 1 to 100 nanometers) and are able to performance a specific task at the nano-level, such as communicating, computing, data storing, sensing and/or actuation" [3, 4]. Due to their own functionality, nano-machines with different architectures can be deployed to fulfil tasks of both the Tx and Rx. There are three potential methods to fabricate nano-machines, i.e. the top-down approach by down-scaling current micro-devices [5, 6, 7, 8], the bottom-up approach by assembling elementary nano-components [3, 9, 10, 11], and the bio-hybrid approach by considering the living organisms as nano-machines [12, 13, 14]. The development of the manufacture limits the implementation of the first two methods, but natural systems, such as cells or bacterium, can be utilised as nano-machines.

As to the information medium, various technologies have been proposed,

where accordingly EM, acoustic, or molecular signals are used. The transmission from a micro-device to a nano-machine can be accomplished by taking advantage of EM [15] or ultrasonic waves [16]. These waves propagate with minimal losses, which can help to establish a reliable communication channel. Thus, it is required that either radio-frequency transceivers or ultrasonic transducers should be integrated in nano-machines. However, due to the size and current complexity of nano-machines, this integration cannot be easily realised [17]. In addition, even if the integration was possible, the energy budget of nano-machines may not be sufficient to undertake these objectives [16].

Alternatively, message symbols can be expressed by molecular signals, which is named as *Molecular Communications* (MC). MC can be observed among living cells [18], bacterias [14], and even social insects [19]. Accordingly, unlike the other two technologies, the integration process of molecular transceivers in nano-machines is more feasible due to the bio-compatibility [1]. To communicate, the Tx makes a physical change to its environment and this change must be measurable at the Rx [20]. Similar to the change of the EM field in CC, the change in MC must be molecular: the Tx emits molecules into a shared environment, and these molecules propagate to (and are detected by) the Rx. In this way, information can be transmitted from a nano-machine to a micro-device or among nano-machines, which therefore provides a potential method to enable the networking of deployed nano-machines [16]. Due to its own superiority, the MC is regarded as the most promising method to solve the problems of nano-communications [21].

1.2 Molecular communications systems

1.2.1 MC system transportation modes

Inspired by the biological systems found in nature, five MC system architectures have been proposed to describe the propagation mechanism of message molecules, which

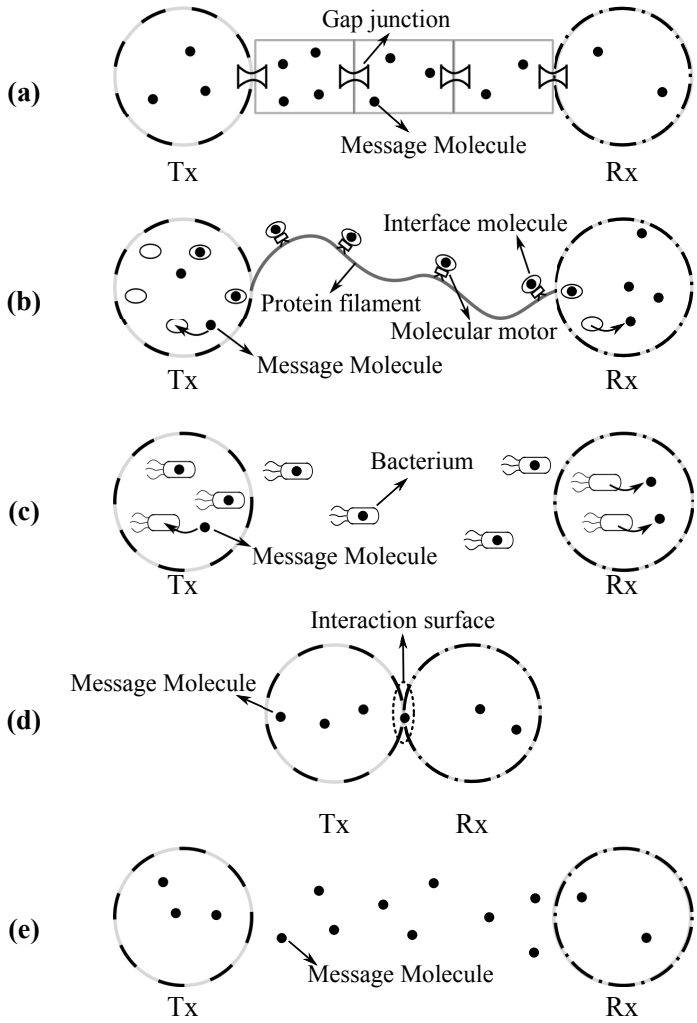

Figure 1.2: Five different MC architectures.

can be grouped into two types, namely the Active Molecular Transporting (AMT) and Passive Molecular Transportation (PMT) [22]. The AMT can be accomplished by four techniques shown in Figs. 1.2 (a) to (d), namely the gap junction channels by taking advantage of the gap junctions between cells [23, 24], the interface molecule carrier channels by using the protein filaments and molecular motors [25, 26], the self-propelling mechanism by embedding message molecules into bacteria [27, 28], and the contact-dependent inter-cellular communications via molecular collisions [29]. To deploy the AMT, the connectivity between nano-machines requires to be established in advance [30].

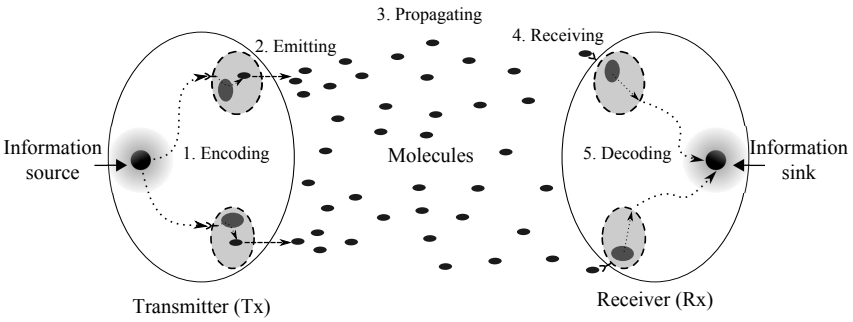

Figure 1.3: The outline of the MC system incorporating nano-machines.

Another transportation mode, the PMT, is achieved by molecular random walk, or free diffusion, in the environment. As is illustrated in the Fig. 1.2 (e), MC systems with the diffusion-based architecture take advantage of the free diffusion of information molecules without guided by any intermediate system. When receiving message molecules, the Rx can be either an absorber to capture molecules and to remove them from the environment [31, 32], or an observer to sense, rather than affecting, the concentration by means of binding a ligand-receptor [33, 34]. Compared with the AMT, the implementation of the PMT requires little effort to establish the MC systems. Therefore, this architecture is a feasible solution to realise the communications between nano-machines, and hence becomes increasingly attractive [35].

1.2.2 Diffusive MC systems

As is shown in the Fig. 1.1, a diffusive MC systems, belonging to nano-communications systems, consist of three main blocks, i.e. the Tx, the diffusive channel, and the Rx. The outline of a typical diffusive MC system is illustrated in the Fig. 1.3 [36]. The capability of the Tx is to generate, encode, and emit information molecules. The Rx is able to receive these molecules and to decode the attached messages. Generated by the information source, information is represented by a sequence of symbols in consecutive time slots, and encoded onto certain molecules. As soon as being

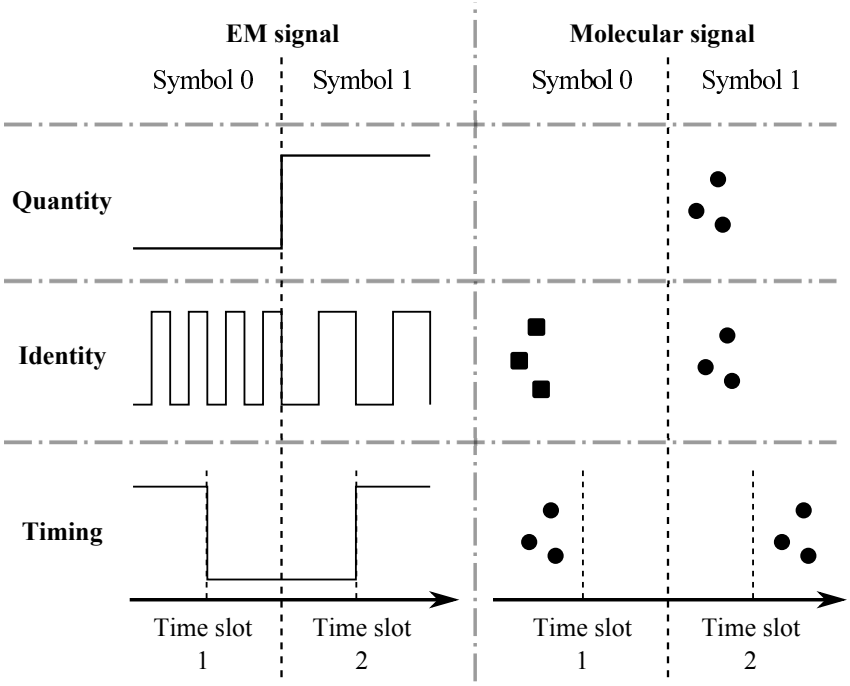

Figure 1.4: Three ways to encode messages into molecular signals.

released by the Tx, message molecules start to propagate towards the Rx. After receiving these molecules, the Rx can decode corresponding information symbols according to certain pre-designed decoding algorithms.

In order to convey information by molecular signals, a unique patten of physical change should be designed for each message symbol, which should also be able to be detected by the Rx. Motivated by EM signals in CC, three encoding methods are utilised in diffusive MC systems [20]. As is illuminated in the Fig. 1.4, different information symbols are expressed by different amounts of emitted molecules, different species of emitted molecules, or different emission time.

Molecules encoded with messages will diffuse independently in the environment. The propagation mechanism of these molecules has been investigated from two angles of views. On one hand, researches are carried out from the micro-scope by focusing on each individual molecule. The movement of each molecule is a random process. The probability can be derived for whether a molecule will be absorbed by

the Rx or move to the infinity. Given this capture probability obtained, the propagation of all these molecules can be treated as a Bernoulli process. In this way, the propagation mechanism can be addressed from the micro level. On the other hand, when dealing with the molecular diffusion, attention is paid on the molecular concentration. No matter how every single molecule moves, they will gradually form a certain concentration distribution in the environment, which provides another method to describe the molecular propagation procedure.

After these message molecules arrive at the Rx, they will trigger the receiving function of the Rx so that these information symbols can be decoded correspondingly. As is also explained in Section 1.2.1, two receiving strategies can be applied. The Rx can be either an active absorber, which is able to capture molecules and remove them from the environment, or an passive observer, which can sense the concentration without affecting the distribution of molecules. The selection of these two kinds of Rx should be made depending on different scenarios. Referring to all the research published, when the molecular propagation is modelled by the motion of individual molecules, the Rx is generally regarded as an absorber; whereas the propagation is characterised by the molecular concentration, the Rx is often considered as an observer.

Similar to the situation in CC systems, there are various types of channel noise in diffusive MC systems. The noise source could be the propagation randomness, the transmitter emission noise, the feature of the environment (such as the temperature and pH level), or even the reactions between molecules. As a consequence, although plenty of effort has been put aiming to illuminate the impact of the channel noise [37, 38, 39, 40, 41, 42, 43, 44, 45, 46, 47], it still remains an open challenge to discover a proper way to model the noise in MC systems.

Another factor influencing MC systems is the channel memory. As is mentioned previously, it is impossible to predict the exact arrival time of message molecules at the Rx due to the randomness of the molecular propagation, and

Table 1.1: Differences between CC and MC

Features	CC	MC
Device	Artificial machines	Bio-hybrid nano-machines
Information carrier	EM waves	Molecules
Type of information	Digital	Chemical or physical
Propagation speed	Light (3×10^8 m/s)	Extremely low
Propagation range	m $\sim$ km	nm $\sim$ µm
Medium	Air or cables	Aqueous
Noise source	EM fields and signals	The medium, Tx and Rx
ISI source	Multi-path	Unpredictable arrival time
Energy consumed	Electrical, high	Chemical, low

molecules remaining in the environment will not vanish until they move to the infinity (only if the time is infinite). Hence, some of messages molecules may reach the Rx in future time slots, and these molecules will cause a form of interference to the detection of that corresponding symbol when they arrive. This is denoted as the Inter-Symbol Interference (ISI) of MC systems, which can seriously degrade the channel reliability. To mitigation the ISI, a wide range of solutions have been proposed, such as implementing advanced modulation schemes [48, 49, 50, 51, 52], applying the Mean Square Error (MSE) decoding algorithm [53, 54], optimising the decoder of the Rx [45, 55, 56], and using Error Control Coding schemes [57, 58].

1.2.3 Comparisons between CC systems and diffusive MC systems

With all preceding explanation on diffusion-based MC systems, it can be summarised that diffusive MC, as a promising form of nano-communications, is not a simple extension of CC networks at the nano-scale. The comparisons between CC and MC are presented in Table 1.1 [1, 20]. Given such many differences between these two communications domains, it can be deduced that existing communication technologies may not suit for the diffusive MC systems and innovative networking techniques are required for the unique characteristics of nano-machines and the molecular communication processes.

1.2.4 Recent advancements in diffusive MC systems

The first research on the diffusive MC systems can be tracked back to a 2005 paper entitled as "Molecular Communication" [59], since when, work on MC systems has accelerated. MC is an increasingly attractive topic, and there is a rapid growth in theoretical and simulation-based analysis within this field. The main three themes of contemporary literature are respectively modelling and analysing the MC channel, investigating performance enhancement techniques, and developing simulation tools. Even though the laboratory experiment on MC systems, compared with the theoretical and simulation-based advancements, is still in its infancy due to the great expense and high difficulty, there have been several heuristic experiments implementations to explore the practicality of MC systems [46, 60, 61].

(1). Channel modelling and analysing

Based on two different propagation mechanisms described in Section 1.2.2, the diffusive MC channel can be divided into two broad categories, i.e., the discrete model with information expressed by the molecular amount, and the continuous model with information expressed by the molecular concentration. Discrete channel models with no ISI or simplified ISI (only one previous bit considered) were established in [38, 62, 63, 64]. In [65], Atakan took a general form of the ISI into account and built the MC system. For continuous models, the first research was present in [66] and expanded in [39] by considering the continuous emission of the Tx. However, there is no widely accepted general channel model or noise model for MC systems. Depending on different scenarios, researchers had to introduce their own specific assumptions of the noise. Hence, it still remains to be an open challenge.

(2). Performance enhancement techniques

Due to the severe attenuation and great randomness, MC channels tend to suffer from a higher Bit Error Rate (BER) and a lose of the capacity. To solve this problem, different techniques have been proposed to improve the system re-

liability. Several examples of such technologies, like novel modulation schemes, MSE decoding algorithms, or error control coding schemes, have been explained in Section 1.2.2. Apart from these, transmission protocols, like those introduced in [27, 53, 67, 68, 69, 70] can bring in benefit by compensating the attenuation of molecular signals. Specifically, in [27], a hybrid communication system is established, where short range communications is achieved by diffusion molecules, medium range communications is accomplished by the bacteria transportation mechanism, and long range communications is realised by using pheromones. Other transmission strategies, such as the Stop-and-Wait Automatic Repeat reQuest (SW-ARQ) techniques [67], the TCP/IP structure [68], and relaying schemes [53, 69, 70], can also enhance the performance. In addition, chemical methods by taking advantage of enzymes can be beneficial as well [71, 72].

(3). Simulation tools

Lacking of reliable experiment platforms, research activities have to rely on simulations to verify the accuracy of the theoretical analysis of MC systems and to evaluate the gain of performance enhancement techniques. Aiming to fulfil this target, several simulators have been developed, such as *eMCS* [73], *NanoNS* [74], *N3Sim* [75], *BINS* [76], and *MUCIN* [77]. These simulators all have their own superiority and drawbacks. Hence, researchers should select the proper simulator according to the specific requirement of their MC systems.

1.3 The aim and specifically divided tasks of the Ph.D. project

Molecular Communications (MC) is an increasingly attractive nano-communications technology to accomplish the information exchange among nano-machines, where messages symbols are expressed by molecular signals. The goal of this Ph.D. project is to establish an diffusive MC system, to apply functional transmission schemes and

to evaluate their performance through both mathematical calculations and simulations. Previous researchers have built the basic MC system models based on different propagation mechanisms of diffusing molecules, and introduced protocols to complete certain tasks. However, their system models should be further improved to be more accurate and closer to the reality. Meanwhile, enhanced transmission approaches need to be proposed to optimise the communication performance. Therefore, aiming to solve these problems, the Ph.D. project has been separated into the following specific tasks with corresponding objectives.

(1). Understanding molecular propagation mechanisms and the MC system models established accordingly

To carry out research on the MC system, it is essential to have a knowledge on how molecules diffuse in the surrounding environment. By assuming each molecule moving independently, studies on describing the propagation mechanism can be classified into two categories. The first classification is to analyse the movement of individual molecules. In this case, molecules reaching the Rx will be absorbed and removed from the channel, and the probability whether or not this molecule will be captured has already been derived by previous researchers. According to this propagation mechanism, an MC system model, represented as Model-I, is designed with information expressed by the number of captured molecules. The second category of researches is to characterise the propagation by investigating the molecular concentration distribution of these message molecules. Under this situation, the capability of the Rx is to sense the concentration around without affecting the distribution. Existing literature has formulated the molecular distribution in the aqueous medium. By taking advantage of the molecular concentration, a different MC system model, represented as Model-II, is established with messages symbols conveyed by the molecular concentrations.

(2). Enhancing both the system models and evaluating their performance

The system Model-I can be enhanced by applying the MSE decoding algo-

rithm, which is a method to alleviate the ISI. As to the system Model-II, not only can the MSE decoding algorithm be utilised, but also can the emission process of the Tx be taken into consideration. Based on these two refined system models, an information theoretical approach should be developed to evaluate the system performance with two features, namely, the BER and the channel capacity. Simulations should also be designed to verify these formulations and to assess the impact of different parameters. Moreover, even though the ISI has been mitigated, it will still influence the channel properties. Thus, further analysis with respect to the ISI needs to be carried out. For theoretical derivations, the ISI length should be regarded as an arbitrary value to maximise the generality. For simulations, the value of ISI length should be sufficiently large such that results are of as a high precision as is reasonably practical.

(3). Proposing distance estimation schemes for each model with a high accuracy and less time consumption

From previous research on measuring the system performance, it can be noticed that the distance between a couple of nano-machines is a vital parameter for both the Tx and Rx. As a consequence, it is highly required to find an appropriate method to estimate the distance. Existing schemes either cost too much time, or cannot provide an sufficiently accurate result. Hence, there is a clear and timely demand for the continued development of distance estimation schemes that are shown to be both accurate and fast. According to these two different system models, distance estimation schemes should be respectively proposed. Simulations should be also conducted to evaluate and compare the performance of these schemes by obtaining the estimation deviation and the time consumption.

(4). Applying transmission schemes to improve the MC system performance

Due to the high randomness and server attenuation of the molecular propagation, the MC systems tend to be susceptible to the channel memory and noise.

To assure the reliable message transmission, communications techniques, such as the SW-ARQ schemes and system relaying schemes, should be implemented in the MC systems. Considering the unique characters of MC, these transmission techniques should be proven to suit for the special conditions in MC systems via both theoretical analysis and simulations. The performance gain needs to be illustrated by numerical results, and it should also be presented how relevant parameters can affect the corresponding system performance.

1.4 Contributions to drive the entire thesis

The following contributions have been produced through the Ph.D. project and will be explained in detail throughout Chapter 2 to Chapter 7.

(1). The MSE decoding algorithm has been deployed to enhance MC system models with information expressed by either the number of absorbed molecules (Model-I) or molecular concentration (Model-II).

(2). The emission process of the Tx has been considered to improve the system model Model-II.

(3). Theoretical expressions of the BER and capacity have been derived for both enhanced MC system models.

(4). The impact of the channel memory has been further investigated by both theoretical derivations and simulations for these two system models.

(5). An algorithmic distance estimation scheme and two parameter optimisation methods have been proposed for the Model-I.

(6). 2 distance estimation schemes have been proposed for the Model-II.

(7). 5 SW-ARQ protocols have been proposed and proven to work on the Model-I.

(8). Decode-and-Forward (DF) relaying schemes have been designed to be deployed on the Model-II aiming to improve the system performance.

1.5 The organisation of the thesis

The entire thesis is organised with 8 chapters. Apart from the first chapter as the introduction chapter and the last chapter summarising the thesis and providing future research suggestions, the rest 6 chapters will describe each individual task accomplished. The highlights of these 6 chapters are respectively presented as follows.

Chapter 2

(1). The system model, Model-I, is established with information conveyed by the number of absorbed molecules.

(2). This model is refined by applying the MSE decoding method.

(3). An information theoretical approach is developed to measure the system performance with regards to the BER and capacity.

(4). Simulations are conducted to prove the derived expressions of the BER and capacity.

(5). Investigation is carried out to analyse how the system performance can be influenced by different parameters assignment.

(6). The impact of the channel memory on the properties of the channel is further explored.

Chapter 3

(1). An algorithmic distance estimation scheme for Model-I is proposed, which can be applied in both unsynchronised and synchronised situations.

(2). Two parameter optimisation methods, i.e. using more molecules and using molecules with larger diffusion coefficient, are introduced to enhance the distance estimation scheme.

(3). Simulations are provided to show the accuracy and time consumption of this estimation scheme and two optimisation methods.

(4). Performance comparisons are also presented with different parameters assignment.

Chapter 4

(1). 5 SW-ARQ schemes are proposed to be implemented on the Model-I.

(2). The performance is evaluated by the averaged time and energy utilisation.

(3). Scheme 1 benefits communications between adjacent nano-machines.

(4). Schemes 2 and 3 exhibit performance benefits for longer range communications.

(5). Schemes 4 and 5 suit for MC systems with unknown or varying channels.

Chapter 5

(1). The system model, Model-II, is built with messages expressed by molecular concentrations.

(2). The model is enhanced by considering the Tx emission process and utilising the MSE to decode information symbols.

(3). Theoretical formulations are derived to analyse the system BER and channel capacity.

(4). Simulations are designed to verify these mathematical expressions of the BER and capacity.

(5). The changes of channel properties with different parameters assignment is explored.

(6). The investigation on the influence of the channel memory on the system performance is expanded.

Chapter 6

(1). Two distance estimation schemes for Model-II are proposed by taking advantage of either the concentration peak time or the concentration energy.

(2). These two schemes are simplified by assuming molecules emitted simultaneously.

(3). Using energy to measure the distance will have a better accuracy at the cost of more energy and higher complexity.

(4). Simulations are carried out to show the performance of these two schemes and their simplification methods.

(5). Improvement of the estimation accuracy by optimising parameters is presented as well.

(6). An MC system without any pre-knowledge of distance is also analysed through both theoretical derivations and simulations.

Chapter 7

(1). Based on the Model-II, two DF relaying schemes are implemented.

(2). Theoretical expressions of the system BER are provided for both DF relaying schemes.

(3). If two different kinds of molecules are utilised respectively by the Tx and Relay Node (RN), the relay system performance can be further enhanced.

(4). Simulations are provided to illuminate the system performance enhancement by deploying these two DF relaying schemes.

(5). Through simulations, the optimal position of the RN is obtained to achieve the minimum system error probability.

Chapter 2

The Design of MC System Model-I and Its Performance Analysis

2.1 Introduction

In Chapter 1, the definition of Molecular Communications (MC) was introduced, which is to use specific molecules to enable the networking of nano-machines. Molecules, encoded by the transmitter (Tx), spread out in the environment and gradually propagate to the receiver (Rx) to accomplish the exchange of information. In this chapter, it is assumed that each molecule diffuses independently. The movement of individual molecules is investigated based on this assumption. Whether or not the message molecules will be absorbed is a random process, whose probability distribution will be presented. According to the analysis of the motion of each molecule, the MC system model is established with information symbols expressed by the numbers of captured molecules. This model is named as Model-I.

In order to carry out further research based on this model, it is essential to develop a method to evaluate the system performance and to figure out how

this performance can be influenced by different parameters. The channel reliability and the reliable transmission rate are two keys features to describe the properties of the channel. The former can be investigated by the Bit Error Rate (BER), and the latter can be characterised by the channel capacity. Deriving theoretical expressions of these two features provides an intuitive approach to measure the system performance and the impact of relevant parameters.

The first attempt to analyse these two channel features in diffusive MC systems was presented in [62], and expanded in [44, 78, 79] by taking the channel memory into consideration. In [37, 50, 52, 64, 80, 81, 82], research that focused on modulation schemes and/or noise modelling, also provided theoretical approaches to evaluate the performance of MC systems. In these studies, molecules were assumed to move independently, and information was decoded by comparing the number of captured molecules to a pre-designed threshold. However, due to the existence of the Inter-Symbol Interference (ISI), such a threshold may be either too large or too small that results in a high error probability. Thus, to achieve the optimisation of the system performance, the threshold should be adaptive, which may exceed the capability of nano-machines. Under this situation, another decoding method by calculating the Mean Square Error (MSE) should be implemented. By taking advantage of previous symbols to assist the decoding procedure of the Rx, the system performance can be enhanced due to the mitigation of the ISI influence.

In this chapter, the system Model-I is introduced based on the motion of individual molecules. To measure the system performance, expressions for the BER and channel capacity are derived. Simulation results are also provided to verify the accuracy of these formulations and to illuminate the performance variation caused by different designs of relevant parameters. Moreover, the influence of the channel memory is further investigated even though it has been alleviated. For theoretical derivations, the ISI length has been regarded as an arbitrary value to maximise the generality. For simulations, it is set to a length of 20 such that results are of as a

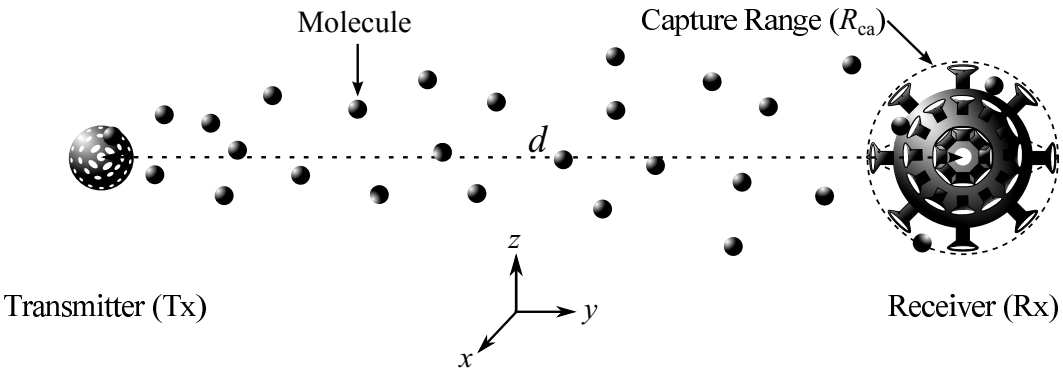

Figure 2.1: The structure of the MC system.

high precision as is reasonably practical.

The remainder of this chapter is organised as follows. The system Model-I, as well as relevant parameters, is described in Section 2.2. In Section 2.3, The channel performance in terms of the BER and capacity is studied for MC systems Model-I. Numerical results are provided in Section 2.4. Finally in Section 2.5, this chapter is concluded.

2.2 The diffusion-based MC system model based on the motion of individual molecules

The first MC system model, denoted as Model-I, is built according to the study on the movement of every single molecule. The system structure is illustrated in the Fig. 2.1. As is shown here, the MC system consists of two nano-machines in a 3D environment, one of which serves as the transmitter (Tx) with the other acting as the receiver (Rx). Information is conveyed by a sequence of symbols in consecutive time slots. In each time slot, to transmit symbol '1', the Tx releases a certain amount of molecules; to transmit '0', the Tx releases nothing. Within one time slot, molecules are assumed to be sent out simultaneously. At the destination end, the Rx captures molecules and removes them from the environment. By counting the number of absorbed molecules, the Rx determines whether '1' or '0' is transmitted. Referring

to the Fig. 2.1, the distance from the Tx to the centre of the Rx is represented by d, the size of Tx is negligible compared with the relative distance between these two nano-machines, and the radius of the capturing spherical surface of the Rx is R_{ca}.

In a 3D space, molecules ongoing Brownian Motion have a chance to escape to the infinity rather than being absorbed by the Rx. The escape probability, $P_{\text{es}}(d,t)$, obeys the following backward difference equation at time t , that is[83]:

$$\frac{\partial P_{\text{es}}(d,t)}{\partial t} = D\nabla^2 P_{\text{es}}(d,t), \tag{2.1}$$

where ∇^2 is the Laplacian operator, and D is the diffusion coefficient (in $\mu\text{m}^2\,\mu\text{s}^{-1}$). The value of D depends on the various factors, such as the temperature, the surrounding fluid, and the radius of the molecules. Correspondingly, the initial condition and boundary conditions are given as [57, 84]:

$$P_{\text{es}}(d, t=0) = 1, \quad \forall d > R_{\text{ca}}, \tag{2.2}$$

$$P_{\text{es}}(d = R_{\text{ca}}, t) = 0, \tag{2.3}$$

$$P_{\text{es}}(d \to \infty, t) = 1, \tag{2.4}$$

where (2.2) means at the time 0 the molecule is not captured by the Rx, (2.3) means the molecule will be absorbed as soon as entering the capture range of the Rx, and (2.4) means Rx is not able to capture the molecule if the distance between the molecule and Rx is infinite.

The capture probability, $P_{\text{ca}}(d,t)$, is more of interest, and can be derived by $P_{\text{ca}}(d,t) = 1 - P_{\text{es}}(d,t)$. Thus, considering (2.1) through (2.4), the capture probability can be obtained as [57, 84, 85]:

$$P_{\text{ca}}(d,t) = \frac{R_{\text{ca}}}{d}\text{erfc}\left(\frac{d - R_{\text{ca}}}{\sqrt{4Dt}}\right). \tag{2.5}$$

where 'erfc' represents the complementary error function. The signal period for each

symbol transmitted is denoted as T_{pd}. Thus, $P_{\mathrm{ca},0}$, which donates the probability for one molecule to be absorbed by the Rx within one signal period, can be derived as:

$$P_{\mathrm{ca},0} = P_{\mathrm{ca}}(d, t = T_{\mathrm{pd}}) = \frac{R_{\mathrm{ca}}}{d}\mathrm{erfc}\left(\frac{d - R_{\mathrm{ca}}}{\sqrt{4DT_{\mathrm{pd}}}}\right). \tag{2.6}$$

In the current time slot, the number of molecules received by the Rx for the current symbol signal is represented as N_0. It can be deduced that N_0 follows a binomial distribution given as [37, 78]:

$$N_0 \sim \mathcal{B}(m, P_{\mathrm{ca},0}), \tag{2.7}$$

where m is the number of molecules emitted by the Tx for one symbol. If m is sufficiently large, the binomial distributed N_0 can be approximated as a normal distribution expressed as:

$$\begin{aligned} N_0 &\sim \mathcal{N}\Big(mP_{\mathrm{ca},0}, mP_{\mathrm{ca},0}(1 - P_{\mathrm{ca},0})\Big) \\ &= \mathcal{N}\Big(\eta_0, \zeta_0\Big), \end{aligned} \tag{2.8}$$

where it is denoted that $\eta_0 = mP_{\mathrm{ca},0}$ and $\zeta_0 = mP_{\mathrm{ca},0}(1 - P_{\mathrm{ca},0})$.

However, molecules will not vanish within one period T_{pd}. The remaining molecules may reach the Rx in the next several time slots, or escape to the infinity. The late-arriving molecules will cause the InterSymbol Interference (ISI) at the Rx. The existence time for newly emitted molecules can be expressed as $(I + 1) \times T_{\mathrm{pd}}$, where I is called the ISI length. After $(I + 1) \times T_{\mathrm{pd}}$, newly emitted molecules are considered to be unable to reach the Rx anymore. If I is infinite, the molecules released in the first symbol time slot will result in the ISI to all the symbols followed; if I is finite, the channel is defined as the Memory Limited Channel (MLC) [86]. It is further assumed that the reception of molecules belonging to the same transmission pulse but arriving during different time slots can be viewed

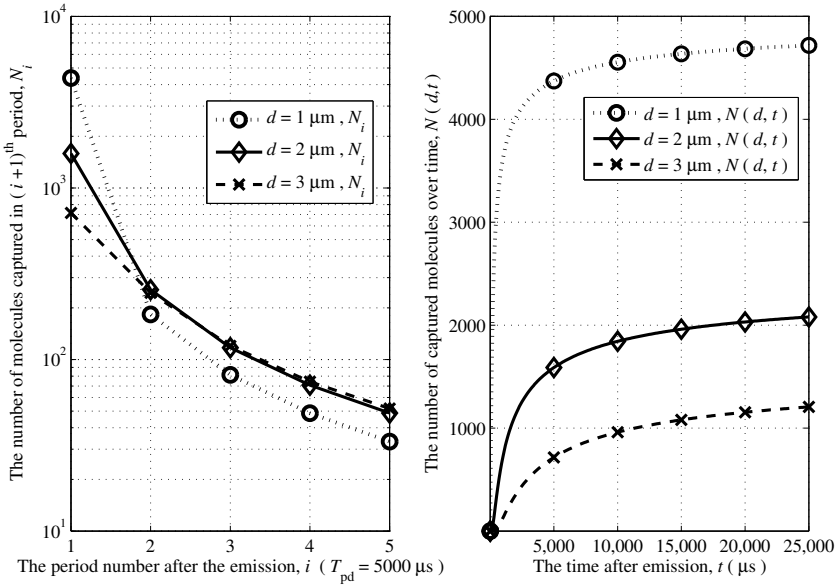

Figure 2.2: The number of captured molecules vs time with $m = 10^4$.

to be independent [52, 58, 87]. For $i = 1, 2, 3, ..., I$, if it is denoted that $P_{\mathrm{ca},i} = P_{\mathrm{ca}}(d, (i+1) \times T_{\mathrm{pd}})$, then, the number of received molecules for the previous i^{th} symbol in the current time slot, represented as N_i, can be derived as [52, 58, 87]:

$$\begin{aligned} N_i &\sim \mathcal{N}\Big(mP_{\mathrm{ca},i}, mP_{\mathrm{ca},i}(1-P_{\mathrm{ca,i}})\Big) - \mathcal{N}\Big(mP_{\mathrm{ca},i-1}, mP_{\mathrm{ca},i-1}(1-P_{\mathrm{ca},i-1})\Big) \\ &= \mathcal{N}\Big(mP_{\mathrm{ca},i} - mP_{\mathrm{ca},i-1}, mP_{\mathrm{ca},i}(1-P_{\mathrm{ca},i}) + mP_{\mathrm{ca},i-1}(1-P_{\mathrm{ca},i-1})\Big) \\ &= \mathcal{N}\Big(\eta_i, \zeta_i\Big), \end{aligned} \tag{2.9}$$

where it is denoted that $\eta_i = mP_{\mathrm{ca},i} - mP_{\mathrm{ca},i-1}$, and $\zeta_i = mP_{\mathrm{ca},i}(1-P_{\mathrm{ca},i}) + mP_{\mathrm{ca},i-1}(1-P_{\mathrm{ca},i-1})$. The Fig. 2.2 is an example showing the number of captured molecules over time, $N(d,t)$, and the number of captured within different periods, N_i, where the number of molecules released per pulse is $m = 10^4$. It can be noticed that with the distance between nano-machines increasing, the distribution gradient of N_i becomes gentler, and the tail of the distribution gets larger. Thus, with other parameters remaining the same, when the Tx is getting far away from the Rx, the

MC system tends to suffer more from the impact of the channel memory, i.e. ISI.

Given (2.8) and (2.9), the overall number of molecules received in one time slot, N^I, can be computed as:

$$\begin{aligned} N^I &= \sum_{i=0}^{I} a_{k-i} N_i \\ &\sim \sum_{i=0}^{I} a_{k-i} \mathcal{N}\Big(\eta_i, \zeta_i\Big) \end{aligned} \tag{2.10}$$

where k represents the k^{th} symbol from the beginning of transmission, the set $\{a_{k-i}, i = 0, 1, ..., I\}$ is the transmitted binary messages sequence, and the element a_{k-i} represents the binary value of each symbol. Within this thesis, the diffusion coefficient D is assumed to remain constant.

The ISI is a factor that has significant impact on the MC system performance. To reduce this influence, the Rx is designed to determine information bits by means of calculating the Mean Square Error (MSE) [88]. The decision variable, L, can be expressed as:

$$L = \text{MSE}_1 - \text{MSE}_0 = [N^I - l_1]^2 - [N^I - l_0]^2, \tag{2.11}$$

where N^I is given by (2.10), and l_1 and l_0 are pre-designed criteria for the Rx to determine the current message bit. The expressions of l_1 and l_0 are:

$$l_1 = \sum_{i=1}^{I} \hat{a}_{k-i} \hat{N}_i + \hat{N}_0, \tag{2.12}$$

$$l_0 = \sum_{i=1}^{I} \hat{a}_{k-i} \hat{N}_i, \tag{2.13}$$

where the set $\{\hat{a}_{k-i}, i = 1, 2, ..., I\}$ is previously decoded bits within the ISI length I, and $\hat{N}_0$ and $\hat{N}_i$ are respectively the corresponding estimated values of N_0 and N_i. Similar to (2.8) and (2.9), it can be deduced that $\hat{N}_0$ and $\hat{N}_i$ obey the normal

distribution, which are respectively represented as:

$$\hat{N}_0 \sim \mathcal{N}\Big(\eta_0, \zeta_0\Big), \tag{2.14}$$

$$\hat{N}_i \sim \mathcal{N}\Big(\eta_i, \zeta_i\Big). \tag{2.15}$$

It can be noticed from (2.12) and (2.13) that the design of l_1 and l_0 has taken the influence of previous symbols into consideration, which is a method to mitigate the ISI.

For theoretical derivations, it is assumed that previously decoded bits will not affect the decoding of the current bit. Thus, in this case, it is assumed that $\hat{a}_{k-i} = a_{k-i}$ for $i = 1, 2, ..., I$. By substituting (2.10), (2.12) and (2.13) into (2.11), the decision variable L can be rewritten as:

$$\begin{aligned}
L &= (N^I - l_1)^2 - (N^I - l_0)^2 \\
&= (a_k N_0 + \sum_{i=1}^{I} a_{k-i} N_i - \sum_{i=1}^{I} \hat{a}_{k-i} \hat{N}_i - \hat{N}_0)^2 - (a_k N_0 + \sum_{i=1}^{I} a_{k-i} N_i - \sum_{i=1}^{I} \hat{a}_{k-i} \hat{N}_i)^2 \\
&= [\sum_{i=1}^{I} a_{k-i}(N_i - \hat{N}_i) + a_k N_0 - \hat{N}_0]^2 - [\sum_{i=1}^{I} a_{k-i}(N_i - \hat{N}_i) + a_k N_0]^2 \\
&= -2\hat{N}_0[\sum_{i=1}^{I} a_{k-i}(N_i - \hat{N}_i) + a_k N_0 - \frac{1}{2}\hat{N}_0].
\end{aligned} \tag{2.16}$$

Thus, the value of L could be computed via (2.16). When $L \geq 0$, '0' is decided; otherwise, '1' is decided. In this way, the information bits can be determined.

2.3 Performance analysis of MC system Model-I

The MC system Model-I is described in Section 2.2. The decision variable for the Rx to decode messages is derived as (2.16), where N_0, N_i, $\hat{N}_0$, and $\hat{N}_i$ are normally distributed with expressions given by (2.8), (2.9), (2.14) and (2.15). To make it

easier to follow, L in (2.16) is rewritten as:

$$\begin{aligned} L &= -2\hat{N}_0[\sum_{i=1}^{I} a_{k-i}(N_i - \hat{N}_i) + a_k N_0 - \frac{1}{2}\hat{N}_0], \\ &= -2\hat{N}_0 \varpi. \end{aligned} \tag{2.17}$$

Since a_k represents the binary value of the k^{th} symbol after the transmission starts, it can be deduced that $a_k^2 = a_k$. Similarly, $a_{k-i}^2 = a_{k-i}$ for $i = 1, 2, ..., I$. Thus, according to properties of the normal distribution, it can be derived that:

$$N_i - \hat{N}_i \sim \mathcal{N}\Big(0, 2\zeta_i\Big), \tag{2.18}$$

$$a_k N_0 \sim \mathcal{N}\Big(a_k\eta_0, a_k\zeta_0\Big), \tag{2.19}$$

$$\frac{1}{2}\hat{N}_0 \sim \mathcal{N}\Big(\frac{1}{2}\eta_0, \frac{1}{4}\zeta_0\Big), \tag{2.20}$$

where m is the number of molecules emitted per pulse, ζ is expressed in (2.9), and $P_{\text{ca},0}$ can be calculated by (2.6). Given (2.18), it can be further obtained that:

$$\sum_{i=1}^{I} a_{k-i}(N_i - \hat{N}_i) \sim \mathcal{N}\Big(0, 2\sum_{i=1}^{I} a_{k-i}\zeta_i\Big). \tag{2.21}$$

Considering (2.19) and (2.20), the distribution of ϖ in (2.17) can be deduced as:

$$\begin{aligned} \varpi &= \sum_{i=1}^{I} a_{k-i}(N_i - \hat{N}_i) + a_k N_0 - \frac{1}{2}\hat{N}_0 \\ &\sim \mathcal{N}\Big((a_k - \frac{1}{2})\eta_0, 2\sum_{i=1}^{I} a_{k-i}\zeta_i + (a_k + \frac{1}{4})\zeta_0\Big). \end{aligned} \tag{2.22}$$

2.3.1 Bit Error Rate analysis

Error occurs only when '0' is transmitted but '1' is received (named as a_k=0 but $\hat{a}_k$=1), or when '1' is transmitted but '0' is received (named as a_k=1 but $\hat{a}_k$=0). Due to the existence of the ISI, different permutations of the values of

$\{a_{k-i}, i = 1, 2, ..., I\}$ will result in different error patterns. Each error pattern will be corresponding to a certain permutation of values of $\{a_{k-i}, i = 1, 2, ..., I\}$. With the ISI length equal to I, there will be 2^I error patterns. In this chapter, 'j' is denoted as the error pattern index, where $j = 1, 2, 3, ..., 2^I$. For the error pattern 'j', the permutation of values of $\{a_{k-i}, i = 1, 2, ..., I\}$ is denoted as $\{a_{k-i}^{(j)}, i = 1, 2, ..., I\}$, the number of '1's within $\{a_{k-i}^{(j)}, i = 1, 2, ..., I\}$ is denoted as ϱ_j, and accordingly, the number of '0's is $(I - \varrho_j)$. The probability of '1' transmitted is denoted as P_{tx}, and the probability of '0' transmitted is $(1 - P_{\text{tx}})$.

(1) a_k=0, but $\hat{a}_k$=1

With $a_k = 0$ and $\hat{N}_0 > 0$, to obtain the condition $L < 0$ in (2.17), it is required that:

$$\varpi > 0. \tag{2.23}$$

Given the distribution of ϖ expressed as (2.22), the probability for the error pattern 'j' can be derived by calculating the probability of $\varpi > 0$, that is:

$$\begin{aligned} P_{\text{er}0j} &= P_{\text{tx}}^{\varrho_j}(1 - P_{\text{tx}})^{I-\varrho_j} \int_0^{+\infty} \frac{1}{\sqrt{2\pi}} \frac{1}{\sigma_{0j}} \exp\Big(- \frac{(\varpi - \vartheta)^2}{2\sigma_{0j}^2} \Big) d\varpi \\ &= P_{\text{tx}}^{\varrho_j}(1 - P_{\text{tx}})^{I-\varrho_j} \left[1 - \int_{-\infty}^{0} \frac{1}{\sqrt{2\pi}} \frac{1}{\sigma_{0j}} \exp\Big(- \frac{(\varpi - \vartheta)^2}{2\sigma_{0j}^2} \Big) d\varpi \right] \\ &= P_{\text{tx}}^{\varrho_j}(1 - P_{\text{tx}})^{I-\varrho_j} \left[1 - \Phi\Big(\frac{0 - \vartheta}{\sigma_{0j}} \Big) \right] \\ &= P_{\text{tx}}^{\varrho_j}(1 - P_{\text{tx}})^{I-\varrho_j} \Phi\Big(\frac{\vartheta}{\sigma_{0j}} \Big), \end{aligned} \tag{2.24}$$

where $\vartheta = -\frac{1}{2}\eta_0$, $\sigma_{0j} = \sqrt{2 \sum_{i=1}^{I} a_{k-i}^{(j)} \zeta_i + \frac{1}{4}\zeta_0}$, and $\Phi(\cdot)$ is the cumulative distribution function (CDF) of the standard normal distribution.

Table 2.1: Model-I: error patterns and their probabilities for ISI length $I = 2$.

Index	ISI		Variance		Probability of each error pattern	
j	a_{k-2}	a_{k-1}	σ_{0j}^2	σ_{1j}^2	P_{er0j} (a_k=0, $\hat{a}_k$=1)	P_{er1j} (a_k=1, $\hat{a}_k$=0)
1	0	0	0	$\frac{5\zeta_0}{4}$	0	$(1-P_{\text{tx}})^2 \cdot \Phi(\frac{\vartheta}{\sigma_{11}})$
2	0	1	$\zeta_1 + \frac{\eta_0}{4}$	$\zeta_1 + \frac{5\zeta_0}{4}$	$P_{\text{tx}}(1-P_{\text{tx}}) \cdot \Phi(\frac{\vartheta}{\sigma_{02}})$	$P_{\text{tx}}(1-P_{\text{tx}}) \cdot \Phi(\frac{\vartheta}{\sigma_{12}})$
3	1	0	$\zeta_2 + \frac{\eta_0}{4}$	$\zeta_2 + \frac{5\zeta_0}{4}$	$P_{\text{tx}}(1-P_{\text{tx}}) \cdot \Phi(\frac{\vartheta}{\sigma_{03}})$	$P_{\text{tx}}(1-P_{\text{tx}}) \cdot \Phi(\frac{\vartheta}{\sigma_{13}})$
4	1	1	$\sum_{i=1}^{2} \zeta_i + \frac{\eta_0}{4}$	$\sum_{i=1}^{2} \zeta_i + \frac{5\zeta_0}{4}$	$P_{\text{tx}}^{\ 2} \cdot \Phi(\frac{\vartheta}{\sigma_{04}})$	$P_{\text{tx}}^{\ 2} \cdot \Phi(\frac{\vartheta}{\sigma_{14}})$

(2) a_k=1, but $\hat{a}_k$=0

With $a_k = 1$ and $\hat{N}_0 > 0$, to obtain the condition $L \geq 0$ in (2.17), it is required that:

$$\varpi \leq 0. \tag{2.25}$$

Given (2.22), the probability for the error pattern 'j' can be obtained as:

$$\begin{aligned} P_{\text{er1}j} &= P_{\text{tx}}^{\varrho_j}(1-P_{\text{tx}})^{I-\varrho_j} \int_{-\infty}^{0} \frac{1}{\sqrt{2\pi}} \frac{1}{\sigma_{0j}} \exp\Big(- \frac{\Big(\varpi - (-\vartheta)\Big)^2}{2\sigma_{0j}^2} \Big) d\varpi \\ &= P_{\text{tx}}^{\varrho_j}(1-P_{\text{tx}})^{I-\varrho_j} \Phi\Big(\frac{\vartheta}{\sigma_{1j}}\Big), \end{aligned} \tag{2.26}$$

where $\sigma_{1j} = \sqrt{2 \sum_{i=1}^{I} a_{k-i}^{(j)} \zeta_i + \frac{5}{4}\zeta_0}$.

(3) Bit Error Rate

The BER can be derived as:

$$\begin{aligned} P_{\text{er}} &= (1-P_{\text{tx}})P_{\text{er0}} + P_{\text{tx}}P_{\text{er1}} \\ &= (1-P_{\text{tx}}) \sum_{j=1}^{2^I} P_{\text{er0}j} + P_{\text{tx}} \sum_{j=1}^{2^I} P_{\text{er1}j}. \end{aligned} \tag{2.27}$$

Table 2.1 is an example showing the probability of each error pattern for $I = 2$.

2.3.2 Capacity analysis

The binary input vector of the system is denoted as $\mathbf{X} = \{X_1, X_2, ..., X_k\}$, and the corresponding binary output vector is denoted as $\mathbf{Y} = \{Y_1, Y_2, ..., Y_k\}$. Thus, the capacity for the memory channel can be calculated by[64, 89]:

$$\text{Capacity} = \lim_{k\to\infty} \max_{P_{\text{tx}}} \sum_{i=1}^{k} \frac{1}{k} \mathcal{I}(X_i; Y_i), \tag{2.28}$$

where $\mathcal{I}(X_i; Y_i)$ is the mutual information defined as [64]:

$$\begin{aligned} \mathcal{I}(X_i; Y_i) &= H(Y_i) - H(Y_i|X_i) \\ &= \mathcal{H}\Big((1 - P_{\text{tx}})(1 - P_{\text{er0}}) + P_{\text{tx}} P_{\text{er1}}\Big) \\ &\quad - P_{\text{tx}} \mathcal{H}(1 - P_{\text{er1}}) - (1 - P_{\text{tx}}) \mathcal{H}(1 - P_{\text{er0}}), \end{aligned} \tag{2.29}$$

where $H(\cdot)$ is named as the *Shannon entropy* representing the averaged information contained in each message, and $\mathcal{H}(\xi) = -\xi \log_2 \xi - (1-\xi) \log_2 (1-\xi)$. If the channel is a memory unlimited channel with an infinite ISI length I, the capacity can be calculated by substituting (2.24), (2.26), (2.27) and (2.29) into (2.28).

For a Memory Limited Channel (MLC) with finite ISI length I, after the i^{th} symbol ($i > I + 1$), the newly emitted molecular signal will be affected by the same amount (equal to I) of previous signals. Referring to (2.24) through (2.27), it can be deduced that the average error probability stays constant after the i^{th} symbol ($i > I + 1$). Thus, with P_{tx} fixed and values of P_{er0} and P_{er1} being constant, it can be proven from (2.29) that:

$$\mathcal{I}(X_i; Y_i) = \mathcal{I}(X_{I+1}; Y_{I+1}), \forall i \in \{I + 1, I + 2, ..., k\}. \tag{2.30}$$

Thus, for the MLC, the capacity calculation can be simplified as:

$$\begin{aligned}
\text{Capacity} &= \lim_{k\to\infty} \max_{P_{\text{tx}}} \{ \sum_{i=1}^{k} \frac{1}{k} \mathcal{I}(X_i; Y_i) \} \\
&= \lim_{k\to\infty} \max_{P_{\text{tx}}} \left\{ \sum_{i=1}^{I} \frac{1}{k} \mathcal{I}(X_i; Y_i) + \sum_{j=I+1}^{k} \frac{1}{k} \mathcal{I}(X_j; Y_j) \right\} \\
&= \lim_{k\to\infty} \max_{P_{\text{tx}}} \left\{ \sum_{i=1}^{I} \frac{1}{k} \mathcal{I}(X_i; Y_i) \right\} + \lim_{k\to\infty} \max_{P_{\text{tx}}} \left\{ \frac{k-I}{k} \mathcal{I}(X_{I+1}; Y_{I+1}) \right\} \\
&= 0 + \max_{P_{\text{tx}}} \{ \mathcal{I}(X_{I+1}; Y_{I+1}) \} \\
&= \max_{P_{\text{tx}}} \{ \mathcal{I}(X_{I+1}; Y_{I+1}) \} . \qquad (2.31)
\end{aligned}$$

By substituting (2.24), (2.26), (2.27) and (2.29) into (2.31), the capacity for MLC can be obtained.

2.3.3 A refined design of the decision variable

The BER of the MC system can be further reduced by applying a new decision variable given as:

$$L = N^I - \sum_{i=1}^{I} a_{k-i} N_i - \frac{\eta_0}{2}, \qquad (2.32)$$

where N^I, N_i, and eta_0 are respectively given in (2.8) to (2.10). Thus, L can be re-written as:

$$L = \sum_{i=0}^{I} a_{k-i} N_i - \sum_{i=1}^{I} a_{k-i} N_i - \frac{\eta_0}{2} = a_k N_0 - \frac{\eta_0}{2}, \qquad (2.33)$$

where $N_0$is given in (2.8). If $L < 0$, symbol '0' is determined; otherwise, symbol '1' is determined. Similar to the derivation in Section 2.3.1, the MC system BER can be derived as:

$$P_{\text{er}} = (1-P_{\text{tx}})P_{\text{er0}} + P_{\text{tx}}P_{\text{er1}} = (1-P_{\text{tx}})\sum_{j=1}^{2^I} P_{\text{er0}j} + P_{\text{tx}}\sum_{j=1}^{2^I} P_{\text{er1}j}$$
$$= (1-P_{\text{tx}})\sum_{j=1}^{2^I} P_{\text{tx}}^{\varrho_j}(1-P_{\text{tx}})^{I-\varrho_j}\Phi\Big(\frac{\vartheta}{\sigma_{0j}}\Big) +$$
$$P_{\text{tx}}\sum_{j=1}^{2^I} P_{\text{tx}}^{\varrho_j}(1-P_{\text{tx}})^{I-\varrho_j}\Phi\Big(\frac{\vartheta}{\sigma_{1j}}\Big) \tag{2.34}$$

where ϱ_j represents the number of '1's within the previous bits $\{a_{k-i}^{(j)}, i = 1, 2, ..., I\}$ for error pattern 'j', $\sigma_{0j} = \sqrt{2\sum_{i=1}^{I} a_{k-i}^{(j)}\zeta_i}$, $\sigma_{1j} = \sqrt{2\sum_{i=1}^{I} a_{k-i}^{(j)}\zeta_i + \zeta_0}$, and ζ_i is given in (2.9). Compared with the expression of the system BER shown in (2.24) and (2.26), it can be noticed that the values of σ_{0j} and σ_{1j} have been decreased, leading to a smaller error probability for each error pattern 'j'. Consequently, the overall system BER has been reduced.

2.4 Numeral results

In this section, numerical results for both theoretical derivations and simulations are presented. During simulations, the Tx emits molecules periodically, and these molecules spread out in the environment. The Rx can capture these molecules, count the number of absorbed molecules, and determine whether '1's or '0's are transmitted. The times of simulation trials are based on the theoretically derived results. For example, if the theoretical BER is 10^{-4}, then 10^8 successive bits are utilised to carry out the corresponding simulations, so that confidence level will be sufficiently large. All results are presented with a common set of parameters assigned in Table 2.2. These values agree with the research in [44, 45, 79].

It should be noticed that when the ISI length I increases, not only the computation of the BER and capacity increases exponentially, but also simulations will become more complex to be performed. Especially, if I is infinite, it is impossible

Table 2.2: Parameters assignment for the analysis of Model-I

1.	The capturing radium of the Rx	R_{ca}	$0.5\,\mu\text{m}$
2.	The distance between Tx and Rx	d	$1 \sim 3\mu\text{m}$
3.	The diffusion coefficient	D	$10^{-3}\mu\text{m}^2\,\mu\text{s}^{-1}$
4.	The pulse period	T_{pd}	$5000\,\mu\text{s}$
5.	The number of transmitted molecules	m	$10^3 \sim 10^4$

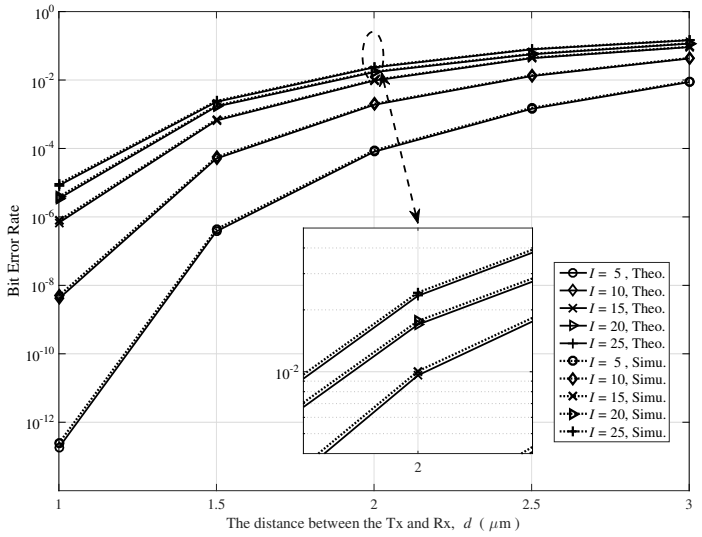

Figure 2.3: BER vs. distances for different I with $m = 5 \times 10^3$.

to obtain the required results. Thus, the channel considered herein is an MLC with a finite I. The value of I used in this chapter has been greatly increased compared with all existing literatures, and we believe it is sufficiently large for the MC system analysis. If further results for larger I are required, readers could compute the BER and capacity based on (2.24) to (2.31).

2.4.1 Channel performance when $P_{\mathbf{tx}} = 0.5$

In Figs. 2.3 through 2.5, the probability of '1's transmitted is considered to be equal to the probability of '0's transmitted, that is, $P_{\text{tx}} = 0.5$. It will be shown later that the channel capacity is proven to be obtained when $P_{\text{tx}} = 0.5$.

Throughout Figs. 2.3 to 2.5, it can be seen that the diffusion-based MC

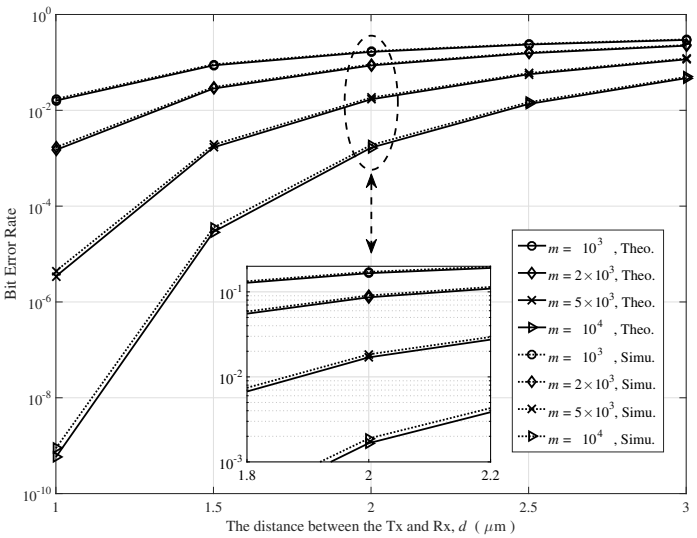

Figure 2.4: BER vs. distances for different m with $I = 20$.

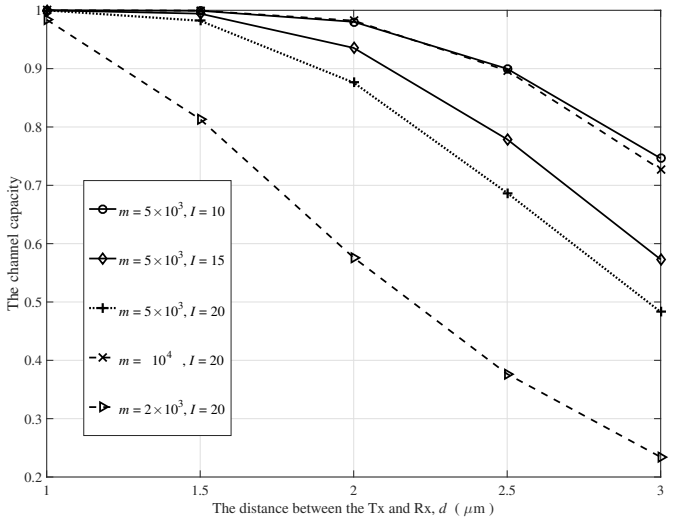

Figure 2.5: Channel capacity vs. distances for different m and I.

system enables the message exchanges among these two nano-machines. The system performance is mainly influenced by three parameters, i.e. the distance d, the ISI length I, and the number of molecules emitted per pulse m.

To be specific, when the Tx is far away from the Rx, the system tends to suffer

from more errors (illustrated by Figs. 2.3 and 2.4) and lower reliable transmission rate (illustrated in the Fig. 2.5). There are two reasons for this phenomenon. Firstly, referring to (2.5), with an increasing d, the capture probability $P_{\mathrm{ca}}(d,t)$ will reduce significantly, leading to fewer molecules reaching the Rx. In this case, the MC system has less resistance to the randomness of the molecular propagation. Considering the decision variables of the Rx represented in (2.11) to (2.13), the difference between l_1 and l_0 becomes smaller. Hence, a slight change in the number of absorbed molecules may lead to a completely different decoding of message symbols. Thus, there tend to be more errors.

Secondly, when d increases with other parameters staying constant, the MC system will suffer more from the impact of the channel memory. As is clearly shown in the Fig. 2.2, when Rx becomes farther away from the Tx, a higher ISI will be resulted because of the reduction of the capture probability. Correspondingly, more molecules will be spreading out in the environment after one pulse period. Some of these diffusing molecules may arrive at the Rx in later time slots, which results in a severe ISI. Therefore, the MC system will have a higher BER and lower channel capacity due to the enlarging distance, d.

Another factor that affects the system BER and capacity is the ISI length I. Even though the influence of the ISI has been mitigated by using the MSE decoding algorithm, it can be deduced that the larger the ISI length I is, the more channel memory will be considered, and correspondingly, the more random the propagation procedure will be. If the ISI can be further alleviated, a smaller BER and higher capacity will be obtained, which shows agreement to the results in the Fig. 2.3 and Fig. 2.5.

Moreover, as can also be seen in the Fig. 2.3, the difference in performance between $I = 20$ and $I = 25$ is quite tiny. Thus, considering the fact that with I rising, the complexity of both the computation of BER and capacity and MATLAB simulations increases exponentially, $I = 20$ is sufficiently large for the system

Table 2.3: The comparison between theoretical and simulated BER with $m = 5\times10^3$, and I=20

Distance d (µm)	Simulated BER	Theoretical BER	The difference
1	7.8136×10^{-5}	6.7656×10^{-5}	1.04801×10^{-5}
1.5	0.02424	0.02290	0.00133
2	0.14672	0.14249	0.00422
2.5	0.29866	0.29321	0.00546
3	0.40424	0.39870	0.00554

performance analysis.

The system performance can also be influenced by the number of molecules emitted per pulse, m. When the Tx encodes message bits with more molecules, the approximation process from (2.7) to (2.8) will be more accurate, and the difference between the real number of captured molecules (N_i) and the estimated number of captured molecules ($\hat{N}_i$) can be statistically reduced. Thus, the channel performance can be improved by releasing more molecules. However, as is also shown in Figs. 2.4 and 2.5, such an enhancement may become less distinct if m has been sufficiently large. Under this circumstance, the impact of m is not as significant as other parameters.

An additional noticeable feature in Figs. 2.3 and 2.4 is that the simulated BER is slightly higher than the theoretical BER even if the deviation is almost negligible. The main reason of the difference herein is that the assumption that "previously decoded bits will not affect the decoding procedure of the current bit", does not hold during simulations. In other words, when decoding the bit a_k, for theoretical derivations, it is assumed that $\hat{a}_{k-i} = a_{k-i}$ for $i = 1, 2, ..., I$; while for simulations, one wrongly decoded bit will affect the decoding of next several symbols. Errors may therefore occur in succession, which is called the *error burst* or *error propagation*. Thus, the existence of the error burst leads to a higher BER for simulations. An example of the BER differences between the simulation and analysis is shown in Table 2.3.

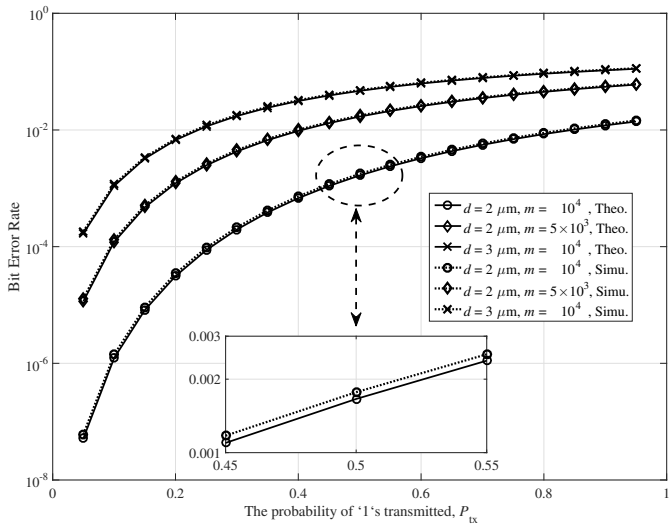

Figure 2.6: BER vs. P_{tx} for different m and d with $I = 20$.

2.4.2 Channel performance with different P_{tx}

In this section, the system performance is evaluated with P_{tx} varied from 0.05 to 0.95. Similar to Section 2.4.1, the channel reliability is measured by the BER, whose values are shown in the Fig. 2.6. In the Fig. 2.7, the corresponding mutual information is also calculated so that the channel capacity can be determined, which is a measurement of the maximum reliable transmission rate of the MC system.

Given (2.24), (2.26), and (2.27), it can be obtained that a lower BER can be achieved by deceasing the probability of symbol '1' transmitted (P_{tx}), which agrees with the results in the Fig. 2.6. If under certain circumstances, the probability of sending symbol '1' (or '0') can be adjusted, it will be beneficial to select a smaller P_{tx} to have less errors. However, as is also shown in the Fig. 2.6, the mutual information, calculated by (2.29), gets its peak value with $P_{\text{tx}} = 0.5$, which means the maximum reliable transmission rate is correspondingly achieved. In this situation, when P_{tx} satisfies the condition of maximising the mutual information, the system will have to suffer from more errors. Thus, when adapting the transmission probability, both the BER and mutual information needs to be considered.

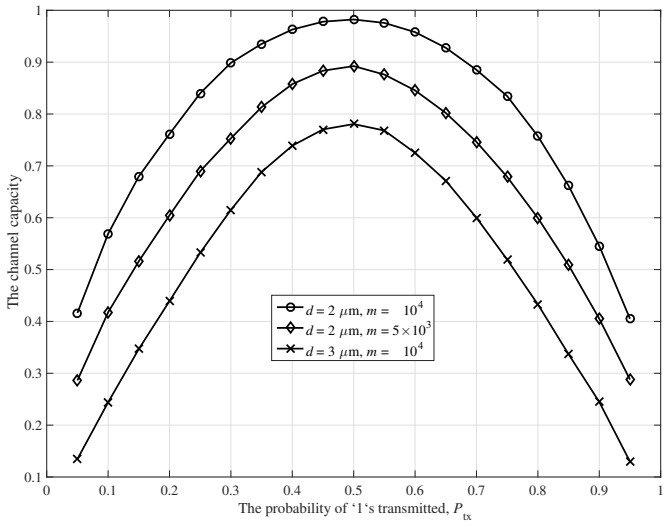

Figure 2.7: Channel capacity vs. P_{tx} for different m and d with $I = 20$.

2.5 Conclusions

In this chapter, an MC system model, namely Model-I, has been introduced, as well as relevant parameters. The Tx encodes information symbol sequences into molecules and releases them periodically. These molecules are regarded to diffuse independently, and when arrived at the Rx, they will be absorbed and removed from the environment. When dealing with the propagation procedure, attention is paid to analyse the motion of every single molecule. Whether or not a specific molecule will reach the Rx is random, the probability (known as the capture probability) of which can be derived by assuming that this molecule moves without being affected by other molecules around. With the capture probability obtained, the molecular propagation can be addressed accordingly. The Rx is designed to be capable of counting the number of captured molecules. The decoding method utilised in the system model is to calculate the Mean Square Error (MSE). In this way, the impact of ISI can be alleviated as remaining molecules of previous symbols within the ISI length have been taken into consideration for decoding.

Chapter 3

An Algorithmic Distance Estimation Scheme Based on System Model-I

3.1 Introduction

In Chapter 2, a diffusion-based Molecular Communication (MC) system model, i.e. Model-I, is introduced. Information molecules are assumed to move independently, and can be captured by the Rx with specific probabilities. The Rx counts the number of obtained molecules, and decodes messages correspondingly. To evaluate the system reliability and achievable transmission rate, Bit Error Rate (BER) and channel capacity are calculated and their results are provided in Section 2.4. It can be noticed from Chapter 2 and other research like [44, 62, 90, 91] that the distance between the source nano-machine and target nano-machine is an essential parameter which has significant influence on the system performance. According to the pre-known distance, nano-machines can coordinate their functionality, such as the transmission rate and the number of molecules emitted per pulse. If the two nano-machines are close to each other, the source nano-machine can trans-

mit messages at a high rate and using less molecules per pulse without decreasing the channel reliability. However, if the distance between these two nano-machines becomes large, either an excessive transmission rate or an insufficient molecules utilisation will cause the system to suffer from more errors. With a prior knowledge of the distance, the source nano-machine can adjust the transmission rate and number of molecules utilised to achieve the optimal system performance. Furthermore, in application areas like drug-delivery systems [92], it is strongly required to know the current locations of both the nano-machine-bound drug and its destination, which can be realised by estimating the distances to certain pre-deployed beacons [93].

Research has been carried out to investigate the distance estimation techniques. Taking advantage of feedback protocols, four distance estimation schemes were introduced in [94, 95, 96]. Another two estimation schemes can be found in [97], in which nano-machines were designed to determine the distance by measuring either the peak concentration or the time interval between the first and second peak. However, all of these aforementioned studies were based on the system model with information conveyed by molecular concentrations. For system model with information expressed by the number of received molecules, the distance measurement method still remains blank. Moreover, these schemes suffers from a low accuracy but a high time cost. There is a clear and timely requirement for the continued development of distance estimation schemes that are shown to be accurate and fast, and proven to work in 3D scenarios.

In this chapter, an algorithmic scheme is proposed to estimate the distance between two nano-machines for MC system Model-I. The Rx computes the distance based on the amount of received molecules. Compared with previous estimation schemes, the accuracy is significantly improved, and this new scheme enjoys a high feasibility due to a low requirement on the complexity of the nano-machines. The mechanism and the computation are sufficiently simple to be implemented into nano-communication systems. Additionally, the performance of the scheme can be

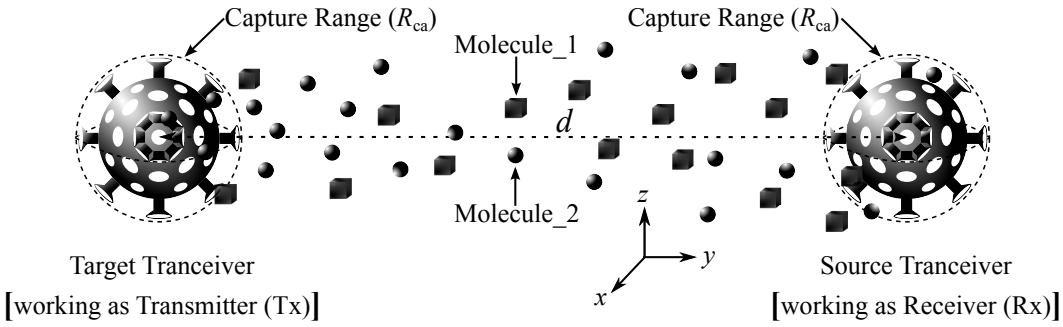

Figure 3.1: The structure of the MC system.

further enhanced by optimising two parameters, namely, the number of transmitted molecules (represented as m), and the diffusion coefficient (represented as D).

The remainder of this chapter is organised as follows. In Section 3.2, the system structure is introduced. The distance estimation scheme and two optimisation methods are explained in Section 3.3. Simulations and comparisons of results are provided in Section 3.4. Finally in Section 3.5, we conclude this chapter.

3.2 Diffusion-Based MC System Structure

The diffusion-based MC system is based on the system Model-I, where information is expressed by the number of captured molecules. The only difference is that the system considered herein consists of two transceiver nano-machines which can both emit and absorb message molecules. As is shown in the Fig. 3.1, the source nano-machine communicates to the target nano-machine by conveying information symbols with a certain kind of molecules (denoted as Molecule_1). However, before this communication is established, the distance between the source nano-machine and the target nano-machine should be measured so that the source nano-machine can accordingly select the optimal transmission rate and number of molecules per pulse.

The source nano-machine determines the distance by taking advantage of the molecules emitted by the target nano-machine, which is denoted as Molecule_2.

Herein, two kinds of molecules are utilised for the purpose that the distribution and reception of 'estimation' molecules (Molecule_2) can be treated to be free from the influence of 'message' molecules (Molecule_1). Thus, during the distance estimation process, the target nano-machine is considered as the Tx, and the source nano-machine is considered as the Rx. Since both the nano-machines are spheres, it can be deduced that molecules can be viewed as being released from the centre of nano-machines due to the symmetry. Referring to the Fig. 3.1, the distance between the Tx and Rx is d, and the capture range of nano-machines is R_{ca}.

To develop a distance estimation method for Model-I, it is assumed that the propagation procedure of Molecule_2 is the same as the system Model-I introduced in Chapter 2, but the counting function of the Rx is slightly different. The Rx is designed to count the captured molecules intermittently. The counting duration is denoted as t_2. The time interval between each counting process is denoted as $\triangle t$. The Tx and Rx may not be synchronised, and the delay between the Tx emission and Rx reception is denoted as t_1. Especially, when $t_1 = 0$, the system is synchronised. The Tx pulse period is T_{pd}. The time for the Rx to estimate the distance is denoted as T_{over}.

The capture probabilities within t_1 and within $t_1 + t_2$ are respectively represented as $P_{\mathrm{ca}}(d, t_1)$ and $P_{\mathrm{ca}}(d, t_1 + t_2)$. Thus, for the newly emitted molecules, the capture probability between t_1 and $t_1 + t_2$, denoted as $P_{0,t_1 \to t_1+t_2}(d, t_1, t_2)$, can be obtained as:

$$P_{0,t_1 \to t_1+t_2}(d, t_1, t_2) = P_{\mathrm{ca}}(d, t_1 + t_2) - P_{\mathrm{ca}}(d, t_1). \tag{3.1}$$

It is assumed that the existence time for newly emitted molecules is longer than the time for Rx to estimate the distance. This assumption is realistic, because for diffusion-based MC system, the channel memory is large. It is therefore denoted that $T_{\mathrm{over}} < (I + 1) \times T_{\mathrm{pd}}$, where I is the ISI length. Thus, for the previous i^{th} symbol ($i = 1, 2, ..., I - 1$), the capture probability between t_1 and $t_1 + t_2$ in each

symbol period can be obtained as:

$$P_{i,t_1\to t_1+t_2}(d,t_1,t_2) = P_{\mathrm{ca}}(d,t_1+t_2+iT_{\mathrm{pd}}) - P_{\mathrm{ca}}(d,t_1+iT_{\mathrm{pd}}). \tag{3.2}$$

where $i = 1, 2, ..., I-1$. Thus, the theoretical probability after the emission of j^{th} symbol ($0 \le j \le I$) is obtained as:

$$P^{(j)}_{t_1\to t_1+t_2} = \sum_{i=0}^{j-1} P_{i,t_1\to t_1+t_2}. \tag{3.3}$$

According to (2.8), among the newly emitted m molecules, the number of captured molecules can be expressed as a normal distribution. Hence, for the current symbol, the number of molecules captured within t_1 and within t_1+t_2 are respectively expressed as:

$$N_{0,t_1} \sim \mathcal{N}\Big(mP_{\mathrm{ca}}(d,t_1), mP_{\mathrm{ca}}(d,t_1)\big(1-P_{\mathrm{ca}}(d,t_1)\big)\Big). \tag{3.4}$$

$$N_{0,t_1+t_2} \sim \mathcal{N}\Big(mP_{\mathrm{ca}}(d,t_1+t_2), mP_{\mathrm{ca}}(d,t_1+t_2)\big(1-P_{\mathrm{ca}}(d,t_1+t_2)\big)\Big). \tag{3.5}$$

Thus, among the current m molecules, the number of captured molecules between time t_1 and t_1+t_2 can be obtained as:

$$\begin{aligned}
N_{0,t_1\to t_1+t_2} &= N_{0,t_1+t_2} - N_{0,t_1} \\
&\sim \mathcal{N}\Big(mP_{\mathrm{ca}}(d,t_1+t_2), mP_{\mathrm{ca}}(d,t_1+t_2)\big(1-P_{\mathrm{ca}}(d,t_1+t_2)\big)\Big) \\
&\quad - \mathcal{N}\Big(mP_{\mathrm{ca}}(d,t_1), mP_{\mathrm{ca}}(d,t_1)\big(1-P_{\mathrm{ca}}(d,t_1)\big)\Big) \\
&= \mathcal{N}\Big(mP_{\mathrm{ca}}(d,t_1+t_2) - mP_{\mathrm{ca}}(d,t_1), \\
&\qquad mP_{\mathrm{ca}}(d,t_1+t_2)\big(1-P_{\mathrm{ca}}(d,t_1+t_2)\big) + mP_{\mathrm{ca}}(d,t_1)\big(1-P_{\mathrm{ca}}(d,t_1)\big)\Big).
\end{aligned} \tag{3.6}$$

Similarly, for the previous i^{th} symbol ($i = 1, 2, ..., I-1$), the number of captured

molecules between t_1 and $t_1 + t_2$ in each symbol period can be obtained as:

$$\begin{aligned} N_{i,t_1\to t_1+t_2} &= N_{i,t_1+t_2} - N_{i,t_1} \\ &\sim \mathcal{N}\Big(mP_{\mathrm{ca}}(d, t_1 + t_2 + iT_{\mathrm{pd}}) - mP_{\mathrm{ca}}(d, t_1 + iT_{\mathrm{pd}}), \\ &\qquad mP_{\mathrm{ca}}(d, t_1 + t_2 + iT_{\mathrm{pd}})\Big(1 - P_{\mathrm{ca}}(d, t_1 + t_2 + iT_{\mathrm{pd}})\Big) \\ &\qquad + mP_{\mathrm{ca}}(d, t_1 + iT_{\mathrm{pd}})\Big(1 - P_{\mathrm{ca}}(d, t_1 + iT_{\mathrm{pd}})\Big)\Big). \end{aligned} \tag{3.7}$$

Thus, the overall number of molecules captured between t_1 and $t_1 + t_2$ after the emission of j^{th} symbol is obtained as:

$$N^{(j)}_{t_1\to t_1+t_2} = \sum_{i=0}^{j-1} N_{i,t_1\to t_1+t_2}, \tag{3.8}$$

where $0 \leq j \leq \lfloor \frac{T_{\mathrm{over}}}{T_{\mathrm{pd}}} \rfloor$, and $\lfloor \xi \rfloor$ represents the biggest integer not larger than ξ.

3.3 Distance estimation scheme

Referring to (2.5) and (3.1) through (3.3), it is obvious that for each value of j, the probability $P^{(j)}_{t_1\to t_1+t_2}$ is highly dependent on the distance d. Thus, the distance can be derived by estimating $P^{(j)}_{t_1\to t_1+t_2}$. With the pre-knowledge of the number of molecules per pulse (m), the estimated capture probability after the emission of j^{th} symbol ($0 \leq j \leq I$) can be expressed as:

$$\hat{P}^{(j)}_{t_1\to t_1+t_2} = \frac{N^{(j)}_{t_1\to t_1+t_2}}{m}. \tag{3.9}$$

By comparing the theoretical and estimated values of the capture probability, respectively given by (3.3) and (3.9), the distance can be determined. The obtained solutions for the distance may not be unique for one trial, which requires iterations to narrow down the range of potential values until a unique value is obtained or T_{over} is reached.

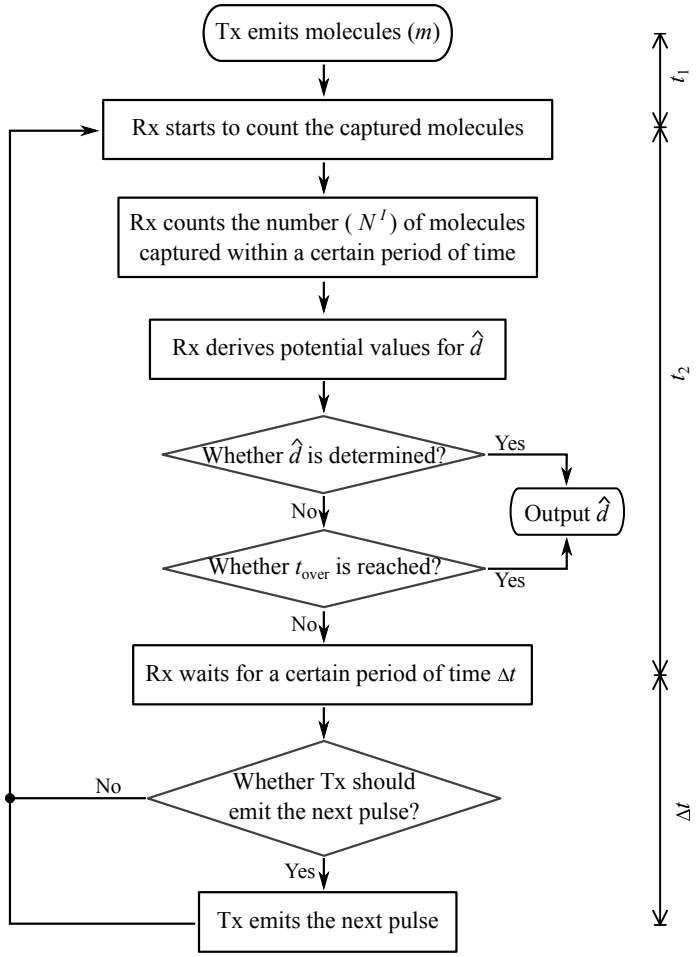

Figure 3.2: The flow chart illustrating the estimation scheme.

3.3.1 The Distance Estimation Scheme in Unsynchronised Conditions

If the system has not been synchronised, the Rx may start the estimation process at any time after the Tx releases molecules, which means the values of t_1 obey the uniform distribution from 0 to T_{pd}. Thus, when solving (3.1) to obtain the estimated distance $\hat{d}$, the value of $\hat{t}_1$ must be determined as well. With pre-designed R_{ca}, D, and t_2, the solution pairs of $\hat{d}$ and $\hat{t}_1$ may not be unique for some certain values of $\hat{P}^{(j)}_{t_1 \to t_1+t_2}$. The set of estimated distance values is represented as $\hat{\mathbf{d}}$. Especially, when $\hat{P}^{(j)}_{t_1 \to t_1+t_2}$ gets smaller, it is hard for the Rx to tell whether the small value

of $\hat{P}^{(j)}_{t_1 \to t_1+t_2}$ is due to a large distance or the unsynchronisation, leading to more potential solutions.

To solve this problem, the scheme illustrated in the Fig. 3.2 is proposed. By periodically counting the number of captured molecules, the Rx can narrow down the range of $\hat{\mathbf{d}}$. After several iterations, the Rx makes a final decision on the estimated distance. If $\hat{\mathbf{d}}$ is not unique when T_{over} is reached, the distance is estimated as the median value of $\hat{\mathbf{d}}$. Thus, the estimation bias between the real distance and estimated distance can be obtained as:

$$\text{Dev} = \hat{d} - d, \tag{3.10}$$

where $\hat{d} = \text{median}(\hat{\mathbf{d}})$.

In the unsynchronised scenario, the values of t_1 obey the uniform distribution between 0 and T_{pd}. For a fixed distance d, the estimation bias obtained from (3.10) varies according to the random value of t_1. In this chapter, it is considered that there are Q values for t_1 ranging from 0 to T_{pd}. Thus, the average bias for a certain distance should be obtained by averaging the corresponding Dev_q for all values of t_1, that is:

$$\text{Dev}_d = \frac{1}{Q} \sum_{q=1}^{Q} \text{Dev}_q. \tag{3.11}$$

3.3.2 The Distance Estimation Scheme in Synchronised Conditions

For the synchronised MC system, it is pre-known that $t_1 = 0$. Thus, (3.1) can be rewritten as:

$$\begin{aligned} P_{\text{sy}}(d, t_2) &= P_{0 \to t_2}(d, 0, t_2) = P_{\text{ca}}(d, t_2) - P_{\text{ca}}(d, 0) \\ &= P_{\text{ca}}(d, t_2) = \frac{R_{\text{ca}}}{d} \text{erfc}\left\{ \frac{d - R_{\text{ca}}}{\sqrt{4Dt_2}} \right\}. \end{aligned} \tag{3.12}$$

In (3.12), when parameters D, R_{ca} and t_2 have been pre-designed, they can

be regarded as constants. Thus the derivative of (3.12) with respect to d is:

$$\begin{aligned} P'_{\text{sy}} =& \Big(P_{\text{ca}}(d,t_2)\Big)' = \left(\frac{R_{\text{ca}}}{d}\text{erfc}\left\{\frac{d-R_{\text{ca}}}{\sqrt{4Dt_2}}\right\}\right)' \\ =& -\frac{R_{\text{ca}}}{d^2}\text{erfc}\left\{\frac{d-R_{\text{ca}}}{\sqrt{4Dt_2}}\right\} - \frac{R_{\text{ca}}}{d}\frac{1}{\sqrt{4\pi Dt_2}}\exp\left(-\frac{(d-R_{\text{ca}})^2}{4Dt_2}\right). \end{aligned} \tag{3.13}$$

In (3.13), with $d > R_{\text{ca}} > 0$, $D > 0$, and $t_2 > 0$, it is clear that $P'_{\text{sy}} < 0$, which means $P_{\text{sy}}(d,t_2)$ is a strictly decreasing function with regards to d. Thus, for a given $P_{\text{sy}}(d,t_2)$, using (3.9) and (3.12), $\hat{d}$ can be determined. Similarly, the estimation bias also exists for this scheme, which is defined by (3.10).

Due to the perfect synchronisation, this scheme enjoys a desirable performance with regards to the bias. However, such an assumption might be premature at present as the synchronisation techniques presented in the literature like [28, 98, 99] so far are still in their early stages with their implementation still an open challenge for researchers. Nevertheless, this assumption will still be tested anticipating further advances in these areas.

3.3.3 Parameter Optimisation Methods

The first method is to convey messages into molecules with a larger diffusion coefficient, D. According to (2.5) and (3.1), the relationship between $P_{0,t_1\to t_1+t_2}(d,t_1,t_2)$ and D can be plotted as the Fig. 3.3. It can be noticed that the larger D is, the sharper the curve will be. This feature will bring two benefits. Firstly, a sharper curve means a higher gradient, leading to a higher distinctiveness for the Rx to narrow down the range of possible values of $\hat{\mathbf{d}}$. Secondly, a sharper curve results in a smaller tail, which means the Rx will suffer less from ISI. Thus, using molecules with a larger diffusion coefficient will improve the performance. However, the increase of D may have a higher requirement on the complexity of the Rx to capture the molecules, and this also needs to be taken into consideration when implementing the distance estimation scheme.

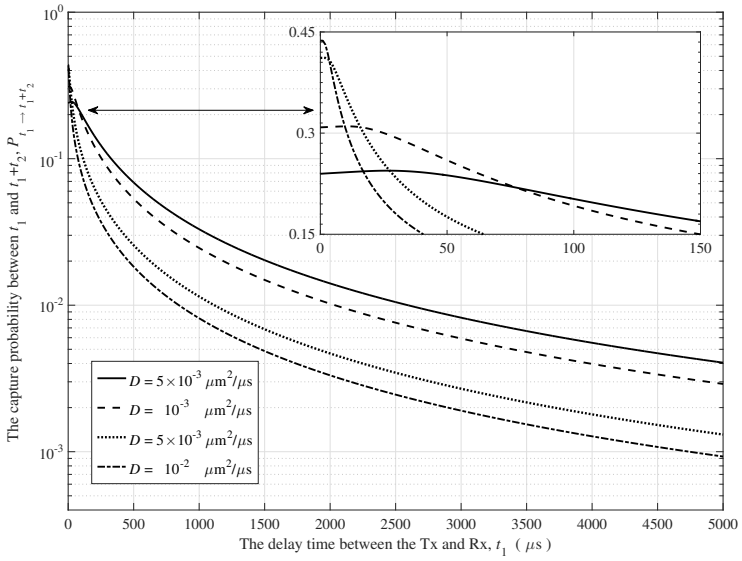

Figure 3.3: $P_{0,t_1 \to t_1+t_2}$ within $t_2 = 500\,\mu\text{s}$ at $d = 1\,\mu\text{m}$.

Alternatively in the section method, the Tx can increase the number of molecules emitted in a single pulse, m. With more molecules emitted, according to (3.9), $\hat{P}^{(j)}_{t_1 \to t_1+t_2}$ can be more accurately estimated, leading to a decrease in the estimation bias. However, increasing m will also result in a higher energy consumption of the system due to two reasons. Firstly, when more molecules are used to decrease the bias, more energy will be needed for the Tx to generate and release these molecules. Secondly, the increase in the number of molecules requires the Rx to have a larger buffer to count and restore the number of captured molecules, which also costs more energy. Such a high energy consumption may exceed the capability of nano-communication systems.

3.4 Numeral results

The main aim is to implement the proposed algorithmic distance estimation scheme in a diffusion-based MC system, and to evaluate the performance of this scheme and the two optimisation methods. Two features are considered as the performance

Table 3.1: Parameters for simulating the distance estimation scheme for Model-I

1.	The capturing radium of nano-machines	R_{ca}	$0.5\,\mu\text{m}$
2.	Distance between Tx and Rx	d	$1 \sim 3\ \mu\text{m}$
3.	Diffusion coefficient	D	$5 \times 10^{-4} \sim 10^{-2}\ \mu\text{m}^2\,\mu\text{s}^{-1}$
4.	Pulse period	T_{pd}	$5000\,\mu\text{s}$
5.	Number of transmitted molecules	m	$10^3 \sim 10^4$
6.	Time for Rx capturing molecules	t_2	$500\,\mu\text{s}$
7.	Time interval between each estimation action	Δt	$750\,\mu\text{s}$
8.	Overall time to measure the distance	T_{over}	$5 \times 10^4 \mu\text{s}$

metrics, namely, the estimation accuracy and the time consumption. The accuracy is measured by calculating the estimation bias using (3.10) and (3.11), and the time consumption is to record the time for the Rx to determine the distance. Simulations are carried out on MATLAB with values of parameters assigned in Table 3.1. All results are obtained after 10^5 trials.

3.4.1 Distance Estimation Scheme in Unsynchronised Condition

In this section, the proposed distance estimation scheme is implemented onto an unsynchronised MC system. Results throughout Figs. 3.4 to 3.7 illustrate that this scheme works well under the unsynchronised circumstances. The performance, with regards to both the accuracy and the time consumption, is mainly affected by four parameters, i.e. the distance between these two nano-machines (d), the ISI length (I), the number of molecules emitted per pulse (m), and the diffusion coefficient (D). The change of these parameters will influence the number of molecules within the estimation duration t_2, leading to the difference in both the estimation bias and the time cost.

To be specific, in the Fig. 3.4 through 3.7, it is shown that when the Rx gets farther away from the Tx, the estimation will become less accurate and cost more time. The capture probability within the estimation duration, $P_{0,t_1 \to t_1+t_2}$, goes down with an increasing distance d, which results in less molecules being captured. On one hand, as is explained in Section 3.3.1, the reduction of the captured molecules

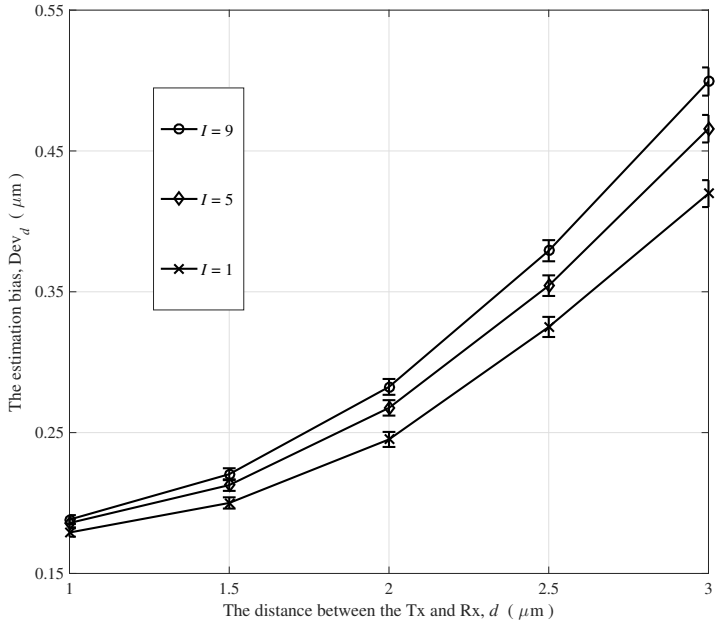

Figure 3.4: Unsynchronised, Dev_d vs d for different I with $m = 5 \times 10^3$ and $D = 5 \times 10^{-3}\mu\text{m}^2\,\mu\text{s}^{-1}$.

leads to a less resistance to the randomness of the propagation, making it harder for the Rx to narrow down the range of possible values for $\hat{\mathbf{d}}$. Correspondingly, the Rx needs more iterations to repeat the estimation procedure, and the final decision is less accurate. On the other hand, less molecules captured within the estimation duration means that more molecules remain in the environment. In this case, the system will have a larger channel memory, which causes the performance being worse.

Another factor that influences the estimation procedure is the ISI length I. As is shown in Figs. 3.4 and 3.7, both the estimation bias and the time consumption increase with an enlarging I, even though the influence of the ISI has been mitigated by considering all previous emitted molecules in equations (3.7) to (3.9). The more the ISI length is, the more molecules will remain in the channel. As a consequence, the molecular propagation will be of higher randomness, and the estimation will

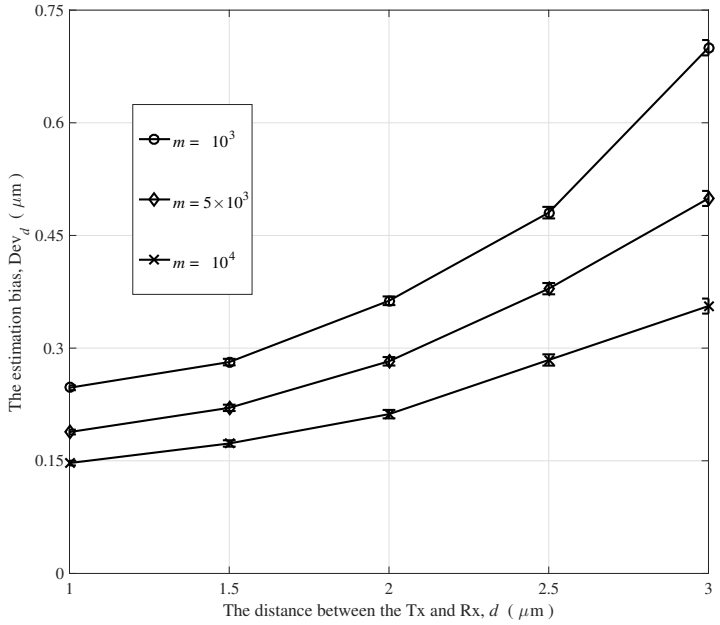

Figure 3.5: Unsynchronised, Dev_d vs d for different m with $I = 9$ and $D = 5 \times 10^{-3}\mu\mathrm{m}^2\,\mu\mathrm{s}^{-1}$.

become less accurate and cost more time. The maximum value of the ISI length considered herein is $I = 9$ because the overall time for estimation is $T_{\mathrm{over}} = 5\times10^4\mu\mathrm{s}$. Under this situation, the maximum interfering time of the molecules emitted in the first period is $9 \times T_{\mathrm{pd}}$.

Figs. 3.5 to 3.7 show the performance enhancement using optimisation methods by changing the two parameters m and D. The accuracy has been improved significantly with less time consumption by either emitting more molecules or using molecules with greater diffusion coefficient D. However, this improvement is not infinite. When m (or D) is sufficiently large, keeping increasing m (or D) will not bring in further benefit., which shows agreement with results in these three figures. Moreover, the drawbacks of these two optimisation methods are intuitive. Increasing m requires Tx to consume more energy for generating and sending out the extra molecules, and requires Rx to have a larger buffer to count the captured molecules.

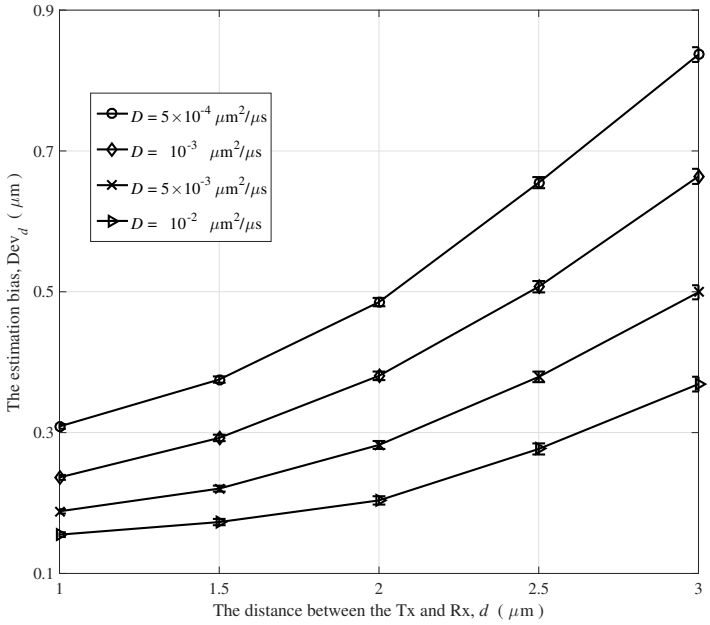

Figure 3.6: Unsynchronised, Dev_d vs d for different D with $I = 9$ and $m = 5 \times 10^3$.

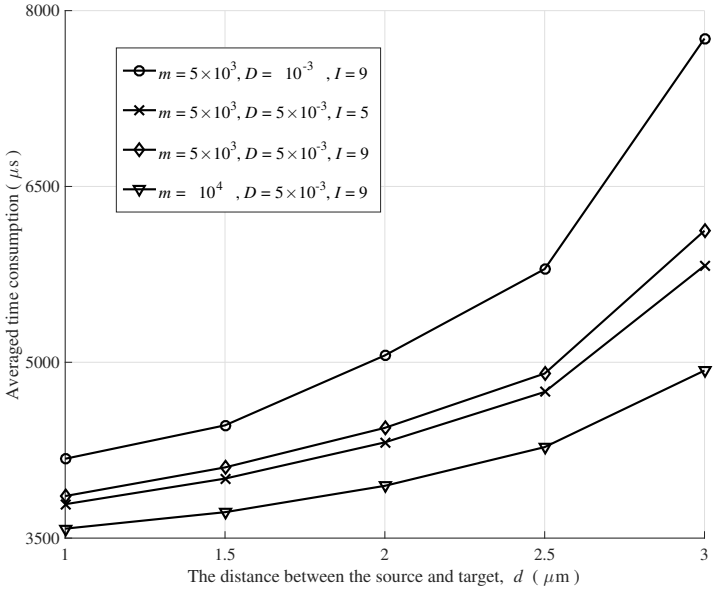

Figure 3.7: Unsynchronised, Time consumption vs d for different I, m and D.

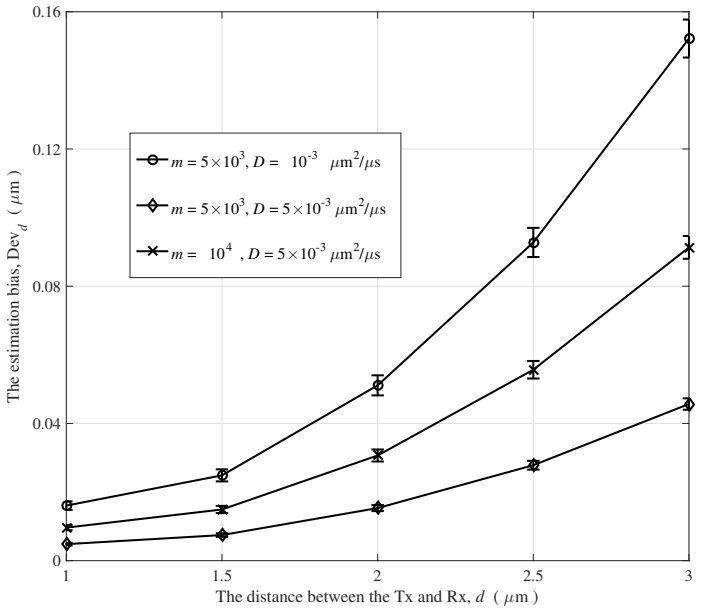

Figure 3.8: Synchronised, Dev_d vs d for different m and D.

Enlarging D means molecules can diffuse faster, which leads to a higher requirement of the Rx to capture these molecules. Therefore, when implementing the distance estimation schemes, not only the accuracy and time consumption should be taken into account, but the energy budget and nano-machine complexity are also required to be considered.

3.4.2 Distance Estimation Scheme in Synchronised Condition

In this section, results for a synchronised MC system are presented. From Figs. 3.8 and 3.9, it can be seen that by using the proposed distance estimation algorithm in the synchronised condition, both the estimation bias and the time consumption are desirable. Even when the distance is large (around 3 µm), the estimation is still quite accurate ($\text{Dev}_d \approx 0.15$ µm) and fast (time consumption $\approx 1\ T_{\text{pd}}$). Furthermore, as is also shown herein, both the parameter optimisation methods, i.e. increasing m and D, can provide great benefit on the estimation performance.

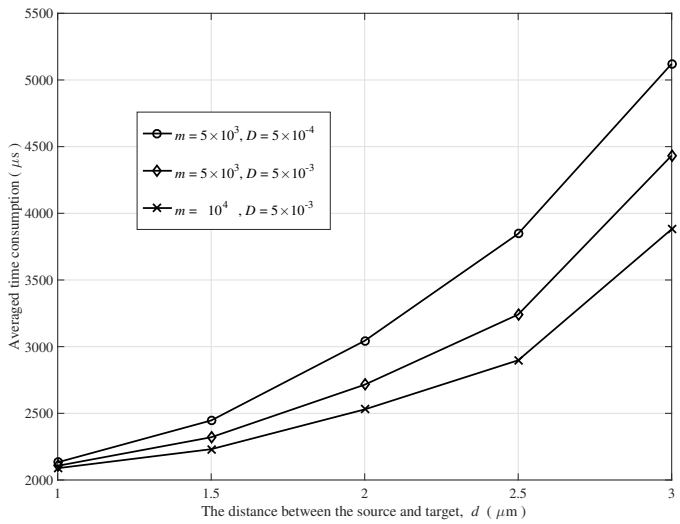

Figure 3.9: Synchronised, time consumption vs d for different m and D.

3.5 Conclusions

In this chapter, based on the MC system Model-I, an algorithmic distance estimation scheme and two optimisation methods have been proposed for both the unsynchronised and synchronised conditions. The estimation bias, Dev_d, and the time consumption are analysed as the measurement to evaluate the performance. It is shown in the simulations that the proposed scheme can provide accurate estimation results, and the time consumption is reasonably low. As to the two optimisation methods, the implementation of these methods will greatly improve the performance even though they have their own drawbacks. Emitting more message molecules means more energy consumption and requires the Rx to have a larger buffer, and enlarging the diffusion coefficient leads to a higher complexity of the Rx. Besides, when the amount of used molecules and the value of the diffusion coefficient are sufficiently large, increasing these two parameters will bring no further benefit. Thus, when designing a communication system, the selection on the optimisation methods should be made according to the specific requirement of the accuracy, time consumption, energy budget and the complexity of the entire system.

Chapter 4

Communication Protocols: SW-ARQ schemes in MC systems

4.1 Introduction

In Chapter 2, based on the movement of individual molecules, the propagation procedure is introduced for a diffusive Molecular Communication (MC) system. Based on this propagation procedure, the MC system Model-I is established with information expressed by the number of captured molecules. The system performance is analysed with regards to the Bit Error Rate (BER) and channel capacity. Alternatively, there is another way to build a diffusive MC system with the same propagation mechanism where a message sequence, containing several successive symbols, is conveyed into a single large molecule, such as the DeoxyriboNucleic Acid (DNA) or RiboNucleic Acid (RNA) [100, 101, 102, 103]. The source nano-machine encodes consecutive bits within one information sequence into a large molecule, and each molecule acts as a message packet. The target nano-machine absorbs these message molecules, and scans each molecule to decode corresponding information symbols.

Based on the system described, communications between the source nano-machine and target nano-machine is achieved. In this chapter, five Stop-and-Wait Automatic Repeat reQuest (SW-ARQ) networking protocols are implemented onto such kind of diffusion-based MC systems.

The SW-ARQ scheme is a method initially proposed in Conventional Communications (CC) systems to ensure that information packets are transmitted successfully between two connected devices[104, 105]. The communication system using the SW-ARQ scheme requires a two-way channel: one for the information packet (hereinafter referred to as packet) transmission, and the other for the acknowledgment (ACK) transmission. With the help of the ACKs, the source nano-machine can know whether packets are transmitted successfully or not. However, due to the retransmission mechanism, this scheme suffers from the reduction of the transmission rate and an increase in the system complexity.

To enable a complete communication framework for MC systems, it is required that various primitives, such as the source nano-machine, the propagation of molecules carrying information, and the target nano-machine, should be combined to define a transmission protocol [1, 106]. The first research to develop such protocols was mentioned in [92], by proposing the idea of *Assured State Transfer*. Similar to the SW-ARQ scheme in CC applications, the goal of Assured State Transfer is designed to enable the reliable transmission of signalling molecules between the source and the target. Molecules encoded with both the message and the index [107, 108], represented as Molecule_1, are emitted by the source nano-machine and propagate to the target nano-machine. Upon reception, these molecules stimulate the target nano-machine to release another type of molecules acting as ACKs, represented as Molecule_2. When Molecule_2 reach the source nano-machine, they stimulate this nano-machine to stop releasing Molecule_1. In this way, this protocol guarantees that no more Molecule_1 are emitted. However, in this research, only the idea of this protocol was described, but no MC system was established to implement this

transmission method. In [107, 109], the nano-logic computation was investigated and a state machine was designed for MC systems. This laid the foundation for applying communication protocols upon nano-machine networks.

In this chapter, a diffusive MC system is described, whose propagation mechanism is the same as the Model-I. Molecules, representing either packets or ACKs, are utilised as the carrier to accomplish the information exchange between the source nano-machine and the target nano-machine. Based on this system, five SW-ARQ transmission schemes are proposed, and simulations of the MC system with these SW-ARQ schemes implemented are carried out. To evaluate the performance for each scheme, two metrics are taken into consideration, namely, the average time cost per successful duplex transmission and the energy cost per successful duplex transmission. Especially, the energy is measured by tracking the amount of overall bits transmitted in both packets and ACKs for a complete duplex transmission. Thus, the unit of the energy consumption is normalised to *bits*, which allows future researches to substitute their own energy model given by their own source-target nano-machines. Numeral results show that all these five methods work well, and can be beneficial depending on different application scenarios.

The remainder of this chapter is organised as follows. In Section 4.2, the MC system structure is introduced. The five SW-ARQ transmission schemes are explained in Section 4.3. Simulations and comparisons of results are provided in Section 4.4 for each scheme. Finally, in Section 4.5, this chapter is concluded.

4.2 System transmission structure

The focus of this chapter is to present how the SW-ARQ protocol can be implemented in MC systems. For the purpose required herein, as is shown in the Fig. 4.1, the system consists of two transceiver nano-machines acting in a way that is analogous to biological entities [13]. One transceiver, working as the source nano-machine,

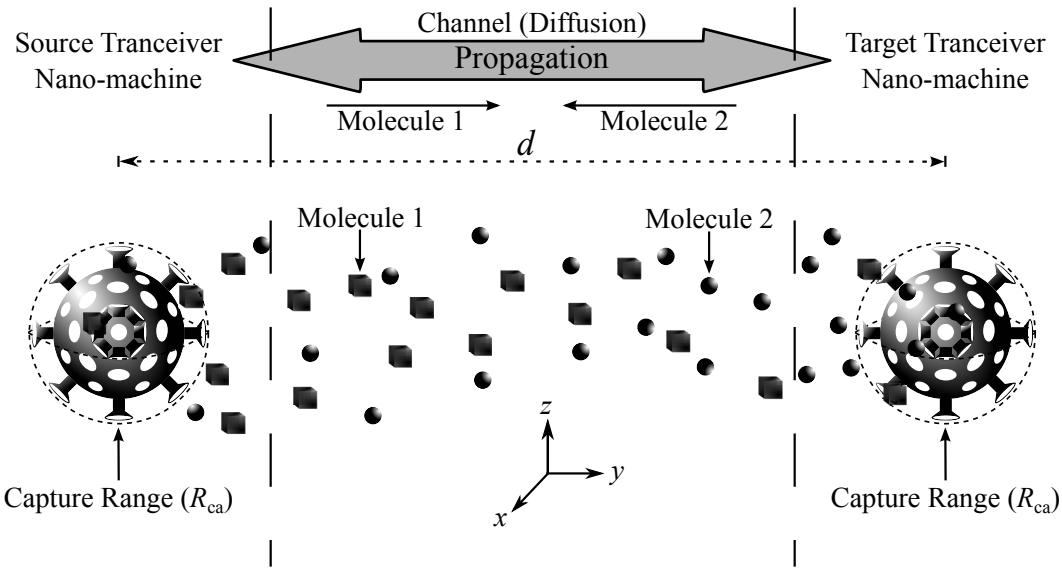

Figure 4.1: The structure of the MC system.

Figure 4.2: The structures of the packets and ACKs in the MC system.

communicates to the other transceiver, working as the target nano-machine, via the diffusion of uniquely identifiable transmission molecules [66]. Each molecule is viewed as an isolate packet or ACK. Structures of packets and ACKs are presented in the Fig. 4.2, whereby it can be seen that the packet is a conjunction of B_{me} message bits and B_{in} index bits, and the corresponding ACK only consists of B_{in} index bits. In the MC system considered herein, packets (or ACKs) with different index sequences will be encoded into different kinds of molecules, and molecules for packets and ACKs are also different. With the index length of B_{in} bits, the index value will range from 0 to $2^{B_{\text{in}}-1}$, and there will be overall $2^{B_{\text{in}}+1}$ kinds of molecules utilised in the MC system, i.e. $2^{B_{\text{in}}}$ kinds for packets, and another $2^{B_{\text{in}}}$ kinds for ACKs. According to the pheromone diversity described in [34], different kinds of molecules will not interfere with each other, and can be recognised by both nano-machines,

which means these two nano-machines can capture wanted molecules accordingly.

Molecules are assumed to diffuse independently in the environment, and the propagation mechanism is the same as the system Model-I. Thus, the capture probability, $P_{\mathrm{ca}}(d,t)$, is expressed by (2.5). Since both of the nano-machines are spheres, it can be deduced that molecules can be viewed as being released from the centre of each nano-machine due to the symmetry. Referring to the Fig. 4.1, the distance between these two nano-machines is d, and the capture range of nano-machines is R_{ca}.

The energy consumption considered in this chapter is measured by calculating the transmitted bits in both packets and ACKs for a complete duplex transmission. Thus, the unit of the energy consumption is normalised to *bits*, which allows readers to substitute their own energy model given by their own source-target nano-machines. Accordingly, the energy is calculated by:

$$\text{Energy} = N_{\mathrm{pa}} \times (B_{\mathrm{me}} + B_{\mathrm{in}}) + N_{\mathrm{ac}} \times B_{\mathrm{in}}, \tag{4.1}$$

where N_{pa} and N_{ac} respectively represent the overall numbers of the released packets and ACKs.

4.3 SW-ARQ schemes

The five proposed transmission schemes are illustrated in the Fig. 4.3, and will be introduced in turn as follows.

4.3.1 Scheme 1

This is similar to the traditional SW-ARQ scheme. As shown in the Fig. 4.3(a), the source nano-machine transmits a packet and waits for the ACK from the target transceiver. If the waiting time is longer than a pre-defined limit, T_{out}, the current packet will be re-transmitted. When receiving the packet, the target nano-machine

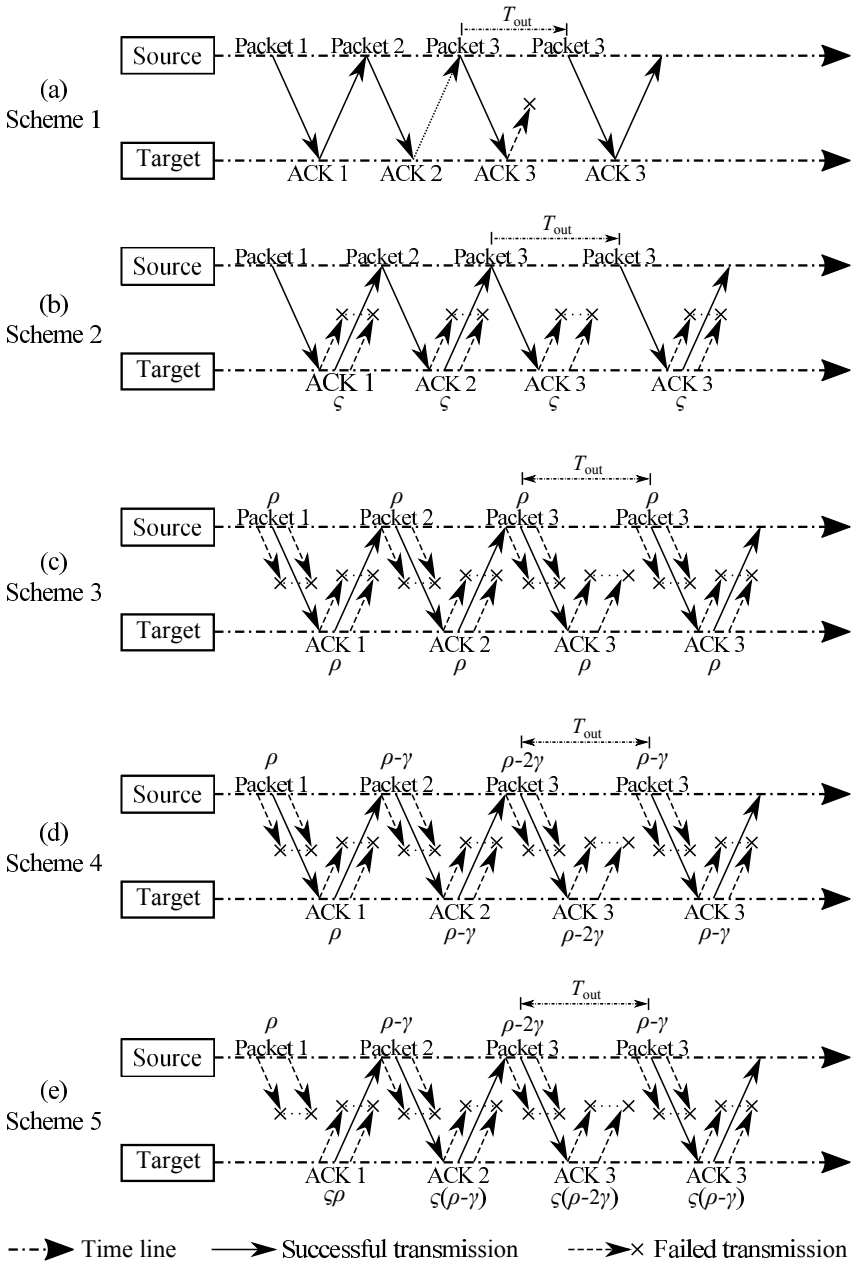

Figure 4.3: The five proposed SW-ARQ transmission schemes.

sends back an ACK and waits for the next packet from the source. Thus, using Scheme 1, the probability for a complete duplex transmission of the wanted packet

can be obtained as:

$$P_{\mathrm{s1}} = P_{\mathrm{ca}}(d,t)^2. \tag{4.2}$$

This scheme enjoys great simplicity but suffers from a high rate of unsuccessful transmissions, especially for long range communications. This limits the application of this scheme to a very narrow area: adjacent range communications. For example in the biomedical field [92], new smart drug delivery systems are designed to adjoin two nano-machines together, one of which has the capability to sense the environment and the other is able to release specific drugs inside the body. The communication between these two adjacent nano-machines could be fulfilled using this scheme. In this scenario, this scheme will be both simple and reliable.

4.3.2 Scheme 2

This scheme, as shown in the Fig. 4.3(b), is an enhancement method over Scheme 1. When the target transceiver receives a packet, it sends back ς copies of the corresponding ACK simultaneously, where $\varsigma \geq 1$. As soon as at least one of the ς ACKs reaches the source transceiver, the next packet will be transmitted. Therefore, using Scheme 2, the probability for a complete duplex transmission of the wanted packet can be derived as:

$$P_{\mathrm{s2}}(\varsigma) = P_{\mathrm{ca}}(d,t) \times \Big(1 - \big(1 - P_{\mathrm{ca}}(d,t)\big)^{\varsigma}\Big). \tag{4.3}$$

Especially, if $\varsigma = 1$, Scheme 2 is the same as Scheme 1.

Based on the structures shown in the Fig. 4.2, a length ratio ψ is defined as the ratio of the length of the packets to the length of the ACKs, that is,

$$\psi = \frac{\text{The length of the packets}}{\text{The length of the ACKs}} = \frac{B_{\mathrm{me}} + B_{\mathrm{in}}}{B_{\mathrm{in}}} = 1 + \frac{B_{\mathrm{me}}}{B_{\mathrm{in}}}. \tag{4.4}$$

If the source is far away from the target, it can be deduced that the larger ψ is, the less time will be cost compared with Scheme 1.

4.3.3 Scheme 3

When the distance between these two nano-machines is quite large, the capture probability is known to be low referring to (2.5), leading to a high probability of re-transmissions. This will potentially cost too much time and energy. This problem can be solved by using the scheme shown in the Fig. 4.3(c). The source nano-machine simultaneously sends ρ copies of the current packet, and as soon as at least one of these copies is received, the target nano-machine will send back ρ copies of the corresponding ACK. Incorporating the capture probability of one packet (or ACK) as expressed by equation (2.5), using Scheme 3, the probability for a complete duplex transmission of the wanted packet is given by:

$$\begin{aligned} P_{\mathrm{s3}}(\rho) &= \left(1-\left(1-P_{\mathrm{ca}}(d,t)\right)^{\rho}\right) \times \left(1-\left(1-P_{\mathrm{ca}}(d,t)\right)^{\rho}\right) \\ &= \left(1-\left(1-P_{\mathrm{ca}}(d,t)\right)^{\rho}\right)^{2}. \end{aligned} \tag{4.5}$$

For $\rho = 1$, P_{s3} is the same as the probability of a successful complete transmission using Scheme 1, that is, with $\rho = 1$, $P_{\mathrm{s3}} = P_{\mathrm{s1}} = P_{\mathrm{ca}}(d,t)^2$. It is therefore obvious that $P_{\mathrm{s3}} \gg P_{\mathrm{s1}}$ when ρ is sufficiently large. In this way, if ρ is properly selected, the time cost will be reduced greatly without consuming too much extra or even less energy. This scheme has relatively higher rate of successful transmissions, but it is more complicated than both Scheme 1 and Scheme 2, which leads to a higher requirement for both nano-machines. The application of this scheme lays on long range communications.

4.3.4 Scheme 4

This scheme is based on scheme 3 and the transmission scheme proposed in [110]. As is shown in the Fig. 4.3(d), the number of copies transmitted for each packet and ACK varies depending on whether the previous duplex transmission is successful or not. The initial number of copies of the first packet (or ACK) is denoted as ρ. If at least one of these ρ copies of the first packet reaches the target and at least one of the ρ ACKs is absorbed by the source, the number of copies of the second packet (or ACK) will reduce to $\rho-\gamma$; otherwise, the source will release $\rho+\gamma$ copies of the first packet and the target will also emit $\rho+\gamma$ copies of the first ACK upon receiving at least of one of these $2\rho+\gamma$ copies of the first packet (previous ρ copies plus current $\rho+\gamma$ copies). It should be noticed that $\gamma<\rho$. Such mechanism goes the same for all the rest packets. With sufficient packets to be transmitted, the number of copies of packets (or ACKs), denoted as χ, will be adaptively altered around a certain value, which could be the optimal number of the copies that need to be transmitted. Using Scheme 3, the probability for a complete duplex transmission of the wanted packet is computed by:

$$\begin{aligned} P_{\mathrm{s4}}(\chi) &= \left(1-\left(1-P_{\mathrm{ca}}(d,t)\right)^{\chi}\right)\times\left(1-\left(1-P_{\mathrm{ca}}(d,t)\right)^{\chi}\right) \\ &= \left(1-\left(1-P_{\mathrm{ca}}(d,t)\right)^{\chi}\right)^{2}. \end{aligned} \tag{4.6}$$

Especially, if $\rho=1$ and $\gamma=0$, Scheme 4 is the same as Scheme 1, and if $\rho>1$ and $\gamma=0$, Scheme 4 is the same as Scheme 3.

If the distance between the source and target is large, based on the equation (4.6), it is obvious that the value of $P_{\mathrm{s4}}(\rho\pm\gamma)$ is close to the value of $P_{\mathrm{s4}}(\rho)$ with a small $P_{\mathrm{ca}}(d,t)$. However, there will be huge differences after accumulations, such as $P_{\mathrm{s4}}(20)\gg P_{\mathrm{s4}}(10)\gg P_{\mathrm{s4}}(1)$. Thus, due to the 'adaptivity' of the system, Scheme 4 can automatically adjust the number of emitted copies to avoid either high time cost or consuming much redundant energy, which has great superiority for a channel with

Table 4.1: Simulation parameters for the investigation of the SW-ARQ schemes

1.	The capturing radium of nano-machines	R_{ca}	$0.5\,\mu\mathrm{m}$
2.	The distance between nano-machines	d	$1 \sim 3\mu\mathrm{m}$
3.	The diffusion coefficient	D	$10^{-3}\mu\mathrm{m}^2\,\mu\mathrm{s}^{-1}$
4.	The timeout limit	T_{out}	$5000\,\mu\mathrm{s}$
5.	The message length	B_{me}	500
6.	The ACK length	B_{in}	5
7.	The amount of successively transmitted packets	10^5	

unknown suitable number of copies to guarantee the successful duplex transmission probability.

4.3.5 Scheme 5

This scheme, as shown in the Fig. 4.3(e), is a combination of Scheme 2 and Scheme 4. The 'adaptive' mechanism is the same as Scheme 4. The only difference is that when source transmits χ packets for a trial, the target will transmit $\varsigma\chi$ copies of corresponding ACKs. Hence, the probability for a complete duplex transmission of the wanted packet can be calculated as:

$$P_{\mathrm{s5}}(\chi,\varsigma) = \left(1-\left(1-P_{\mathrm{ca}}(d,t)\right)^{\chi}\right) \times \left(1-\left(1-P_{\mathrm{ca}}(d,t)\right)^{\varsigma\chi}\right). \tag{4.7}$$

For $\varsigma = 1$, $P_{\mathrm{s5}}(\chi,\varsigma) = P_{\mathrm{s4}}(\chi)$. It is clear that the successful probability using Scheme 5 has been increased compared with the successful probability using Scheme 4. By carefully choosing χ and ς, the time cost will be greatly reduced without using too much or even less energy.

4.4 Numeral results

In this section, these five transmission schemes are simulated to be implemented on a diffusive MC system. Information molecules representing either packets or ACKs can propagate independently. Both the source and target transceivers can recognise

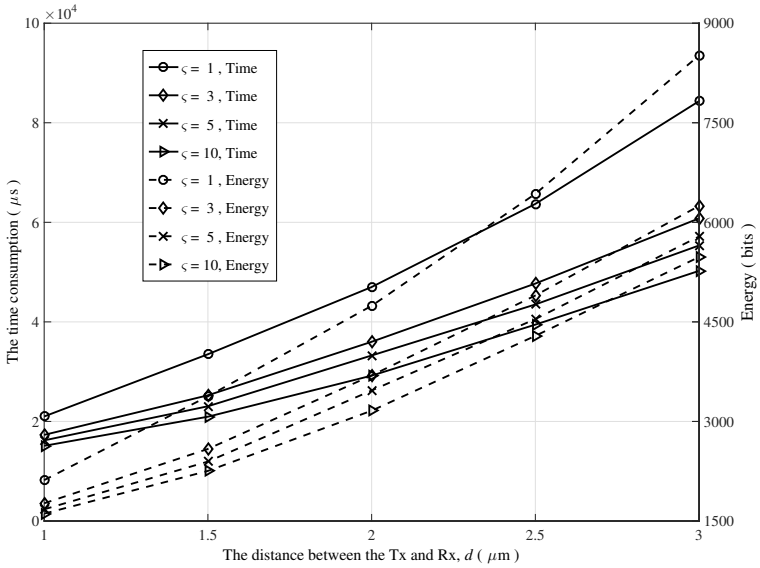

Figure 4.4: The time and energy required for a successful duplex transmission using Scheme 1 and Scheme 2 ($\varsigma = 1$ represents the results for Scheme 1) .

and capture corresponding molecules encoded with wanted packets (or ACKs), and leave the rest untouched. The system performance is analysed mainly regarding to two features, the energy consumption and the time requirement per complete duplex transmission. Simulation parameters assignment is presented in Table 4.1.

4.4.1 Results for Scheme 1 and 2

The Fig. 4.4 presents that both Scheme 1 and Scheme 2 can be successfully deployed into the diffusion-based MC system, and for a larger distance d, more time and energy is required to accomplish a successful duplex transmission. It can be also noticed that by using Scheme 2, the time cost and the energy consumption can be significantly reduced. Referring to (4.3), increasing ς results in a higher probability of a successful duplex transmission. However, a larger ς requires a higher energy budget to transmit the extra copies of ACKs. The energy consumption for transmitting these additional ACKs may outweigh the energy gain in requiring a lower number of transmission packets. Meanwhile, it can be noticed that the gain

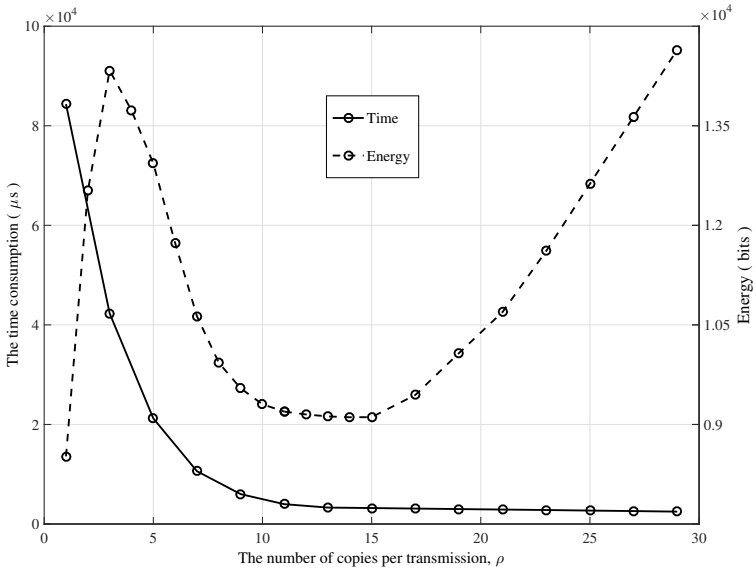

Figure 4.5: The time and energy required for a successful duplex transmission using Scheme 3 at $d = 3\,\mu\text{m}$ (Note: $\rho = 1$ is also Scheme 1).

difference between values of ς becomes small with the increasing ς. Hence, when ς is sufficiently large, keeping enlarging ς may be just a waste of the energy without bringing in any benefit in reducing the time cost. Additionally, it can be deduced that the higher the length ratio ψ is, the larger ς can be selected to achieve the optimal system performance with regards to both the time and energy.

4.4.2 Results for Scheme 3

Results in the Fig. 4.5 reveal that Scheme 3 can perform well in the diffusive MC system. As is clearly shown herein, by sending more copies of each packet and ACK, the system can use less time to achieve the duplex transmissions. According to (4.5), it can be deduced that by increasing ρ, the successful duplex transmission probability will be improved, leading to a lower re-transmission rate. Thus, the time cost per successful duplex transmission is correspondingly reduced.

Another feature in the Fig. 4.5 is that with ρ getting larger, there exists a minimal value for the energy consumption. The corresponding value of ρ, repre-

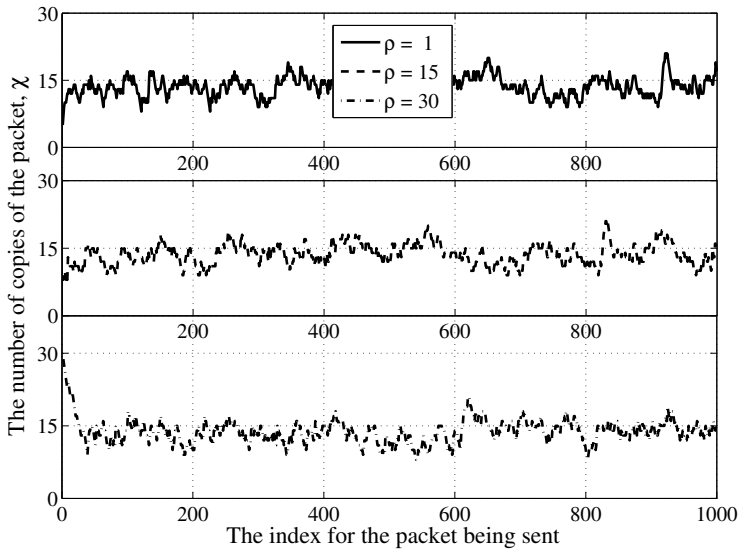

Figure 4.6: The number of copies transmitted χ changes with each transmitted packet for Scheme 4 at $d = 3\,\mu\text{m}$. Results only show the fist 1000 packets.

sented as ρ_{opt}, can be viewed as the optimal design, which is to achieve the trade-off between the time and energy requirement. If $\rho > \rho_{\text{opt}}$, the decrease of the time cost is not quite obvious, but the system has to utilise plenty of extra energy. Thus, when implementing Scheme 3 to accomplish communications between two nano-machines, the number of copies of each packet and ACK, ρ, needs to be carefully designed.

4.4.3 Results for Scheme 4

As is illuminated in Figs. 4.6 and 4.7, the 'adaptive' transmission scheme, Scheme 4, can be implemented to enable the networking of these two nano-machines. No matter what the initial number of copies is, with sufficient packets, the source transceiver can coordinate χ based on whether the previous packet is successfully transmitted. An example of such scheme is illustrated in the Fig. 4.6. At $d = 3\,\mu\text{m}$, regardless of whether $\rho = 1, 15$, or 30, after certain time, the number of emitted copies gradually fluctuate around $\chi = 14$. The Fig. 4.7 provides a more intuitive way to show that there will be a higher probability for the values of χ to be around 14 even though

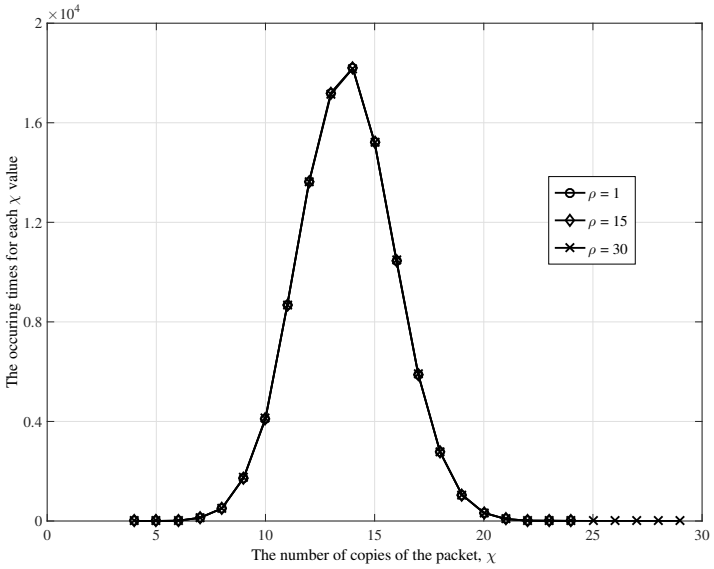

Figure 4.7: The distribution of the occurrence times for each value of χ for Scheme 4 at $d = 3\,\mu\text{m}$. The amount of successively transmitted packets is 10^5.

Table 4.2: Time cost and energy consumption for Scheme 4 and Scheme 3 at $d = 3\,\mu\text{m}$.

Scheme	ρ	Time cost	Energy consumption
Scheme 4	1	7560 µs	14531 bits
Scheme 4	15	7560 µs	14531 bits
Scheme 4	30	7560 µs	14531 bits
Scheme 3	15	3206 µs	9110 bits

the initial numbers of copies are different.

The time cost and energy consumption is shown in Table 4.2. Compared with Scheme 3, Scheme 4 will use more time and energy to achieve successful duplex transmissions. This is mainly due to the fluctuation of the number of copies. Using Scheme 3, with parameters carefully designed, the probability of re-transmission can be reduced to be negligible; while for Scheme 4, the source nano-machine adjusts the number of emitted copies according to the previous trials, which means the re-transmission is unavoidable. Therefore, using Scheme 4 will have a higher time and energy requirement. Although compared with Scheme 3, using Scheme 4 may

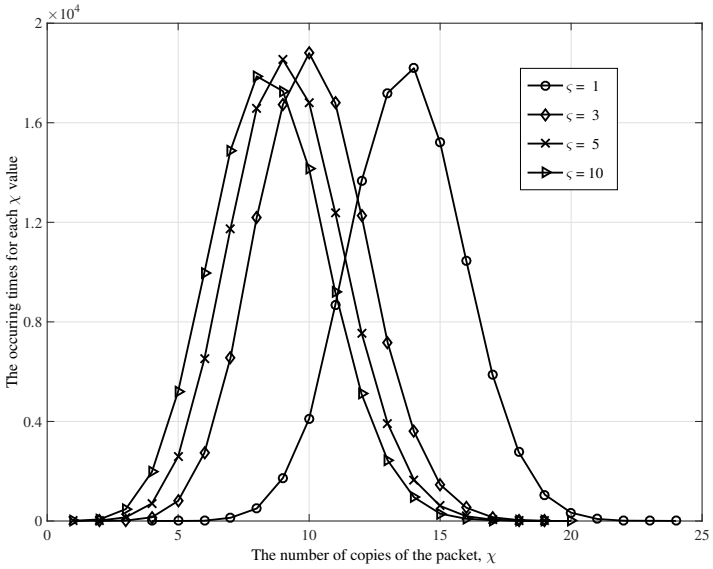

Figure 4.8: The distribution of the occurrence times for each value of χ at $d = 3\,\mu\text{m}$ for Scheme 5. The amount of successively transmitted packets is 10^5. (Note: $\varsigma = 1$ represents the results for Scheme 4.)

Table 4.3: Time cost and energy consumption for Scheme 5 at $d = 3\,\mu\text{m}$.

ρ	ς	Time cost	Energy consumption
1	1	7560 µs	14531 bits
1	3	7541 µs	10956 bits
1	5	7527 µs	10090 bits
1	10	7435 µs	9620 bits

consume more time and energy, it will still be a priori option for the MC system without pre-knowledge of the channel properties due to its own superiority of the 'adaptivity'.

4.4.4 Results for Scheme 5

Results in the Fig. 4.8 present that the source nano-machine can communicate to the target using Scheme 5. Similar to the situation in Scheme 4, the value of χ tends to progressively alter around a certain value, represented as χ_0. Referring to (4.7), it can be deduced that χ_0 varies according to different ς, and by increasing ς, a smaller

Table 4.4: Time cost and energy consumption for all five schemes at $d = 3\,\mu m$.

Schemes	Relevant Parameters	Time cost	Energy consumption
Scheme 1	-	84 350 µs	8514 bits
Scheme 2	$\varsigma = 5$	55 350 µs	5787 bits
	$\varsigma = 10$	50 250 µs	5478 bits
Scheme 3	$\rho = 15$	3206 µs	9110 bits
Scheme 4	$\rho = 1$	7560 µs	14531 bits
Scheme 5	$\rho = 1$, $\varsigma = 5$	7527 µs	10090 bits
	$\rho = 1$, $\varsigma = 10$	7435 µs	9620 bits

value of χ_0 will be caused, which agrees with the results in the Fig. 4.8. With ς getting larger, the target nano-machine has to use more energy to transmit the extra copies of ACKs, but due to the reduction of χ_0, less energy will be required for the packets transmission. Especially when the length ratio ψ is large, the decrease of the energy due to a smaller χ_0 may overweight the additional energy for a larger ς. As a consequence, the overall energy consumption is reduced. Table 4.3 gives the time and energy requirement for $\varsigma = 1, 3, 5$ and 10.

Table 4.4 provides an example of the performance comparison between these 5 schemes. At $d = 3\,\mu m$, all these five schemes can achieve the packet transmission from the source nano-machine to the target nano-machine. If the channel is pre-known to the source nano-machine, by using the Scheme 3, both the time and energy consumption can be reduced with parameter $\rho = 15$ optimised. However, if the source nano-machine has no knowledge of the channel properties, the Scheme 4 or 5 will be a superior option due to the 'adaptivity'.

4.5 Conclusions

In this Chapter, simulation results are provided for the implementation of five SW-ARQ schemes on a diffusion-based MC system. The performance is analysed with regards to the time cost (average time per successful duplex transmission) and the energy consumption (average energy per successful duplex transmission). It is shown

that all five schemes can be used as communication protocols between two nano-machines, and they all have their own superiority according to different scenarios. To be specific, Scheme 1 is the first choice for adjacent communications due to its own simplicity, while Schemes 2 and 3 (especially Scheme 3), will improve the performance significantly with sufficient energy for longer range communications. Unlike Schemes 1 through 3 whose target application is on the pre-known channel, Schemes 4 and 5 are designed for a unknown channel or a varying channel due to the 'adaptivity'. Similar to the comparisons between Scheme 2 and Scheme 1, Scheme 5 will provide a better performance than Scheme 4 with carefully designed parameters and sufficient energy. Besides, when designing an MC system, the complexity of the system should also be taken into consideration. In the future, for specific systems with limitation on time cost or energy consumption, optimising the trade-off between the time and energy requirement will be of great importance.

Chapter 5

The Design of MC System Model-II and The Performance Analysis

5.1 Introduction

In Chapter 2, one molecular communication (MC) system model, named as Model-I, is introduced, where information is conveyed into the number of captured molecules. On the contrary, in this chapter, a different MC system model, represented as Model-II, is described, where messages are encoded into the molecular concentration. The concentration distribution changes with respect to the time, and can be detected by the Rx. By calculating the Mean Square Error (MSE), the Rx can decode messages accordingly. Similar to the situation for Model-I, it is also required to develop a method to evaluate the performance of Model-II by means of both theoretical derivations and simulations.

The concentration-based MC system was first presented in [111], and expanded in [55] by specifying the influence of the Inter-Symbol Interference (ISI) and channel noise. In [112], expressions of the ISI and noise were provided, and the

formulas of various channel parameters, such as the pulse delay, pulse amplitude, and pulse duration, were derived. Further enhancement of the system model was found in [77, 88], where for the first time, the emission process of the Tx was taken into consideration. However, in these literatures, only simulations were carried out, but no theoretical derivations were obtained. Moreover, in all aforementioned publications, when dealing with the ISI, the impact from only one previous symbol was taken into consideration. Therefore, more effort should be put on studying how the channel memory affects the system performance.

In this chapter, the encoding mechanism, transmission procedure, and decoding process for MC system Model-II are described. Compared with previous researches, the Model-II is enhanced by formulating the emission process and implementing the MSE decoding method. Both theoretical and simulated results are presented to illuminate the system reliability (represented by the BER) and reliable transmission rate (represented by the capacity). It is shown that different designs of channel parameters can bring in significant impact on the system performance. Further investigation is also carried out to study the influence of the channel memory. The ISI length, similar to the situation in Model-I, is regarded as an arbitrary value for theoretical derivations, and set to a length of 20 for simulations to maximise the precision as is reasonably practical.

The remainder of this chapter is organised as follows. In Section 5.2, the system Model-II and related parameters are introduced. The channel performance is analysed in Section 5.3, and numerical results are provided in Sectoin 5.4. Finally in Section 5.5, this chapter is concluded.

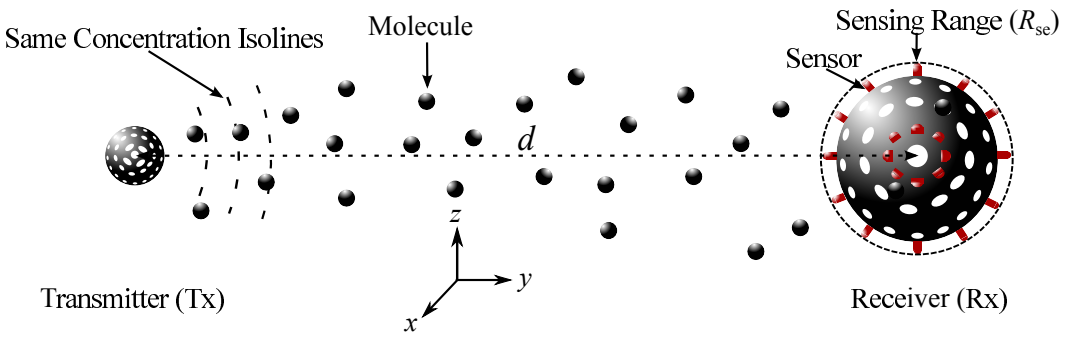

Figure 5.1: The structure of the MC system.

5.2 The diffusion-based MC system model based on molecular concentrations

As is introduced in Chapter 2, for the Model-I, attentions are paid to investigate the movement of individual molecules, where the capture probability, P_{ca} is derived to describe the propagation mechanism. On the contrary, the diffusion process can be alternatively addressed from a macroscopic angle. Regardless how each single molecule moves, they will form a certain concentration distribution after being released by the Tx, and the resultant concentration is easy to be addressed. Based on this phenomenon, the second model is established, that is, the Model-II.

The Fig. 5.1 shows the structure of the MC system model-II. Similar to the case described in Sec. 2.2, messages are expressed as successive binary symbols and encoded by the Tx into molecules. At the beginning of each time slot, the Tx either emits a pulse of molecules to transmit symbol '1', or remains silent to transmit symbol '0'. Molecules diffuse in the 3D environment, and the concentration distribution is formed, which attenuates with the increasing distance, and changes with respect to the time t. At the other end, it is assumed that the Rx is a passive observer [62, 88], which means the Rx will not affect the molecular concentration distribution. The Rx is designed to determine messages bits by sensing the concentration around, rather than counting the number of captured molecules. As is shown in the

Fig. 5.1 , the distance between the Tx and Rx is d, and the sensing range of the Rx is R_{se}. Similar to the results shown in [39, 55, 70, 88, 112, 113], the concentration at the Rx can be considered as the concentration at the centre of sphere.

The molecular concentration in a 3D environment, represented as $c(d,t)$, can be obtained by solving the following equation [88]:

$$\frac{1}{D}\frac{\partial c(d,t)}{\partial t} = \nabla^2 c(d,t), \tag{5.1}$$

where D is the diffusion coefficient (in $\mu\text{m}^2\,\mu\text{s}^{-1}$), and ∇^2 is the Laplacian operator. Thus, the concentration can be derived as [55, 88]:

$$c(d,t) = \frac{m}{(4\pi t D)^{3/2}} \exp\left(-\frac{d^2}{4tD}\right), \tag{5.2}$$

where m is the number of molecules emitted by the Tx in one pulse. Therefore, the impulse response for the diffusion channel, $h(d,t)$, is given as:

$$h(d,t) = \frac{1}{(4\pi t D)^{3/2}} \exp\left(-\frac{d^2}{4tD}\right). \tag{5.3}$$

The emission process of the Tx, rather than being simplified as an impulse, can be regarded as a rectangular pulse expressed as:

$$s(t) = A \cdot \text{rect}\left(\frac{t - T_{\text{em}}/2}{T_{\text{em}}}\right), 0 \le t \le T_{\text{pd}}, \tag{5.4}$$

where A is the emission rate (in number/μs), T_{em} is the emission pulse duration, T_{pd} is the emission pulse period, and $T_{\text{em}} < T_{\text{pd}}$. Since m is denoted as the number of molecules released per pulse, it can be deduced that $m = A \times T_{\text{em}}$. Thus, the theoretical concentration at the Rx, $u(d,t)$, formed by the newly emitted molecules,

can be obtained by the convolution operation $u(d,t) = s(t) * h(d,t)$ [111], that is:

$$u(d,t) = s(t) * h(d,t) = \int_{-\infty}^{+\infty} s(t-\tau)h(d,\tau)d\tau. \tag{5.5}$$

When $t \leq T_{\text{em}}$, $u(d,t)$ in (5.5) can be derived as:

$$\begin{aligned} u(d,t) &= \int_0^t s(t-\tau)h(d,\tau)d\tau = \int_0^t A\frac{1}{(4\pi\tau D)^{3/2}}\exp\left(-\frac{d^2}{4\tau D}\right)d\tau \\ &= \frac{A}{(4\pi D)^{3/2}}\int_0^t \frac{1}{\tau^{3/2}}\exp\left(-\frac{d^2}{4\tau D}\right)d\tau. \end{aligned} \tag{5.6}$$

To make it easy to follow, it is denoted that:

$$\lambda = \frac{A}{(4\pi D)^{3/2}}, \varepsilon = \frac{d^2}{4D}, \omega^2 = \frac{\varepsilon}{\tau}. \tag{5.7}$$

By substituting (5.7) into (5.6), $u(d,t)$ for $t \leq T_{\text{em}}$ can be obtained as:

$$\begin{aligned} u(d,t) &= \frac{A}{(4\pi D)^{3/2}}\int_0^t \frac{1}{\tau^{3/2}}\exp\left(-\frac{d^2}{4\tau D}\right)d\tau \\ &= \lambda\int_{+\infty}^{\sqrt{\varepsilon/t}} \frac{1}{(\varepsilon/\omega^2)^{3/2}}\cdot\Big(-\frac{2\varepsilon}{\omega^3}\Big)\cdot\exp(-\omega^2)d\omega \\ &= \lambda\int_{\sqrt{\varepsilon/t}}^{+\infty} \frac{\omega^3}{\varepsilon^{3/2}}\cdot\frac{2\varepsilon}{\omega^3}\cdot\exp(-\omega^2)d\omega \\ &= \frac{2\lambda}{\sqrt{\varepsilon}}\int_{\sqrt{\varepsilon/t}}^{+\infty}\exp(-\omega^2)d\omega \\ &= \frac{2\lambda}{\sqrt{\varepsilon}}\frac{\sqrt{\pi}}{2}\text{erfc}(\sqrt{\varepsilon/t}) = \lambda\sqrt{\frac{\pi}{\varepsilon}}\text{erfc}(\sqrt{\varepsilon/t}). \end{aligned} \tag{5.8}$$

When $t > T_{\text{em}}$, $u(d,t)$ can be calculated as:

$$\begin{aligned} u(d,t) &= \int_{t-T_{\text{em}}}^t s(t-\tau)h(d,\tau)d\tau = \int_{t-T_{\text{em}}}^t A\frac{1}{(4\pi\tau D)^{3/2}}\exp\left(-\frac{d^2}{4\tau D}\right)d\tau \\ &= \frac{A}{(4\pi D)^{3/2}}\int_{t-T_{\text{em}}}^t \frac{1}{\tau^{3/2}}\exp\left(-\frac{d^2}{4\tau D}\right)d\tau. \end{aligned} \tag{5.9}$$

With the same denotation as (5.7), $u(d,t)$ in (5.9) can be rewritten as:

$$\begin{aligned} u(d,t) &= \frac{A}{(4\pi D)^{3/2}} \int_{t-T_{\mathrm{em}}}^{t} \frac{1}{\tau^{3/2}} \exp\Big(-\frac{d^2}{4\tau D}\Big) d\tau \\ &= \lambda \int_{\sqrt{\varepsilon/(t-T_{\mathrm{em}})}}^{\sqrt{\varepsilon/t}} \frac{1}{(\varepsilon/\omega^2)^{3/2}} \cdot \Big(-\frac{2\varepsilon}{\omega^3}\Big) \cdot \exp\big(-\omega^2\big) d\omega \\ &= \frac{2\lambda}{\sqrt{\varepsilon}} \int_{\sqrt{\varepsilon/t}}^{\sqrt{\varepsilon/(t-T_{\mathrm{em}})}} \exp\big(-\omega^2\big) d\omega \\ &= \frac{2\lambda}{\sqrt{\varepsilon}} \frac{\sqrt{\pi}}{2} \cdot \Big[\mathrm{erfc}\big(\sqrt{\frac{\varepsilon}{t}}\big) - \mathrm{erfc}\big(\sqrt{\frac{\varepsilon}{t-T_{\mathrm{em}}}}\big)\Big] \\ &= \lambda \sqrt{\frac{\pi}{\varepsilon}} \Big[\mathrm{erfc}\big(\sqrt{\frac{\varepsilon}{t}}\big) - \mathrm{erfc}\big(\sqrt{\frac{\varepsilon}{t-T_{\mathrm{em}}}}\big)\Big] \end{aligned} \tag{5.10}$$

Thus, it can be summarised that for $t \leq T_{\mathrm{em}}$, $u(d,t)$ is expressed as (5.8), and for $t > T_{\mathrm{em}}$, the expression of $u(d,t)$ is given by (5.10). By taking (5.7) into consideration, $u(d,t)$ can be derived as:

$$u(d,t) = \begin{cases} \frac{A}{4\pi d D} \mathrm{erfc}\big(\frac{d}{\sqrt{4tD}}\big), & t \leq T_{\mathrm{em}} \\ \frac{A}{4\pi d D} \Big[\mathrm{erfc}\big(\frac{d}{\sqrt{4tD}}\big) - \mathrm{erfc}\big(\frac{d}{\sqrt{4(t-T_{\mathrm{em}})D}}\big)\Big], & t > T_{\mathrm{em}} \end{cases} \tag{5.11}$$

The Rx is designed to sample the concentration at the time when the theoretical concentration reaches the peak value. By deriving the equation $\frac{\partial u(d,t)}{\partial t} = 0$, the relationship between the distance d and the sampling time T_{sa} can be obtained as:

$$d^2 = \frac{6D}{T_{\mathrm{em}}} \cdot (T_{\mathrm{sa}} - T_{\mathrm{em}}) \cdot T_{\mathrm{sa}} \cdot \ln\Big(\frac{T_{\mathrm{sa}}}{T_{\mathrm{sa}} - T_{\mathrm{em}}}\Big). \tag{5.12}$$

Thus, by solving (5.12), the sampling time can be determined.

Furthermore, similar to the situation as in Model-I, the channel is also influenced by the ISI due to the existence of previously emitted molecules. Considering the ISI, the noiseless concentration at the Rx can be regarded as the sum of the

current signal concentration and previous ones, that is [88, 112, 113]:

$$u^I(d,t) = \sum_{i=0}^{I} a_{k-i} u(d, T_{\text{sa}} + i \times T_{\text{pd}}) = \sum_{i=0}^{I} a_{k-i} u_i, \tag{5.13}$$

where I is the ISI length, k represents the k^{th} symbol from the beginning of transmission, the set $\{a_{k-i}, i = 0, 1, ..., I\}$ is the binary messages sequence, and the element a_{k-i} represents the binary value of each symbol. During the diffusion process, an additive signal-dependent noise, $n(t)$, will also affect the concentration at the Rx. The noise, $n(t)$, obeys the normal distribution with the expression given as [39]:

$$n(t) \sim \mathcal{N}(0, \sigma^2), \tag{5.14}$$

where $\sigma^2 = \frac{3}{4\pi R_{\text{se}}^3} u^I(d,t) = \frac{3}{4\pi R_{\text{se}}^3} \sum_{i=0}^{I} a_{k-i} u_i$.

Given $u^I(d,t)$ in (5.13) and $n(t)$ in (5.14), the Rx received concentration, $r(d,t)$, can be represented by:

$$r(d,t) = u^I(d,t) + n(t) = \sum_{i=0}^{I} a_{k-i} u_i + n(t). \tag{5.15}$$

As to the decoding procedure, similar to the case in Model-I, the Rx is also designed to determine information symbols by calculating the Mean Square Error (MSE). Thus, the decision variable L is expressed as:

$$L = \text{MSE}_1 - \text{MSE}_0 = [r(d,t) - l_1]^2 - [r(d,t) - l_0]^2, \tag{5.16}$$

where l_1 and l_0 are pre-designed criteria for the Rx to decide whether '1' or '0' is transmitted. When $L \geq 0$, '0' is decided; otherwise, '1' is decided. The expressions

of l_1 and l_0 are given as:

$$l_1 = \sum_{i=1}^{I} u_i \hat{a}_{k-i} + u_0, \tag{5.17}$$

$$l_0 = \sum_{i=1}^{I} u_i \hat{a}_{k-i}, \tag{5.18}$$

where the set $\{\hat{a}_{k-i}, i = 1, 2, ..., I\}$ is previously decoded bits within the ISI length I. It is assumed that previously decoded bits will not affect the decoding of the current symbol. Thus, in this case, it is assumed that $\hat{a}_{k-i} = a_{k-i}$ for $i = 1, 2, ..., I$. By substituting (5.15), (5.17) and (5.18) into (5.16), L can be derived as:

$$L = -2u_0[n(t) + (a_k - \frac{1}{2})u_0]. \tag{5.19}$$

Thus, the value of L can be determined by (5.16), based on which, the Rx decodes the current information bit.

5.3 Performance analysis of MC system Model-II

The MC system Model-II is described in Section 5.2. The signal concentration is given as (5.13), and the noise is given as (5.14). As is defined in [88], the signal power and noise power of the MC system are respectively expressed as:

$$W_u = \frac{u_0^2}{4}, \tag{5.20}$$

$$W_n = E[n(t)^2], \tag{5.21}$$

where $E[\cdot]$ represents the expected value. Considering (5.14), $E[n(t)]$ can be obtained as:

$$E[n(t)^2] = E[\sigma^2] = E\left[\frac{3u^I(d,t)}{4\pi R_{\text{se}}^3}\right] = \frac{3}{4\pi R_{\text{se}}^3}E[u^I(d,t)]$$
$$= \frac{3}{4\pi R_{\text{se}}^3}E\left[\sum_{i=0}^{I} u_i a_{k-i}\right] = \frac{3P_{\text{tx}}}{4\pi R_{\text{se}}^3}\sum_{i=0}^{I} u_i, \tag{5.22}$$

where P_{tx} is the probability of symbol '1' transmitted. Given (5.20) and (5.22), the Signal-to-Noise-Ratio (SNR) of the Model-II can be calculated by:

$$\text{SNR} = \frac{W_u}{W_n} = \frac{u_0^2}{4 \times \frac{3P_{\text{tx}}}{4\pi R_{\text{se}}^3}\sum\limits_{i=0}^{I} u_i} = \frac{\pi R_{\text{se}}^3 u_0^2}{3P_{\text{tx}}\sum\limits_{i=0}^{I} u_i}. \tag{5.23}$$

5.3.1 Bit Error Rate analysis

The Rx in the MC system Model-II is designed to determine messages by calculating the MSE. The decision variable is given as (5.19). When $L \geq 0$, '0' is decoded; otherwise, '1' is decoded. Similar to the case in Model-I, there are two scenarios for the error occurrence: when '0' is transmitted but '1' is received (named as a_k=0 but $\hat{a}_k$=1), or when '1' is transmitted but '0' is received (named as a_k=1 but $\hat{a}_k$=0). Due to the existence of the ISI, different permutations of the values of $\{a_{k-i}, i = 1, 2, ..., I\}$ will result in different error patterns. Each error pattern will be corresponding to a certain permutation of values of $\{a_{k-i}, i = 1, 2, ..., I\}$. With the ISI length equal to I, there will be 2^I error patterns. In this chapter, 'j' is denoted as the error pattern index, where $j = 1, 2, 3, ..., 2^I$. For the error pattern 'j', the permutation of values of $\{a_{k-i}, i = 1, 2, ..., I\}$ is denoted as $\{a_{k-i}^{(j)}, i = 1, 2, ..., I\}$, the number of '1's within $\{a_{k-i}^{(j)}, i = 1, 2, ..., I\}$ is denoted as ϱ_j, and accordingly, the number of '0's is $(I - \varrho_j)$. The probability of '1' transmitted is denoted as P_{tx}, and the probability of '0' transmitted is $(1 - P_{\text{tx}})$.

(1) a_k=0 but $\hat{a}_k$=1

With $a_k = 0$, to obtain the condition $L < 0$ in (5.19), it is required that:

$$n(t) > \frac{u_0}{2}. \tag{5.24}$$

Given (5.14), the probability for the error pattern 'j' can be derived by calculating the probability of $n(t) > \frac{u_0}{2}$, that is:

$$\begin{aligned} P_{\text{er}0j} &= P_{\text{tx}}^{\varrho_j}(1-P_{\text{tx}})^{I-\varrho_j}\int_{\frac{u_0}{2}}^{\infty}\frac{1}{\sqrt{2\pi}}\frac{1}{\sigma_{0j}}\exp\Big(-\frac{v^2}{2\sigma_{0j}^2}\Big)dv \\ &= P_{\text{tx}}^{\varrho_j}(1-P_{\text{tx}})^{I-\varrho_j}\int_{\frac{u_0}{2\sigma_{0j}}}^{\infty}\frac{1}{\sqrt{2\pi}}\exp\Big(-\frac{\omega^2}{2}\Big)d\omega \\ &= P_{\text{tx}}^{\varrho_j}(1-P_{\text{tx}})^{I-\varrho_j}\Big(1-\Phi(\frac{u_0}{2\sigma_{0j}})\Big) = P_{\text{tx}}^{\varrho_j}(1-P_{\text{tx}})^{I-\varrho_j}\cdot\Phi\Big(\frac{-u_0}{2\sigma_{0j}}\Big), \end{aligned} \tag{5.25}$$

where $\sigma_{0j} = \sqrt{\frac{3}{4\pi R_{\text{se}}^3}\sum_{i=1}^{I} a_{k-i}^{(j)}u_i}$.

(2) a_k=1 but $\hat{a}_k$=0

With $a_k = 1$, to obtain the condition $L \geq 0$ in (5.19), it is required that:

$$n(t) \leq -\frac{u_0}{2}. \tag{5.26}$$

Given (5.14), the probability for the error pattern 'j' can be obtained as:

$$\begin{aligned} P_{\text{er}1j} &= P_{\text{tx}}^{\varrho_j}(1-P_{\text{tx}})^{I-\varrho_j}\int_{-\infty}^{-\frac{u_0}{2}}\frac{1}{\sqrt{2\pi}}\frac{1}{\sigma_{1j}}\exp\Big(-\frac{v^2}{2\sigma_{1j}^2}\Big)dv \\ &= P_{\text{tx}}^{\varrho_j}(1-P_{\text{tx}})^{I-\varrho_j}\int_{-\infty}^{-\frac{u_0}{2\sigma_{1j}}}\frac{1}{\sqrt{2\pi}}\exp\Big(-\frac{\omega^2}{2}\Big)d\omega \\ &= P_{\text{tx}}^{\varrho_j}(1-P_{\text{tx}})^{I-\varrho_j}\Big(1-\Phi(\frac{u_0}{2\sigma_{1j}})\Big) = P_{\text{tx}}^{\varrho_j}(1-P_{\text{tx}})^{I-\varrho_j}\cdot\Phi\Big(\frac{-u_0}{2\sigma_{1j}}\Big), \end{aligned} \tag{5.27}$$

where $\sigma_{1j} = \sqrt{\frac{3}{4\pi R_{\text{se}}^3}(\sum_{i=1}^{I} a_{k-i}^{(j)}u_i + u_0)}$.

Table 5.1: Model-II: error patterns and their probabilities for ISI length $I = 2$.

Index	ISI		Variance		Probability of each error pattern	
j	a_{k-2}	a_{k-1}	σ_{0j}^2	σ_{1j}^2	P_{e0j} (a_k=0 but $\hat{a}_k$=1)	P_{e1j} (a_k=1 but $\hat{a}_k$=0)
1	0	0	0	$\frac{3u_0}{4\pi R_{\text{se}}^3}$	0	$(1-P_{\text{tx}})^2 \cdot \Phi(\frac{-u_0}{2\sigma_{11}})$
2	0	1	$\frac{3u_1}{4\pi R_{\text{se}}^3}$	$\frac{3(u_1+u_0)}{4\pi R_{\text{se}}^3}$	$P_{\text{tx}}(1-P_{\text{tx}}) \cdot \Phi(\frac{-u_0}{2\sigma_{02}})$	$P_{\text{tx}}(1-P_{\text{tx}}) \cdot \Phi(\frac{-u_0}{2\sigma_{12}})$
3	1	0	$\frac{3u_2}{4\pi R_{\text{se}}^3}$	$\frac{3(u_2+u_0)}{4\pi R_{\text{se}}^3}$	$P_{\text{tx}}(1-P_{\text{tx}}) \cdot \Phi(\frac{-u_0}{2\sigma_{03}})$	$P_{\text{tx}}(1-P_{\text{tx}}) \cdot \Phi(\frac{-u_0}{2\sigma_{13}})$
4	1	1	$\frac{3(u_1+u_2)}{4\pi R_{\text{se}}^3}$	$\sum_{i=0}^{2} \frac{3u_i}{4\pi R_{\text{se}}^3}$	$P_{\text{tx}}^{\ 2} \cdot \Phi(\frac{-u_0}{2\sigma_{04}})$	$P_{\text{tx}}^{\ 2} \cdot \Phi(\frac{-u_0}{2\sigma_{14}})$

(3) Bit Error Rate

The BER can be derived by:

$$\begin{aligned} P_{\text{er}} &= (1-P_{\text{tx}})P_{\text{er0}} + P_{\text{tx}}P_{\text{er1}} \\ &= (1-P_{\text{tx}}) \sum_{j=1}^{2^I} P_{\text{er0}j} + P_{\text{tx}} \sum_{j=1}^{2^I} P_{\text{er1}j}, \end{aligned} \tag{5.28}$$

where $P_{\text{er0}} = \sum_{j=1}^{2^I} P_{\text{er0}j}$, and $P_{\text{er0}j} = \sum_{j=1}^{2^I} P_{\text{er0}j}$. Table 5.1 is an example showing the probability of each error pattern for $I = 2$. Comparing the probability calculated by (5.25) and (5.27), it is easy to obtain that $P_{\text{er0}j} < P_{\text{er1}j}$ due to $\sigma_{0j} < \sigma_{1j}$. Thus, the BER can be reduced by trying to decrease the probability of '1' transmitted, P_{tx}.

5.3.2 Capacity analysis

The capacity calculation method for the Model-II is the same as the method for the Model-I, just with different expressions of error probabilities. Thus, as is derived in Section 2.3.2, the capacity for infinity ISI length I can be computed by substituting (5.25), (5.27), (5.28) and (2.29) into (2.28). For Memory Limited Channel (MLC) with finite ISI length I, the capacity can be obtained by substituting (5.25), (5.27),

Table 5.2: Parameter assignment to analyse the performance of Model-II

1.	The sensing radium of the Rx	R_{se}	$0.5\,\mu\text{m}$
2.	The distance between Tx and Rx	d	$1 \sim 3\mu\text{m}$
3.	The diffusion coefficient	D	$10^{-3}\mu\text{m}^2\,\mu\text{s}^{-1}$
4.	The emission duration	T_{em}	$100 \sim 2000\mu\text{s}$
5.	The pulse period	T_{pd}	$5000\,\mu\text{s}$
6.	The number of transmitted molecules	m	$10^3 \sim 10^5$

(5.28) and (2.29) into (2.31).

5.4 Numeral results

In this section, both theoretical and simulated results are presented. For simulations, the Tx emits molecules periodically. Such molecules spread out and form a concentration distribution in the environment. The Rx samples the concentration around itself at time T_{sa} in each period, based on which, the Rx determines whether '1's or '0's are transmitted. The times of simulation trials are based on the theoretically derived results. For example, if the theoretical BER is 10^{-4}, then 10^8 successive bits are utilised to carry out the corresponding simulations. All results are presented with a common set of parameters assigned in Table 5.2. These values agree with the ones used throughout the thesis and the research in [44, 55, 79].

It should be noticed that when ISI length I increases, not only the computation of the BER and capacity increases exponentially, but also simulations will become more complex to be performed. Especially, if I is infinite, it is impossible to obtain the required results. Thus, the channel considered herein is an MLC with a finite I. The value of I used in this chapter has been greatly increased compared with all existing literatures, and we believe it is sufficiently large for the MC system analysis. If further results for larger I are required, readers could compute the BER and capacity based on the description in Chapter 2 and Chapter 5.

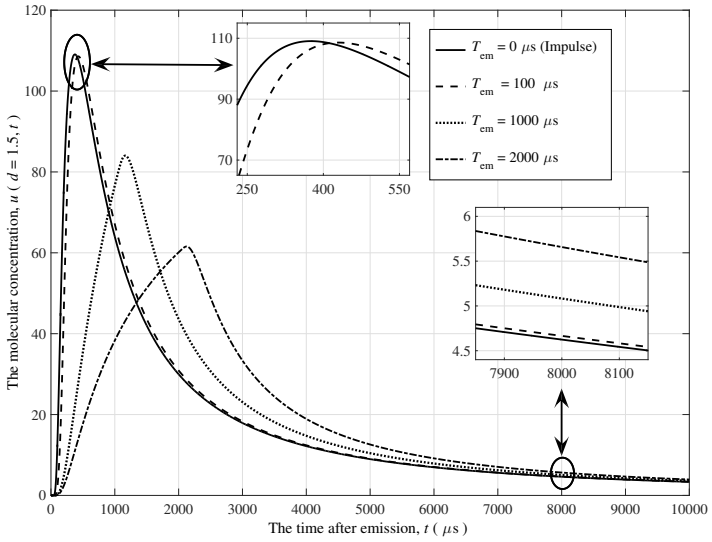

Figure 5.2: The changing concentration over time for different T_{em} at $d = 1.5\,\mu\text{m}$ with $m = 5 \times 10^3$.

5.4.1 The concentration with different emission durations

The Fig. 5.2 shows the concentration around the Rx changes with respect to time. It can be noticed that the emission duration T_{em} is influential to the concentration distribution. Firstly, the rising T_{em} will lead to the decrease in the peak concentration u_0. The increase of T_{em} means the Tx emits molecules more slowly, and these molecules start to propagate to the infinite border immediately upon being released. By the time Tx finishes the emission, a certain amount of molecules have diffused widely in the environment. Thus, the peak concentration around the Rx would be correspondingly smaller.

Secondly, the rising T_{em} will result in an increasing concentration tail after one pulse period, namely $u_i, i = 1, 2, ..., I$. It has been explained that a smaller u_0 will be obtained by enlarging T_{em}. Accordingly, the concentration gradient is gentler, and therefore after the peak time, molecules will diffuse to the infinite border in a lower speed, which means the attenuation of the concentration will be correspondingly slower. As a consequence, the concentration tail will be enlarged.

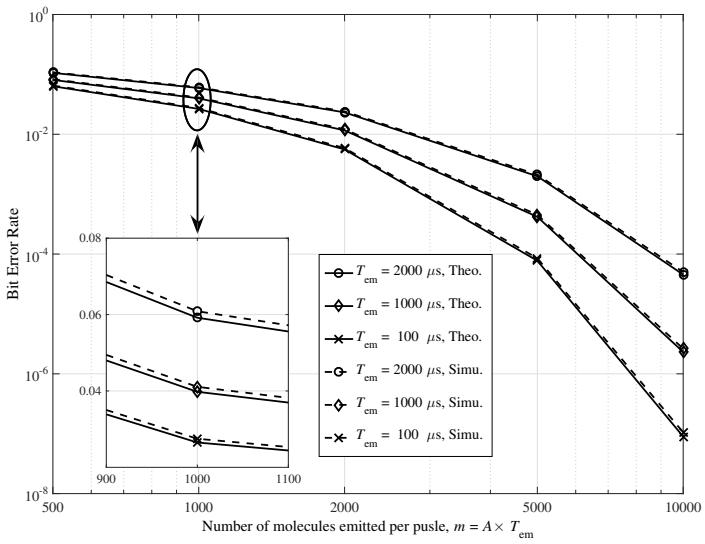

Figure 5.3: BER vs. m for different T_{em} at $d = 1.5\,\mu\text{m}$ with $I = 20$.

Referring to (5.23), either the decrease of the peak concentration (u_0) or the increase of the tail ($u_i, i = 1, 2, ..., I$) will lead to a smaller SNR. Then, it can be deduced that the MC system with a large T_{em} will suffer from a worse performance, which agrees with the curves shown in Figs. 5.3 to 5.4.

5.4.2 Performance analysis for Model-II at one distance

Results for the performance analysis at one single distance ($d = 1.5\,\mu\text{m}$) are presented in Figs. 5.3 to 5.7, and the performance evaluation at different distances will be shown later. It can be seen that the BER and capacity are mainly influenced by three factors, namely, the number of molecules emitted per pulse (m), the emission duration (T_{em}), and the ISI length (I). According to (5.20) through (5.23), the change of these three parameters affects the SNR of the channel, which will have a corresponding impact on the channel performance in terms of the BER and capacity.

To be specific, through Figs. 5.3 to 5.7, increasing m will help the system to suffer less from errors and achieve a higher capacity. The reason is that with more molecules emitted per pulse, the system will have a stronger resistance against the

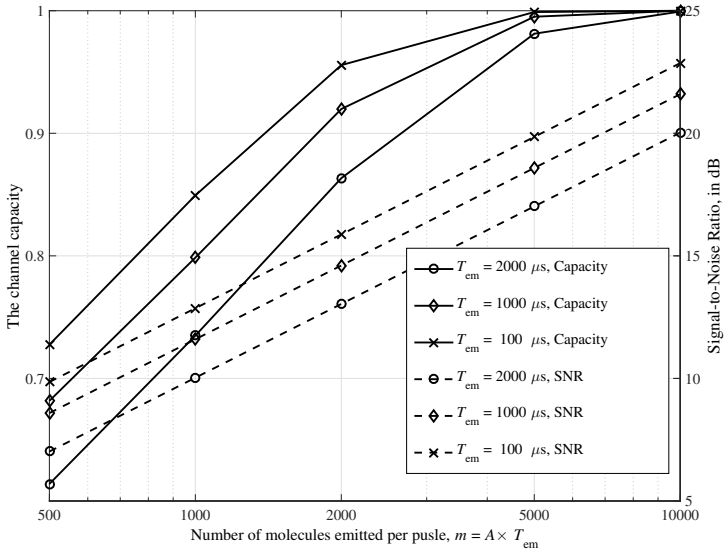

Figure 5.4: Capacity and SNR vs. m for different T_{em} at $d = 1.5\,\mu\text{m}$ with $I = 20$.

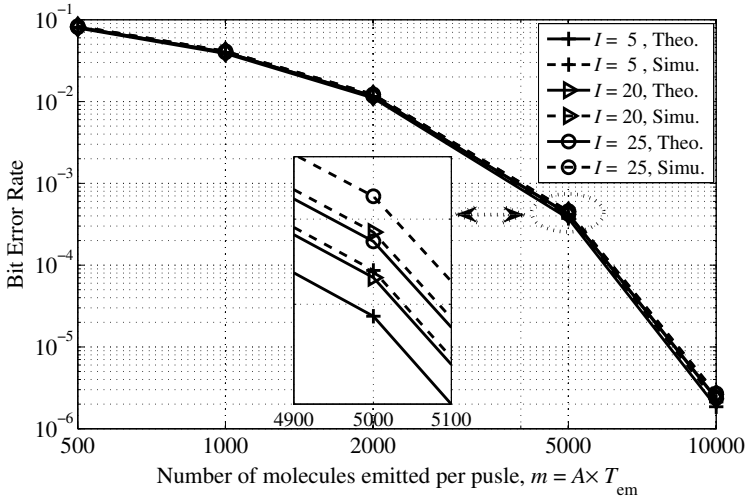

Figure 5.5: BER vs. m for different I at $d = 1.5\,\mu\text{m}$ with $T_{\text{em}} = 1000\,\mu\text{m}$.

noise and ISI. Referring to (5.20) through (5.23), amplifying m leads to a larger SNR, which guarantees a better performance.

The change in T_{em} will also affect the BER and capacity of the system. In Figs. 5.3 and 5.4, decreasing T_{em} leads to a smaller BER and higher capacity. As is explained in Section 5.4.1, the reduction of T_{em} brings about a larger SNR. Thus, if

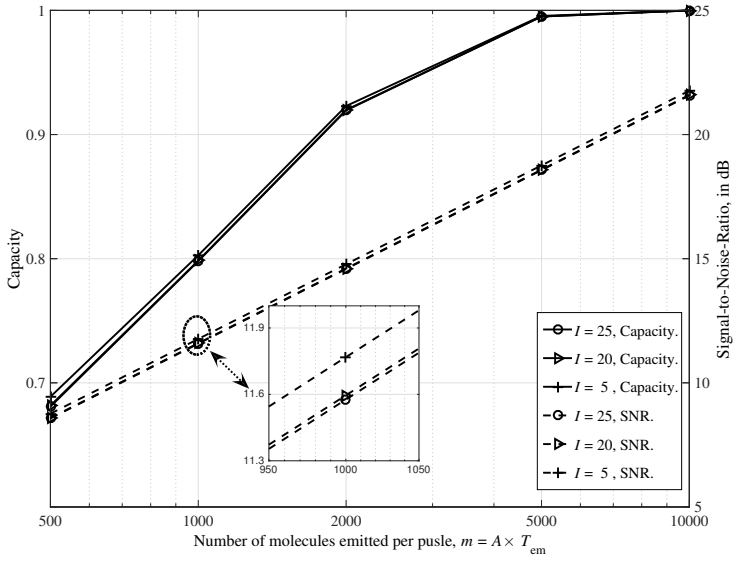

Figure 5.6: Capacity and SNR vs. m for different I at $d = 1.5\,\mu\text{m}$ with $T_{\text{em}} = 1000\,\mu\text{m}$.

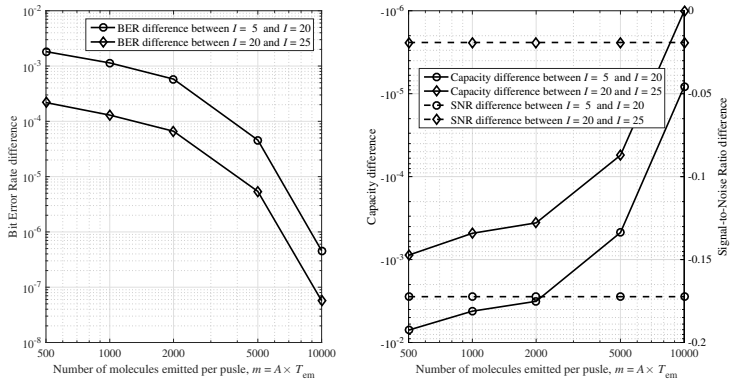

Figure 5.7: The corresponding difference of BER, capacity, and SNR for increasing I at $d = 1.5\,\mu\text{m}$ with $T_{\text{em}} = 1000\,\mu\text{m}$.

the Tx emits molecules as fast as possible, the channel performance can be enhanced.

Another factor that influences the system is the ISI length. Although the influence of the ISI has been mitigated by implementing the MSE decoding method described through (5.16) to (5.19), it can be deduced from (5.14) that the remaining concentrations of previous bits will still affect the channel performance by contribut-

ing to the noise effect. If the ISI can be further alleviated, a smaller BER and higher capacity will be obtained. This shows agreement with the results in the Figs. 5.6 and 5.7 that the decrease of I also results in a larger SNR because molecules vanish more quickly so that less influence will be brought onto the upcoming signals. Moreover, as is also clearly shown here, there is no significant difference in performance between $I = 15, 20$, and 25. Thus, considering the fact that with I rising, the complexity of both the computation of BER and capacity and MATLAB simulations increase exponentially, $I = 20$ is sufficiently large for the system performance analysis.

It should also be noticed that the simulated BER is slightly higher than the theoretical BER even if the deviation is almost negligible. This also happens for the performance analysis of the system Model-I, which has been explained in Section 2.4. Similarly, the main reason for the deviation herein is due to the assumption "previously decoded bits will not affect the decoding procedure of the current bit" when deriving the theoretical formulas. However, this assumption does not hold during simulations where one wrongly decoded bit will affect the decoding of next several symbols. Thus, for simulation, errors often occur in succession, which is known as the *error propagation*. Additionally, during simulations, there is a chance that the concentration may burst into a high value and it takes time to recover to a normal level, which also affects the decoding of next several symbols. This also causes the error propagation. Thus, the existence of the error propagation leads to a higher BER for simulations.

5.4.3 Performance analysis for Model-II at different distances

The performance evaluation at different distances is presented in Figs. 5.8 and 5.9. As is clearly shown, with the distance d getting larger, the system trends to suffer from a higher BER and correspondingly lower capacity. When d increases, it can be deduced from (5.11) that fewer molecules will arrive at the Rx. In this case, any

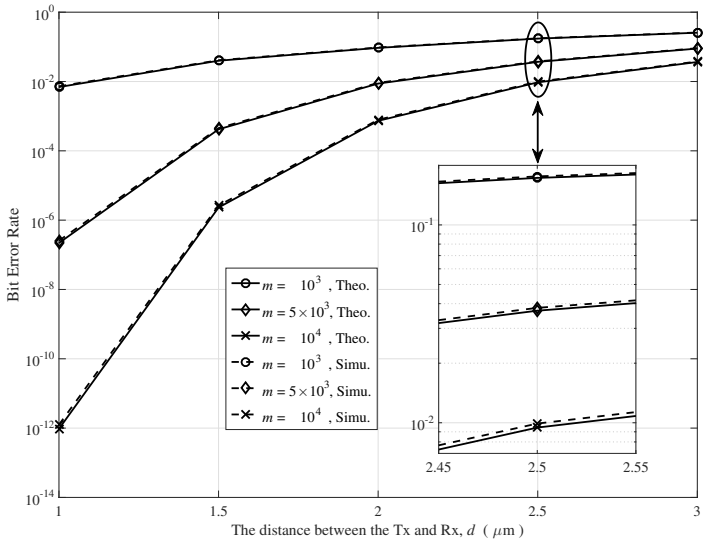

Figure 5.8: BER vs. d for different m with $T_{\text{em}} = 1000\,\mu\text{m}$ and $I = 20$.

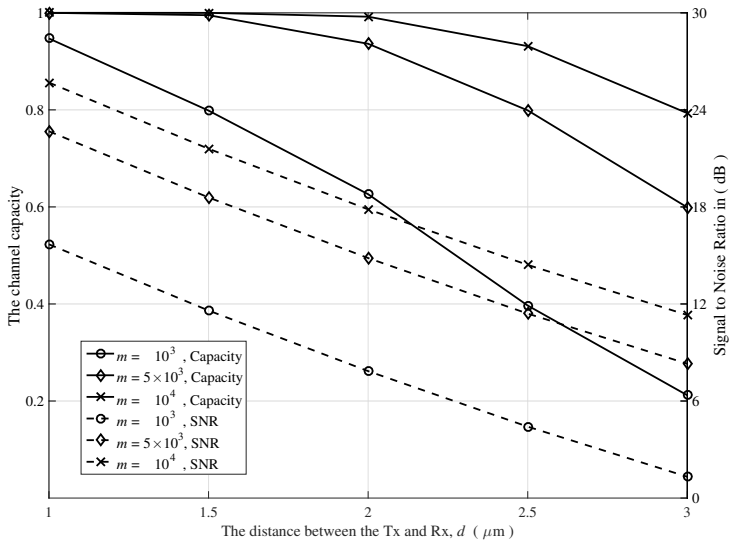

Figure 5.9: Capacity and SNR vs. d for different m with $T_{\text{em}} = 1000\,\mu\text{m}$ and $I = 20$.

slight change of the concentration will significantly affect the decoding process of the Rx, which can be also explained as the system has a smaller SNR according to (5.20) through (5.23). Thus, the system will have a weak resistance against the influence of the noise and ISI.

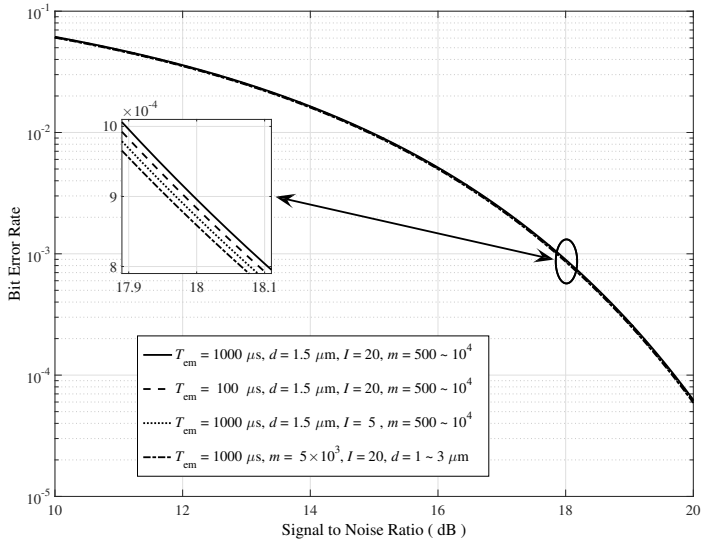

Figure 5.10: BER vs. SNR for different m, d, I, and T_{em}.

An important but not intuitive feature shown throughout Figs. 5.3 to 5.9 is that no matter how parameters are selected, the performance almost remains the same if the system SNR keeps constant. An example is shown in the Fig. 5.10 where the BER for MC systems with different parameters are presented. As is illustrated here, although the assignment of parameters varies, the difference in the error probabilities of MC systems with the same SNR is so small that can be neglected. Therefore, the SNR, defined in (5.23), can be considered as a reasonable metric to evaluate the diffusive concentration-based MC system performance.

5.5 Conclusions

In this chapter, a mathematical method has been developed to evaluate the system performance of the Model-II. The impact of the Tx emission process has been taken into account, as well as the influence of the channel noise and memory. At the Rx, a decoding method by calculating the MSE is utilised to alleviate the ISI as remaining concentrations of previous symbols within the ISI length have been considered

when conveying messages. Expressions of the BER and channel capacity have been derived and simulations are also designed accordingly to verify the accuracy of these analytical formulations. Results reveal the agreement between theoretical and simulated BER, and the cause of the slight deviation in between has been explained. Furthermore, as is also illuminated, the BER and capacity are highly dependent on the number of molecules emitted per pulse (m), the emission duration (T_{em}), the ISI length (I) and the distance between the Tx and Rx (d). After establishing the Model-II, further research on MC systems can be carried out, such as the distance estimation schemes in Chapter 6, and the relaying system analysis in Chapter 7.

Chapter 6

Distance estimation schemes based on system Model-II

6.1 Introduction

In Chapter 5, the diffusive Molecular Communication (MC) system Model-II is developed. Message symbols are encoded by the source nano-machine into the molecular concentration, which changes with regards to the time and distance. The target nano-machine samples the concentration around itself, and determines the transmitted information bits accordingly. The system performance, measured by the Bit Error Rate (BER) and the channel capacity, is analysed by both theoretical derivations and simulations. Similar to the reasons explained in Chapter 3, the distance between two nano-machines is an essential parameters for the MC system, due to the fact that distance will have a great influence on the system performance. One additional cause for the significance of the distance for the system Model-II is that the target nano-machine needs to coordinate the sampling time and decision variables to make better decisions on the incoming bits. How to design the sampling time and decision variables is introduced in Section 5.2, and will be further discussed in this chapter.

Relative research has been briefly mentioned in Section 3.1, and will be described in detail as follows. The first attempt to investigate the distance estimation method was in [94], and this idea was expanded in [95, 96]. In these literature, four estimation schemes were proposed based on feedback protocols in a 2D channel. The distance is determined by means of tracking the round-trip time or the fading of the signal amplitude (or frequency). These schemes are heuristic, but the estimation suffers from a low accuracy and a high time cost. Another two estimation schemes proposed in [97] only suited for the 1D situation, where the nano-machine measured either the peak concentration or the time interval between the first and second peak to estimate the distance. By using these two schemes, the time cost is significantly decreased, but no intuitive benefit on accuracy is presented. In [114], an approach for bounding the estimation accuracy was described to provide a possible method to evaluate distance estimation schemes. However, this bound is only accessible with certain optimal criteria, which means this approach can be only served as the guide for finding optimal estimation protocols rather than as a specific estimation scheme. Motivated by these research, advanced distance estimation schemes should be developed which enjoy a higher accuracy, consume less time, and suit for the 3D scenarios.

In this chapter, two distance estimation schemes are proposed to estimate the distance between two nano-machines for a 3D concentration-based MC system. The source nano-machine senses the surrounding concentration, and determines the distance according to either the concentration peak time or the concentration energy. Simulations are carried out to compare the performance of each scheme and to discover how it will be influenced by different designs of channel parameters. Results show that compared with all aforementioned researches, the estimation can be more accurate by implementing either of these two schemes introduced herein, and using energy to measure distance will provide a further enhancement on the accuracy.

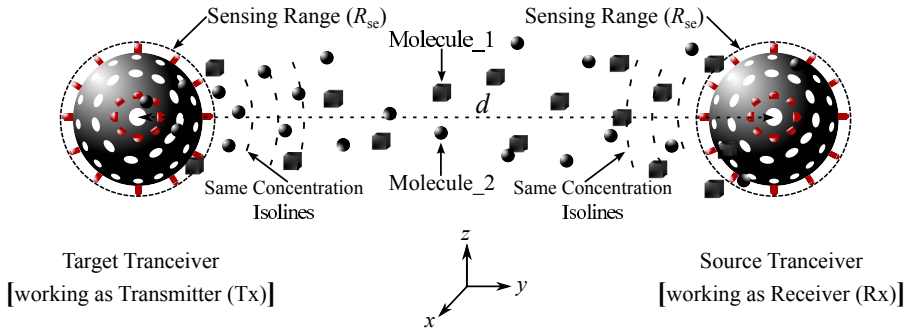

Figure 6.1: The structure of the MC system.

The remainder of this chapter is organised as follows. In Section 6.2, the concentration-based MC system structure is introduced. The distance estimation schemes and their simplification methods are explained in Section 6.3. Simulations and comparisons of results are provided in Section 6.4. Finally in Section 6.5, this chapter is concluded.

6.2 Concentration-Based MC System Structure

The diffusive MC system considered herein is on the basis of the system Model-II, where messages are expressed by molecular concentrations. The only difference is that this system consists of two transceiver nano-machines, which can both release encoded molecules and sense the surrounding concentration to determine the incoming information symbols. As is shown in the Fig. 6.1, the source nano-machine periodically sends out molecules (represented as Molecule_1)to accomplish the communication to the target nano-machine. However, before the establishment of this communication, the distance between these two nano-machines should be measured, so that accordingly, the source nano-machine can adjust both the number of molecules emitted per pulse and the transmission period, and the target nano-machine can set up the sampling time as will as the decision variables.

The distance is determined by taking the advantage of molecules emitted by the target nano-machine, which is denoted as (Molecule_2). Similar to the sit-

uation in Section 3.2, two kinds of molecules are utilised for the purpose that the distribution and reception of 'estimation' molecules (Molecule_2) can be treated to be free from the influence of 'message' molecules (Molecule_1). During the distance estimation process, the target nano-machine is considered as the Tx, and the source nano-machine is considered as the Rx. The Tx emits a single pulse of molecules, and the Rx is designed to keep sensing the concentration all the time until it can determine the distance. Since both the nano-machines are spheres, it can be deduced that molecules can be viewed as being released from the centre of the nano-machines due to the symmetry [113]. Referring to the Fig. 6.1, the distance between the Tx and Rx is d, and the sensing range of nano-machines is R_{se}.

After being released from the Tx, molecules forms the concentration distribution in the environment. The noiseless concentration around the Rx for a single pulse, $u(d,t)$ is given by (5.11), and the channel noise expressed in (5.14) can be rewritten as:

$$n(t) \sim \mathcal{N}(0, \sigma^2), \tag{6.1}$$

where $\sigma^2 = \frac{3}{4\pi R_{\text{se}}^3} u(d,t)$. The Signal-to-Noise Ratio (SNR) of the MC system is defined as (5.23).

6.3 Distance estimation schemes

6.3.1 Using the peak time to estimate the distance

As is shown in the Fig. 6.2, the concentration distribution formed by molecules varies at different distances. The time when the concentration around the Rx peaks is named as the *peak time* and denoted as T_{pk}. It can be noticed that if the Rx is farther away from the Tx, it will take a longer time for the concentration to reach the peak value at the Rx. Thus, motivated by this phenomenon, the estimation

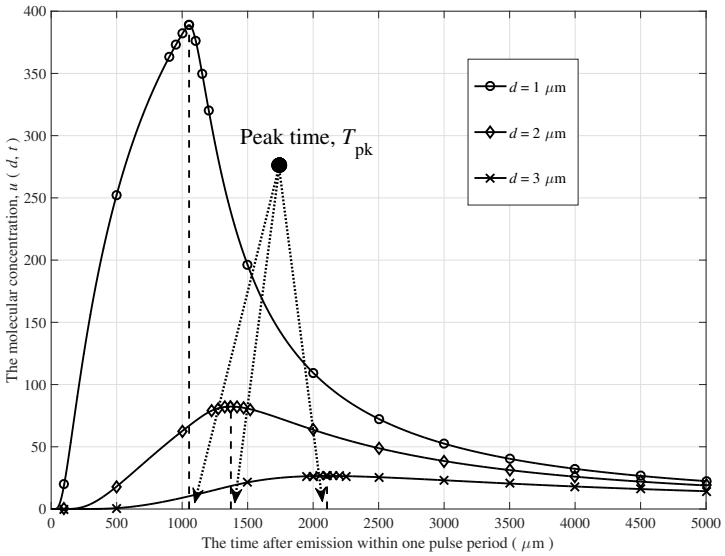

Figure 6.2: The peak concentration time illumination at different distances with $T_{\text{em}} = 10^3$µs and $T_{\text{em}} = 5 \times 10^3$µs.

scheme by means of measuring the peak time is proposed.

Considering $u(d,t)$ given as (5.11), by deriving the equation $\frac{\partial u(d,t)}{\partial t} = 0$, the relationship between the distance d and the peak time T_{pk} can be obtained. The peak time is the same as the sampling time described in Section 5.2, whose value can be calculated by (5.12). Thus, by rewriting the equation (5.12), the estimated distance, represented as $\hat{d}$, can be obtained as:

$$\hat{d} = \sqrt{\frac{6D}{T_{\text{em}}} \cdot (T_{\text{pk}} - T_{\text{em}}) \cdot T_{\text{pk}} \cdot \ln\left(\frac{T_{\text{pk}}}{T_{\text{pk}} - T_{\text{em}}}\right)}, \tag{6.2}$$

where D is the diffusion coefficient, and T_{em} is the emission duration.

Especially, if T_{em} is small, the estimation equation (6.2) can be simplified as:

$$\begin{aligned} \hat{d}_{\text{si}} &= \lim_{T_{\text{em}} \to 0} \hat{d} = \lim_{T_{\text{em}} \to 0} \sqrt{\frac{6D}{T_{\text{em}}} \cdot (T_{\text{pk}} - T_{\text{em}}) \cdot T_{\text{pk}} \cdot \ln\left(\frac{T_{\text{pk}}}{T_{\text{pk}} - T_{\text{em}}}\right)} \\ &= \sqrt{6 T_{\text{pk}} D}. \end{aligned} \tag{6.3}$$

This method enjoys great benefit for its simplicity. The Rx senses the concentration and picks out the peak time T_{pk}. Using (6.2) or (6.3), the distance can be estimated. However, due to the channel noise, it is quite hard to precisely find the peak time, which will influence the estimation accuracy.

6.3.2 Using the energy to estimate the distance

The energy of the signal in the MC system is defined as the sum of the molecular concentrations [39]. Given (5.11), the received noiseless energy, Ω_u, within one signal period, T_{pd}, can be obtained by:

$$\Omega_u = \int_0^{T_{\mathrm{pd}}} u(d,t)dt = \frac{Am}{4\pi dD}\left[\int_0^{T_{\mathrm{pd}}} \mathrm{erfc}(\frac{d}{\sqrt{4tD}})dt - \int_{T_{\mathrm{em}}}^{T_{\mathrm{pd}}} \mathrm{erfc}(\frac{d}{\sqrt{4(t-T_{\mathrm{em}})D}})dt\right] \tag{6.4}$$

If T_{em} is quite small, the input can be simplified as an impulse signal. Thus, the energy can be computed as [112]:

$$\begin{aligned}\Omega_{u,\mathrm{si}} &= \lim_{T_{\mathrm{em}}\to 0} \Omega_u \\ &= \frac{m}{4\pi Dd}\mathrm{erfc}\left(\frac{r}{2\sqrt{DT_{\mathrm{pd}}}}\right).\end{aligned} \tag{6.5}$$

The channel noise is a main factor that affects the accuracy of the distance estimation. To minimise the influence, adding all values of the sensed concentrations is a simple solution, because the noise has a zero mean [88]. Thus, given (5.15), the energy at the Rx can be derived as:

$$\Omega_r = \int_0^{T_{\mathrm{pd}}} r(d,t)dt = \int_0^{T_{\mathrm{pd}}} u(d,t)dt + \int_0^{T_{\mathrm{pd}}} n(t)dt \approx \int_0^{T_{\mathrm{pd}}} u(d,t)dt \tag{6.6}$$

Theoretically, using energy to estimate the distance provides better performance on the accuracy than using the peak time, but it has a higher requirement of

the complexity in the MC system. Both schemes can be simplified by decreasing the emission time, T_{em}, so that the system can be viewed as the impulse response. The performance comparisons between the two estimation schemes, respectively using the peak time and energy, and their simplification methods will be shown later in this chapter.

6.3.3 Applying the estimated distance to decode messages

Before transmitting messages to the target nano-machine, the source nano-machine measures the distance from itself to the target. After the estimation procedure is completed, the source nano-machine encodes information symbols with another kind of molecules (Molecule_1), whose distribution is free from influence of the molecules emitted by the target nano-machine, Molecule_2.

Given the peak time to be T_{pk}, the sampling time of the target nano-machine will be designed as T_{pk}. Thus, for the communications stage, the sampled concentration $r(d,t)$ can be expressed as:

$$\begin{aligned} r(d,t) &= \sum_{i=0}^{I} a_{k-i} u(d; t = T_{\text{pk}} + iT_p) + n(t) \\ &= \sum_{i=0}^{I} a_{k-i} u_{d,i} + n(t), \end{aligned} \tag{6.7}$$

where k represents the k^{th} symbol from the beginning of transmission, the set $\{a_{k-i}, i = 0, 1, ..., I\}$ is the binary messages sequence, and the element a_{k-i} represents the binary value of each symbol. The pre-designed criteria for the target nano-machine to decode message bits are respectively:

$$l_1 = \sum_{i=1}^{I} \hat{a}_{k-i} u(\hat{d}, t = T_{\text{pk}} + iT_{\text{pd}}) + u(\hat{d}, t = T_{\text{pk}}) = \sum_{i=1}^{I} \hat{a}_{k-i} u_{\hat{d},i} + u_{\hat{d},0}, \tag{6.8}$$

$$l_0 = \sum_{i=1}^{I} \hat{a}_{k-i} u(\hat{d}, t = T_{\text{pk}} + iT_{\text{pd}}) = \sum_{i=1}^{I} \hat{a}_{k-i} u_{\hat{d},i}. \tag{6.9}$$

Similarly, it is also assumed that $\hat{a}_{k-i} = a_{k-i}$ for $i = 1, 2, ..., I$. By substituting (6.7) through (6.9) into (5.16), L can be derived as:

$$L = -2u_{\hat{d},0}\Big[\sum_{i=1}^{I} a_{k-i}(u_{d,i} - u_{\hat{d},i}) + a_k u_{d,0} - \frac{1}{2}u_{\hat{d},0} + n(t)\Big]. \tag{6.10}$$

Similar to the derivation in Section 5.3.1, for the error pattern 'j', the permutation of values of $\{a_{k-i}, i = 1, 2, ..., I\}$ is denoted as $\{a_{k-i}^{(j)}, i = 1, 2, ..., I\}$, the number of '1's within $\{a_{k-i}^{(j)}, i = 1, 2, ..., I\}$ is denoted as ϱ_j, and accordingly, the number of '0's is $(I - \varrho_j)$. The probability of '1' transmitted is denoted as P_{tx}, and the probability of '0' transmitted is $(1 - P_{\text{tx}})$. Thus, the probability for the error pattern j can be obtained as:

$$P_{\text{er}1j} = P_{\text{tx}}^{\varrho_j}(1 - P_{\text{tx}})^{I-\varrho_j}\Phi(\frac{\tau_{1j}}{\sigma_{1j}}), \tag{6.11}$$

$$P_{\text{er}0j} = P_{\text{tx}}^{\varrho_j}(1 - P_{\text{tx}})^{I-\varrho_j}\Big(1 - \Phi(\frac{\tau_{0j}}{\sigma_{0j}})\Big), \tag{6.12}$$

where

$$\tau_{1j} = -\sum_{i=1}^{I} a_{k-i}^{(j)}(u_{d,i} - u_{\hat{d},i}) - u_{d,0} + \frac{1}{2}u_{\hat{d},0}, \tag{6.13}$$

$$\tau_{0j} = -\sum_{i=1}^{I} a_{k-i}^{(j)}(u_{d,i} - u_{\hat{d},i}) + \frac{1}{2}u_{\hat{d},0}, \tag{6.14}$$

$$\sigma_{1j} = \sqrt{\frac{3}{4\pi R_{\text{se}}^3}(\sum_{i=1}^{I} a_{k-i}^{(j)}u_{d,i} + u_{d,0})}, \tag{6.15}$$

$$\sigma_{0j} = \sqrt{\frac{3}{4\pi R_{\text{se}}^3}(\sum_{i=1}^{I} a_{k-i}^{(j)}u_{d,i})}. \tag{6.16}$$

Thus, the BER when the distance estimation scheme utilised can be computed by substituting (6.11) and (6.12) into (5.28). As to the channel capacity, the formulation is the same as the explanation in Section 2.3.2 just with different values for $P_{\text{er}1}$ and $P_{\text{er}0}$. The capacity for infinity ISI length I can be computed by substituting

Table 6.1: Parameters to simulate the distance estimation schemes for Model-II.

1.	The sensing radium of nano-machines	R_{se}	$0.5\,\mu\text{m}$
2.	The distance between the Tx and Rx	d	$1 \sim 3\mu\text{m}$
3.	The diffusion coefficient	D	$10^{-3}\mu\text{m}^2\,\mu\text{s}^{-1}$
4.	The emission duration	T_{em}	$50 \sim 1000\mu\text{s}$
5.	The pusle period	T_{pd}	$5000\,\mu\text{s}$
6.	The number of transmitted molecules	m	$10^3 \sim 10^4$

(6.11), (6.12), (5.28) and (2.29) into (2.28). For Memory Limited Channel (MLC) with finite ISI length I, the capacity can be obtained by substituting (6.11), (6.12), (5.28) and (2.29) into (2.31).

6.4 Numeral results

Simulations on MATLAB are carried out to implement these two distance estimation schemes into MC systems. The accuracy of these two schemes is evaluated by means of obtaining the distance estimation bias between the exact and estimated values of distances, which can be expressed as:

$$\text{Dev}_d = \hat{d} - d, \tag{6.17}$$

where $\hat{d}$ represents the estimated distance. Furthermore, the reliability of a MC system with distance estimation schemes implemented is also analysed with regards to the BER. Comparisons between systems with and without pre-knowledge of the distance are made to show how the system performance can be influenced by the estimation accuracy. All results presented herein are presented with a common set of parameters assigned in Table 6.1. These values agree with the ones used throughout the thesis and the research in [44, 55, 79].

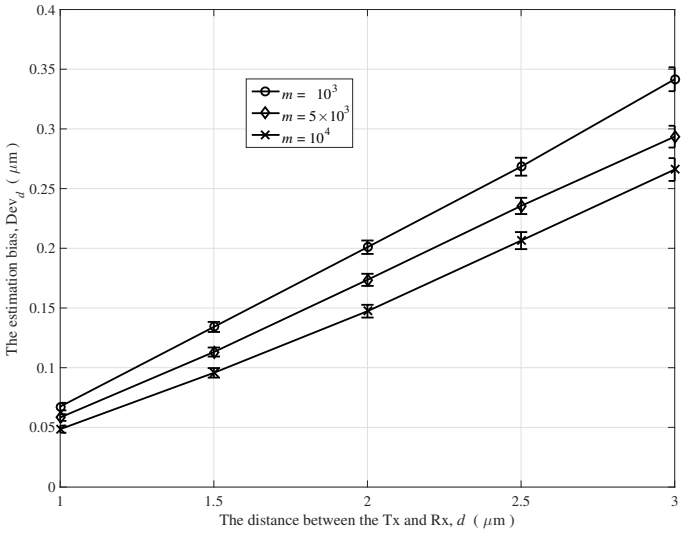

Figure 6.3: Using peak time, Dev_d vs. d for different m with $T_{\mathrm{em}} = 1000\,\mu\mathrm{s}$.

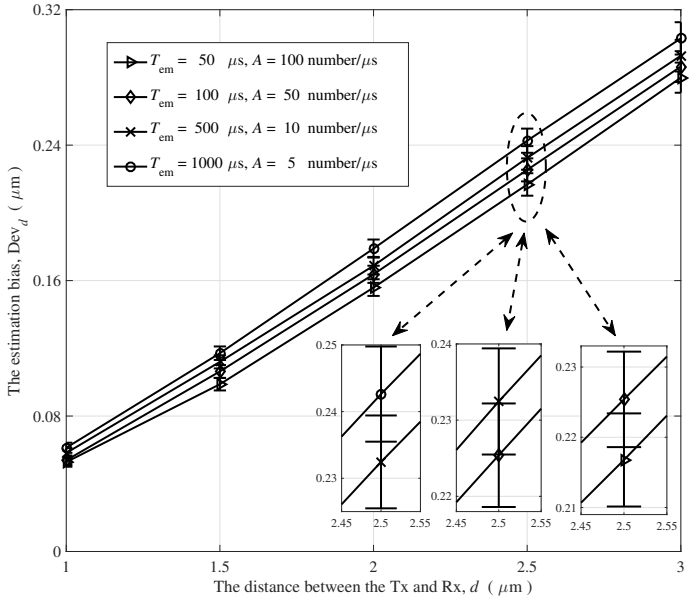

Figure 6.4: Using peak time, Dev_d vs. d for different A and T_{em} with $m = A \times T_{\mathrm{em}} = 5 \times 10^3$.

6.4.1 Using the peak time to estimate the distance

In Figs. 6.3 to 6.4, it is clearly illuminated that this estimation scheme works well. It can be noticed that the accuracy is mainly affected by three parameters, namely,

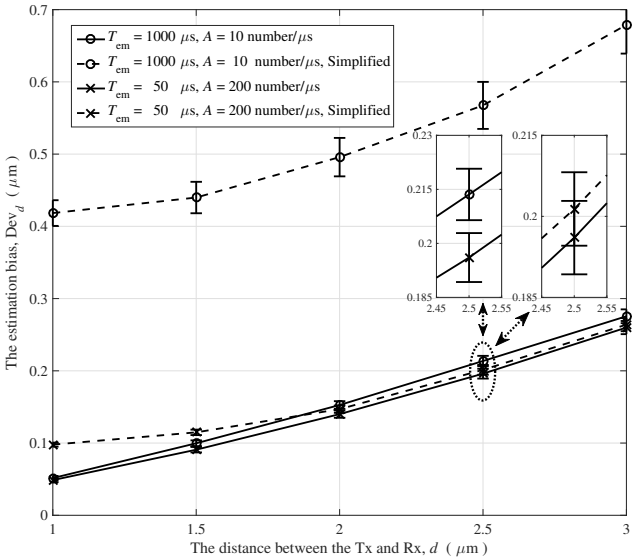

Figure 6.5: Using peak time, Dev_d vs. d for original and simplified schemes with $m = A \times T_{\mathrm{em}} = 10^4$.

the distance d, the emission duration T_{em}, and the number of utilised molecules m. Different selections of these parameters will result in a different concentration around the Rx and a corresponding different system SNR. Thus, the estimation performance varies depending on the designing of each parameter.

To be specific, as is explained in Chapter 5, a larger peak concentration u_0 can be obtained by decreasing the distance d, enlarging the number of molecules emitted per pulse m, or reducing the emission duration T_{em}. Under this circumstance, the system SNR has been increased, which makes the estimation procedure less susceptible to the influence of the noise. In other words, the system has a stronger resistance to the noise, so that the peak time can be more accurately determined. Therefore, the estimation performance is enhanced correspondingly. It can be deduced that the larger the SNR is, the less significant the influence of the noise will become, and the higher the achieved estimation accuracy can be.

In the Fig. 6.5, results of the simplified estimation scheme are compared with the original scheme. Obviously, when T_{em} is so small to be negligible (in this

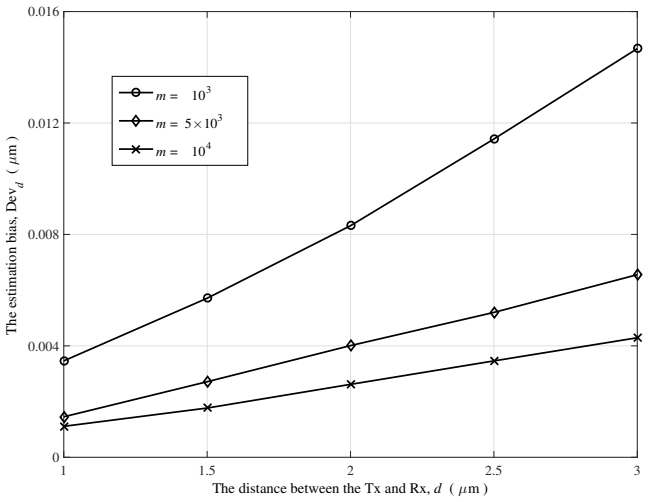

Figure 6.6: Using energy, Dev_d vs. d for different m with $T_{\mathrm{em}} = 1000\,\mu\mathrm{s}$.

case $T_{\mathrm{em}} = 50\,\mu\mathrm{m}$), the performance using the simplified scheme is almost as good as the one using original scheme; but when T_{em} is not able to be neglected, the bias increases greatly, which means the simplified method is not suitable for this case.

Results in Figs. 6.3 to 6.5 show that both the original and simplified estimation schemes perform well in the MC system, and the simplified scheme can estimate the distance as accurately as the original scheme if T_{em} is quite small. To get the best performance, the target nano-machine is required to emit sufficient molecules as fast as possible.

6.4.2 Using the energy to estimate the distance

As is shown in Figs. 6.6 and 6.7, the performance of this estimation scheme is more desirable than the scheme using the peak time. Similarly, the accuracy for this scheme goes down with a larger d, a smaller m, or a longer T_{em} due to the reduce of the system SNR. However, the decrease of the accuracy is not significantly severe. This is mainly due to the superiority that the Rx offsets the influence of the noise by adding all the sensed concentrations.

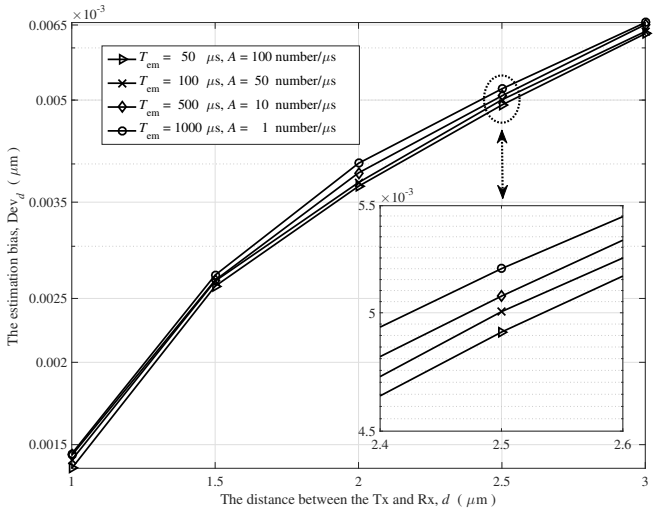

Figure 6.7: Using energy, Dev_d vs. d for different A and T_{em} with $m = A \times T_{\mathrm{em}} = 5 \times 10^3$.

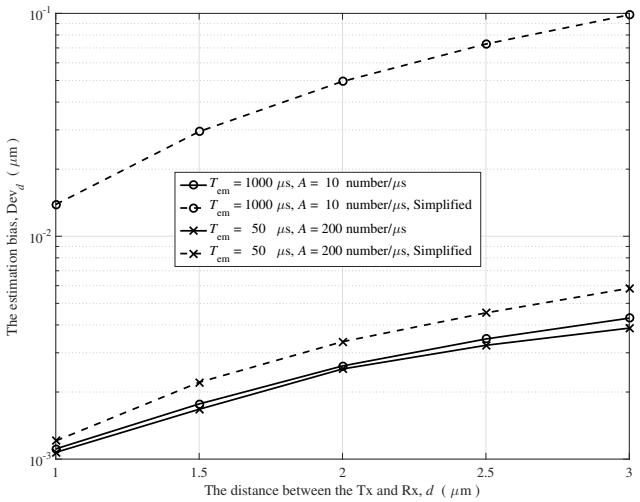

Figure 6.8: Using energy, Dev_d vs. d for original and simplified schemes with $m = A \times T_{\mathrm{em}} = 10^4$.

Performance of the corresponding simplified estimation scheme is shown in the Fig. 6.8. Similar to the situation described in Section 6.4.1, when T_{em} is small, using the simplified method can be as accurate as the original method, but if T_{em} is large, the difference between the simplified and original schemes can not be

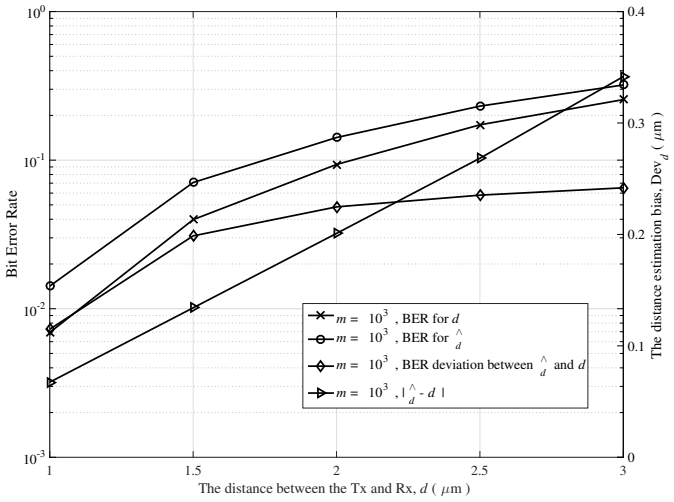

Figure 6.9: BER and Dev_d vs. d with $m = 1000$.

neglected. Furthermore, considering the results shown through Figs. 6.3 to 6.8, it is clear that using energy to estimate the distance, even the simplified scheme, will provide a much better performance than using the peak time.

6.4.3 System BER analysis with distance estimation scheme applied

The performance evaluation at different distances is presented in Figs. 6.9 and 6.10. As is clearly shown, with d rising, the distance estimation accuracy goes down, leading to a larger difference in the BER between the system with and without pre-knowledge of the distance. It can therefore be deduced that by improving the estimation accuracy, there will be less error occurrence in the system. An obvious method to enhance the performance is to increase the SNR of the MC system. With a larger SNR, not only can the estimation be more accurate, but also the system will suffer less from the impact of the channel noise and memory. It can be further deduced from Section 5.4 that three options can be applied to increase the SNR, i.e., increasing m, decreasing T_{em}, and further mitigating the influence of the ISI.

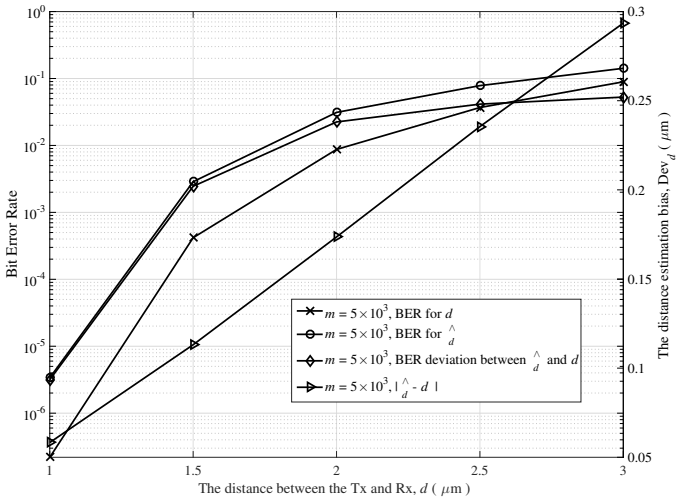

Figure 6.10: BER and Dev_d vs. d with $m = 5000$.

6.5 Conclusions

In this chapter, two distance estimation schemes and their own simplification methods have been introduced. The performance is analysed mainly with regards to the accuracy in terms of the estimation bias. Simulation results show that these proposed schemes can provide reasonable accuracy with well-designed parameters such as T_{em} and m. Using energy to measure the distance enjoys a much more accurate estimation, but has a much higher requirement on the system complexity to compute the distance, which may limit the implementation of this estimation scheme. Moreover, the scheme using the peak time to determine the distance is applied into a MC diffusive system with information expressed by the molecular concentration. This is the first investigation on the performance of MC systems with the distance unknown for nano-machines. Comparisons between distance-pre-known systems and distance-unknown systems have been made, and results reveal that the performance can be enhanced by three methods, sending out more molecules, releasing in a faster rate, and mitigating the influence of the ISI.

Chapter 7

Performance analysis of the relaying MC system based on Model-II

7.1 Introduction

In Chapter 5, the concentration-based diffusive Molecular Communication (MC) system model, namely Model-II, is introduced, and the system performance is evaluated with regards to the Bit Error Rate (BER) and channel capacity by means of both theoretical deviations and simulations. Numerical results presented in Section 5.4 and in other research like [43, 64, 82], intuitively illuminate that BER increases with the rising distance between the transmitter (Tx) and receiver (Rx) due to the severe attenuation of the molecular concentration. Thus, for long-range communications, the channel reliability still remains a key challenge.

To solve this problem, a relay node (RN) can be implemented into the system to assist the transmission and reception of messages molecules. Equivalently, the distance between a pair of communicating nano-machines has been reduced. Consequently, the entire MC system may tend to suffer less from symbol errors. The first

attempt to investigate the relaying system was shown in [69], and further expanded to investigate the performance improvement of Decode-and-Forward (DF) relaying schemes in [115, 116] and Sense-and-Forward (SF) relaying schemes in [117, 118]. However, these schemes were implemented in an MC system with steady-state concentrations. For each symbol transmitted, the Tx had to keep emitting molecules continuously and the theoretical period must be infinite. Hence, this is undesirable, as not only is the transmission rate lowered, but the idea of a continuous and infinitely-lasting emission, raises practical concerns. Conversely, the only publication on relay systems with the time-dependent concentrations can be found in [119]. However, the transmission model needs refined by considering the emission process and clarifying the noise influence. A decoding method to mitigate the Inter-Symbol Interference (ISI) can also be utilised.

In this chapter, a DF relaying scheme is implemented onto the system Model-II, which has been analysed in Chapter 5. Time-dependent molecular concentrations are utilised as the information carrier, which will be influenced by the noise and channel memory. The RN can decode messages, and forward them by using either the same kind of molecules or a different kind of molecules as the Tx sends. Within the emission duration, molecules are viewed to be released in a constant rate by the Tx and RN, rather than emitting simultaneously like in all the aforementioned literature. The decoding algorithm of the RN and Rx is to determine symbols by means of calculating the Mean Square Error (MSE). The system reliability, represented by the BER, is evaluated by deriving theoretical expressions as well as through simulations. Furthermore, the impact of positions of the RN on relay systems performance is also investigated. The optimal positions of the RN have been obtained through simulations according to different initial conditions. Both theoretical and simulated results show that the relaying scheme will bring significant benefits to the communication reliability.

The remainder of this chapter is organised as follows. In Section 7.2, the

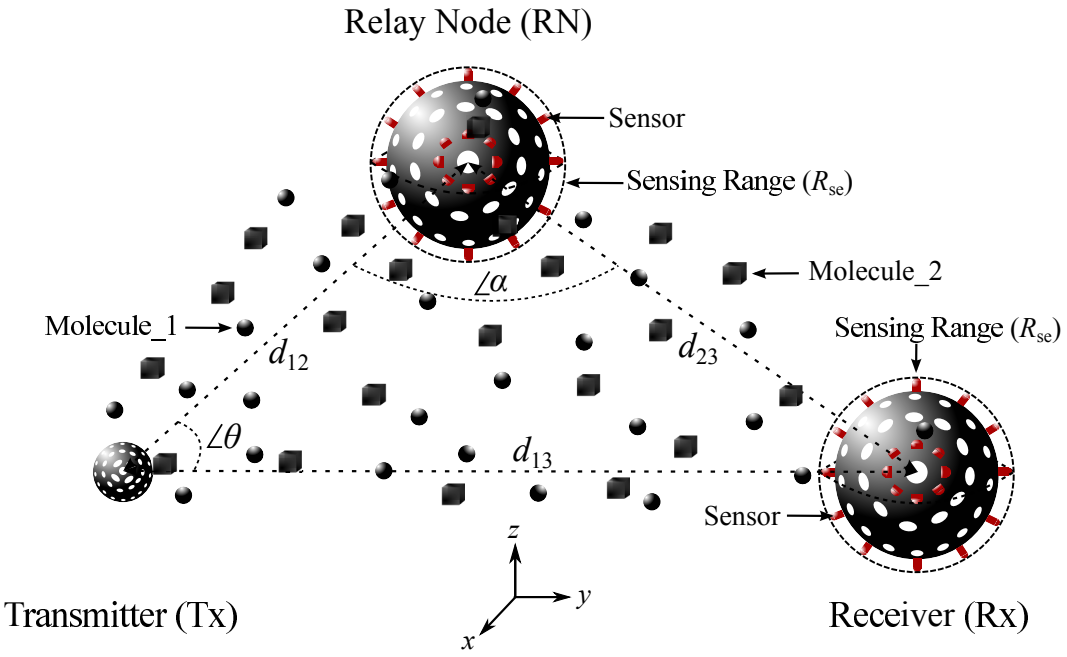

Figure 7.1: The structure of the MC relay system.

relaying system model is introduced. The system performance is studied in Section 7.3. Simulation description and numerical results are provided in Section 7.4. Finally in Section 7.5, the chapter is concluded.

7.2 Relaying system structure

The relaying MC system considered herein is based on the system Model-II described in Chapter 5. As is shown in the Fig. 7.1, the relaying system consisting of three nano-machines. The transmitter nano-machine (Tx) periodically releases a fixed amount of certain molecules (named as Molecule_1) to convey a sequence of message symbols. These molecules diffuse in the environment and form a time-dependent concentration gradient. The DF relay node (RN) senses the surrounding concentration, determines the information bits correspondingly, and forwards these bits to the receiver (Rx) at the destination end. The RN can use the same kind of molecules as the Tx (i.e. Molecule_1) to forward these messages, or can use a

different kind of molecules (named as Molecule_2). If Molecule_1 are utilised by the RN, molecules emitted by the Tx and RN will affect the concentration distribution of each other. As a consequence, molecules released by the RN will have an impact on the decoding process of itself, and molecules released by the Tx will influence the decoding procedure of the Rx. This is known as the *self interference*. If Molecule_2 are used by the RN, then these two kinds of molecules can diffuse separately, which means they will not affect the concentration distribution of each other. In this way, the self interference can be avoided. The performance analysis of these two scenarios will be discussed respectively later in this chapter.

In this MC system, the size of the Tx is negligible compared with the relative distance between nano-machines. Similar to the assumption made in Chapter 5 and Chapter 4 , the concentration at the RN or Rx can be considered as the concentration at the centre of the sphere. Referring to the Fig. 7.1, the distances between the Tx, RN, and Rx are respectively d_{12}, d_{13} and d_{23}. The angle between d_{12} and d_{13} is represented by θ, and the angle between d_{12} and d_{23} is represented by α. The sensing ranges of the RN and Rx are both R_{se}. The decoding algorithm of calculating the MSE is same as the mechanism explained by Section 5.2, with the decision variable given by (5.16).

Considering the emission process of the source nano-machine and the influence of the channel memory and noise, the molecular concentration formed by message molecules can be expressed as (5.11) through (5.15). The sampling time of the target nano-machine can be obtained as (5.12). By substituting the values of parameters d_{12}, d_{13}, d_{23} into these equations, the corresponding sampling time of the RN and Rx can be obtained, and the concentrations around RN and Rx can be also determined. Thus, the sampling time of the RN is represented as $T_{\text{sa,RN}}$, and the sampling time of the Rx is represented as $T_{\text{sa,Rx}}$. It is further denoted that for the i^{th} signal period, where $i = 0, 2, ..., I$, the RN-sampled concentration of the molecules emitted by only the Tx is expressed as $u_i^{(12)} = u\big(d = d_{12}, t = T_{\text{sa,RN}} + i \times T_{\text{pd}}\big)$, the Rx-

sampled concentration of molecules emitted by only the RN is expressed as $u_i^{(23)} = u\big(d = d_{23}, t = T_{\text{sa,Rx}} + i \times T_{\text{pd}}\big)$, and the Rx-sampled concentration of molecules emitted by only the Tx is expressed as $u_i^{(13)} = u\big(d = d_{13}, t = T_{\text{sa,Rx}} + T_{\text{proc}} + i \times T_{\text{pd}}\big)$, where T_{pd} is the pulse period, and T_{proc} is the time for the RN to process the relay function. Herein, it is assumed that $T_{\text{proc}} = 0$.

7.3 Relay channel analysis

This DF relaying system can be viewed as a two-hop transmission, where in the first hop (represented as the HOP1), the Tx transmits information symbols to the RN with Molecule_1, and in the second hop (represented as the HOP2), after decoding messages from the Tx, the RN sends this symbol sequence to the Rx. For the HOP2, to express the information, the Rx can use either Molecule_1 (denoted as 'Relay-1') or Molecule_2 (denoted as 'Relay-2'). The detailed analysis for the DF relaying system is presented as follows.

7.3.1 BER for 'Relay-1'

First, the HOP1 is considered. Molecules emitted by the RN will affect the distribution of molecules emitted by the Tx. The concentration around the RN can be viewed as a combination of the molecules from the Tx and itself, and the concentration of molecules from the RN can be treated as the average concentration over the sphere. When the k^{th} symbol is transmitted by the Tx ($k > I$), due to the existence of the ISI, previously emitted molecules still remain in the environment. For the $(k-i)^{\text{th}}$ symbol, where $i = 1, 2, ..., I$, at the RN sampling time, the propagation time for molecules released by the Tx is $(T_{\text{sa,RN}} + i * T_{\text{pd}})$, and the propagation time for molecules released by the RN is $(i * T_{\text{pd}})$. Thus, when the RN detects the concentration of the k^{th} symbol from the Tx, previous emitted molecules representing

the $(k-i)^{\text{th}}$ symbol will form a concentration given as:

$$r^{(1)}_{\text{RN},k-i} = a_{k-i}u^{(12)}_i + a_{k-i}\int_0^{R_{\text{se}}} \frac{3}{4\pi R^3_{\text{se}}} u\Big(d = w, t = i * T_{\text{pd}}\Big) \cdot 4\pi w^2 dw$$
$$= a_{k-i}u^{(12)}_i + a_{k-i}\bar{u}_{i-1} = a_{k-i}\Big(u^{(12)}_i + \bar{u}_{i-1}\Big), \tag{7.1}$$

where superscript '(1)' denotes 'Relay-1', I is the ISI length, the set $\{a_{k-i}, i = 0, 1, ..., I\}$ is the binary messages sequence, and the element a_{k-i} represents the binary value of each symbol. Specifically, $\bar{u}_0 = 0$. Thus, for the RN in 'Relay-1', the sensed concentration and the pre-designed criteria are respectively given as:

$$r^{(1)}_{\text{RN}} = \sum_{i=0}^{I} r^{(1)}_{\text{RN},k-i} = a_k u^{(12)}_0 + \sum_{i=1}^{I} a_{k-i}\Big(u^{(12)}_i + \bar{u}_{i-1}\Big) + n(t), \tag{7.2}$$

$$l^{(1)}_{\text{RN1}} = \sum_{i=1}^{I} \hat{a}_{k-i}\Big(u^{(12)}_i + \bar{u}_{i-1}\Big) + u^{(12)}_0, \tag{7.3}$$

$$l^{(1)}_{\text{RN0}} = \sum_{i=1}^{I} \hat{a}_{k-i}\Big(u^{(12)}_i + \bar{u}_{i-1}\Big), \tag{7.4}$$

where $\{\hat{a}_{k-i}, i = 1, 2, ..., I\}$ is previously decoded symbols. Herein, it is also assumed that $\hat{a}_{k-i} = a_{k-i}$ for $i = 1, 2, ..., I$. Substituting (7.2) through (7.4) into (5.16), the decision variable of the RN can written as:

$$L^{(1)}_{\text{RN}} = -2u^{(12)}_0[n(t) + (a_k - \frac{1}{2})u^{(12)}_0]. \tag{7.5}$$

Similar to derivations in Section 5.3.1, for the error pattern j, the number of '1's within the previous symbols $\{a_{k-i}, i = 1, 2, ..., I\}$ is denoted as ϱ_j. Since there are 2^I error patterns, there will be 2^I values of corresponding ϱ_j. For the error pattern 'j', the permutation of values of $\{a_{k-i}, i = 1, 2, ..., I\}$ is denoted as $\{a^{(j)}_{k-i}, i = 1, 2, ..., I\}$, the number of '1's within $\{a^{(j)}_{k-i}, i = 1, 2, ..., I\}$ is denoted as ϱ_j, and accordingly, the number of '0's is $(I - \varrho_j)$. The probability of '1' transmitted is denoted as P_{tx}, and the probability of '0' transmitted is $(1 - P_{\text{tx}})$. Thus, the probability of the HOP1

in 'Relay-1' for the error pattern j can be obtained as:

$$P^{(1)}_{\mathrm{er}0j,\mathrm{RN}} = P^{\varrho_j}_{\mathrm{tx}}(1-P_{\mathrm{tx}})^{I-\varrho_j}\Phi\Big(-\frac{u^{(12)}_0}{\sigma^{(1)}_{\mathrm{RN}0j}}\Big), \tag{7.6}$$

$$P^{(1)}_{\mathrm{er}1j,\mathrm{RN}} = P^{\varrho_j}_{\mathrm{tx}}(1-P_{\mathrm{tx}})^{I-\varrho_j}\Phi\Big(-\frac{u^{(12)}_0}{\sigma^{(1)}_{\mathrm{RN}1j}}\Big), \tag{7.7}$$

where

$$\begin{aligned}\sigma^{(1)}_{\mathrm{RN}0j} &= \sqrt{\frac{3}{4\pi R^3_{\mathrm{se}}}\sum_{i=1}^{I} a^{(j)}_{k-i}\Big(u^{(12)}_i + \bar{u}_{i-1}\Big)},\\ \sigma^{(1)}_{\mathrm{RN}1j} &= \sqrt{\frac{3}{4\pi R^3_{\mathrm{se}}}\Big[\sum_{i=1}^{I} a^{(j)}_{k-i}\Big(u^{(12)}_i + \bar{u}_{i-1}\Big) + u^{(12)}_0\Big]}.\end{aligned} \tag{7.8}$$

Thus, the BER for the HOP1 in 'Relay-1' can be computed by substituting (7.7) and (7.6) into (5.28), that is:

$$\begin{aligned}P^{(1)}_{\mathrm{er,RN}} &= P_{\mathrm{tx}}P^{(1)}_{\mathrm{er}1,\mathrm{RN}} + (1-P_{\mathrm{tx}})P^{(1)}_{\mathrm{er}0,\mathrm{RN}}\\ &= P_{\mathrm{tx}}\sum_{j=1}^{2^I} P^{(1)}_{\mathrm{er}1j,\mathrm{RN}} + (1-P_{\mathrm{tx}})\sum_{j=1}^{2^I} P^{(1)}_{\mathrm{er}0j,\mathrm{RN}}.\end{aligned} \tag{7.9}$$

Second, the HOP2 is considered. Molecules from both the Tx and RN will form concentration distribution around the Rx, Thus, the concentration surrounding the Rx can be viewed as the sum of molecular concentrations of molecules from both the Tx and RN. Thus, the sensed concentration and the pre-designed criteria of the Rx in 'Relay-1' will be respectively expressed as:

$$r^{(1)}_{\mathrm{Rx}} = \sum_{i=0}^{I} a_{k-i}\times(u^{(13)}_i + u^{(23)}_i) + n(t), \tag{7.10}$$

$$l^{(1)}_{\mathrm{Rx}1} = \sum_{i=1}^{I} \hat{a}_{k-i}\times(u^{(13)}_i + u^{(23)}_i) + u^{(13)}_0 + u^{(23)}_0, \tag{7.11}$$

$$l^{(1)}_{\mathrm{Rx}0} = \sum_{i=1}^{I} \hat{a}_{k-i}\times(u^{(13)}_i + u^{(23)}_i). \tag{7.12}$$

By substituting (7.10) through (7.12) into (5.16), the decision variable of the Rx in 'Relay-1' can be obtained as:

$$L_{\mathrm{Rx}}^{(1)} = -2(u_0^{(13)} + u_0^{(23)})[n(t) + (a_k - \frac{1}{2})(u_0^{(13)} + u_0^{(23)})]. \tag{7.13}$$

Thus, similarly, the error probability of HOP2 in 'Relay-1' for the error pattern j can be derived as:

$$P_{\mathrm{er}0j,\mathrm{Rx}}^{(1)} = P_{\mathrm{tx}}^{\varrho_j}(1-P_{\mathrm{tx}})^{I-\varrho_j}\Phi\Big(-\frac{u_0^{(12)}+u_0^{(13)}}{\sigma_{\mathrm{Rx}0j}^{(1)}}\Big), \tag{7.14}$$

$$P_{\mathrm{er}1j,\mathrm{Rx}}^{(1)} = P_{\mathrm{tx}}^{\varrho_j}(1-P_{\mathrm{tx}})^{I-\varrho_j}\Phi\Big(-\frac{u_0^{(12)}+u_0^{(13)}}{\sigma_{\mathrm{Rx}1j}^{(1)}}\Big), \tag{7.15}$$

where

$$\sigma_{\mathrm{Rx}0j}^{(1)} = \sqrt{\frac{3}{4\pi R_{\mathrm{se}}^{\,3}}\sum_{i=1}^{I} a_{k-i}^{(j)} \times (u_i^{(13)} + u_i^{(23)})},$$

$$\sigma_{\mathrm{Rx}1j}^{(1)} = \sqrt{\frac{3}{4\pi R_{\mathrm{se}}^{\,3}}\Big[\sum_{i=1}^{I} a_{k-i}^{(j)} \times (u_i^{(13)} + u_i^{(23)}) + u_0^{(13)} + u_0^{(23)}\Big]}. \tag{7.16}$$

Thus, the average bit error rate for the HOP2 in 'Relay-1' can be computed by substituting (7.15) and (7.14) into (5.28), that is:

$$\begin{aligned} P_{\mathrm{er,Rx}}^{(1)} &= P_{\mathrm{tx}}P_{\mathrm{er1,Rx}}^{(1)} + (1-P_{\mathrm{tx}})P_{\mathrm{er0,Rx}}^{(1)} \\ &= P_{\mathrm{tx}}\sum_{j=1}^{2^I} P_{\mathrm{er}1j,\mathrm{Rx}}^{(1)} + (1-P_{\mathrm{tx}})\sum_{j=1}^{2^I} P_{\mathrm{er}0j,\mathrm{Rx}}^{(1)} \end{aligned} \tag{7.17}$$

Throughout the system, an error occurs if the detection is erroneous in either the HOP1 or HOP2. Thus, the overall BER for 'Relay-1' can be calculated by:

$$P_{\mathrm{er}}^{(1)} = (1-P_{\mathrm{er,RN}}^{(1)})P_{\mathrm{er,Rx}}^{(1)} + P_{\mathrm{er,RN}}^{(1)}(1-P_{\mathrm{er,Rx}}^{(1)}). \tag{7.18}$$

7.3.2 BER for 'Relay-2'

First, the HOP1 is considered. Molecule_1 emitted by the Tx will not affect the concentration distribution of the Molecule_2 emitted by the RN. Thus, the sensed concentration and the pre-designed criteria of the RN in 'Relay-2' are respectively given as:

$$r_{\mathrm{RN}}^{(2)} = \sum_{i=0}^{I} u_i^{(12)} a_{k-i} + n(t), \tag{7.19}$$

$$l_{\mathrm{RN1}}^{(2)} = \sum_{i=1}^{I} u_i^{(12)} \hat{a}_{k-i} + u_0^{(12)}, \tag{7.20}$$

$$l_{\mathrm{RN0}}^{(2)} = \sum_{i=1}^{I} u_i^{(12)} \hat{a}_{k-i}. \tag{7.21}$$

where the superscript '(2)' represents 'Relay-2'. By substituting (7.19) through (7.21) into (5.28), the decision variable for the RN in 'Relay-2' can be obtained as:

$$L_{\mathrm{RN}}^{(2)} = -2u_0^{(12)}[n(t) + (a_k - \frac{1}{2})u_0^{(12)}]. \tag{7.22}$$

Thus, the error probability of the HOP1 in 'Relay-2' for the error pattern j can be derived as:

$$P_{\mathrm{er}0j,\mathrm{RN}}^{(2)} = P_{\mathrm{tx}}^{\varrho_j}(1 - P_{\mathrm{tx}})^{I-\varrho_j}\Phi\Big(-\frac{u_0^{(12)}}{\sigma_{\mathrm{RN}0j}^{(1)}}\Big), \tag{7.23}$$

$$P_{\mathrm{er}1j,\mathrm{RN}}^{(2)} = P_{\mathrm{tx}}^{\varrho_j}(1 - P_{\mathrm{tx}})^{I-\varrho_j}\Phi\Big(-\frac{u_0^{(12)}}{\sigma_{\mathrm{RN}1j}^{(1)}}\Big), \tag{7.24}$$

where

$$\sigma_{\mathrm{RN}0j}^{(2)} = \sqrt{\frac{3}{4\pi R^3}\sum_{i=1}^{I} a_{k-i}^{(j)} u_i^{(12)}},$$

$$\sigma_{\mathrm{RN}1j}^{(2)} = \sqrt{\frac{3}{4\pi R^3}\Big[\sum_{i=1}^{I} a_{k-i}^{(j)} u_i^{(12)} + u_0^{(12)}\Big]}. \tag{7.25}$$

Thus, the BER for the HOP1 in 'Relay-2' can be computed by substituting (7.24) and (7.23) into (5.28), that is:

$$\begin{aligned} P_{\text{er,RN}}^{(2)} &= P_{\text{tx}} P_{\text{er1,RN}}^{(2)} + (1 - P_{\text{tx}}) P_{\text{er0,RN}}^{(2)} \\ &= P_{\text{tx}} \sum_{j=1}^{2^I} P_{\text{er1}j,\text{RN}}^{(2)} + (1 - P_{\text{tx}}) \sum_{j=1}^{2^I} P_{\text{er0}j,\text{RN}}^{(2)}. \end{aligned} \tag{7.26}$$

Second, the HOP2 is considered, which can be viewed as the same process from Tx to RN but with different parameters. Thus, the BER for the HOP2 in 'Relay-2' can be derived as:

$$\begin{aligned} P_{\text{er,Rx}}^{(2)} &= P_{\text{tx}} P_{\text{er1,Rx}}^{(2)} + (1 - P_{\text{tx}}) P_{\text{er0,Rx}}^{(2)} \\ &= P_{\text{tx}} \sum_{j=1}^{2^I} P_{\text{er1}j,\text{Rx}}^{(2)} + (1 - P_{\text{tx}}) \sum_{j=1}^{2^I} P_{\text{er0}j,\text{Rx}}^{(2)} \\ &= P_{\text{tx}} \sum_{j=1}^{2^I} P_{\text{tx}}^{\varrho_j} (1 - P_{\text{tx}})^{I - \varrho_j} \Phi\Big(- \frac{u_0^{(23)}}{\sigma_{\text{Rx1}j}^{(1)}} \Big) + \\ &\qquad (1 - P_{\text{tx}}) \sum_{j=1}^{2^I} P_{\text{tx}}^{\varrho_j} (1 - P_{\text{tx}})^{I - \varrho_j} \Phi\Big(- \frac{u_0^{(23)}}{\sigma_{\text{Rx0}j}^{(1)}} \Big) \end{aligned} \tag{7.27}$$

Thus, the overall BER for 'Relay-2' can be calculated by:

$$P_{\text{er}}^{(2)} = (1 - P_{\text{er,RN}}^{(2)}) P_{\text{er,Rx}}^{(2)} + P_{\text{er,RN}}^{(2)} (1 - P_{\text{er,Rx}}^{(2)}). \tag{7.28}$$

7.3.3 An alternative way to obtain the system BER

The system BER can be calculated in a way given by (7.18) for 'Relay-1' and (7.28) for 'Relay-2'. The error probabilities are respectively averaged for HOP1 and HOP2, and the system BER can be obtained by combining the averaged BER. Alternatively, these is another method to calculate the system BER. The derivation of the BER for 'Relay-1' is taken as an example, and the BER for 'Relay-2' can be obtained by substituting the superscript '(1)' with '(2)'.

Table 7.1: Simulation parameters for the analysis of the relaying system

1.	The sensing radium of the Rx and RN	R_{se}	$0.5\,\mu\text{m}$
2.	The distance between Tx and Rx	d_{13}	$5\,\mu\text{m}$
3.	The diffusion coefficient	D	$10^{-3}\mu\text{m}^2\,\mu\text{s}^{-1}$
4.	The emission duration	T_{em}	$1000\,\mu\text{s}$
5.	The pulse period	T_{pd}	$5000\,\mu\text{s}$
6.	The number of molecules per pulse	m	2×10^5
7.	The ISI length	I	20

For error pattern 'j' of the 'Relay-1' system, the error probabilities for '0 transmitted or '1 transmitted in HOP1 are separated expressed as $P^{(1)}_{\text{er0}j,\text{RN}}$ and $P^{(1)}_{\text{er1}j,\text{RN}}$ in (7.6) to (7.8), and those probabilities in HOP2 are expressed as $P^{(1)}_{\text{er0}j,\text{Rx}}$ and $P^{(1)}_{\text{er1}j,\text{Rx}}$ in (7.14) to (7.16), Thus, for error pattern 'j', the system error probability can be calculated as:

$$\begin{aligned} P^{(1)}_{\text{er}j} = {} & (1-P_{\text{tx}})(1-P^{(1)}_{\text{er0}j,\text{RN}})P^{(1)}_{\text{er0}j,\text{Rx}} + (1-P_{\text{tx}})P^{(1)}_{\text{er0}j,\text{RN}}(1-P^{(1)}_{\text{er1}j,\text{Rx}}) \\ & + P_{\text{tx}}(1-P^{(1)}_{\text{er1}j,\text{RN}})P^{(1)}_{\text{er1}j,\text{Rx}} + P_{\text{tx}}P^{(1)}_{\text{er1}j,\text{RN}}(1-P^{(1)}_{\text{er0}j,\text{Rx}}). \end{aligned} \tag{7.29}$$

Therefore, the system BER for 'Relay-1' can be derived by:

$$P^{(1)}_{\text{er}} = \sum_{j=1}^{2^I} P^{(1)}_{\text{er}j}. \tag{7.30}$$

7.4 Numeral results

In this section, both theoretical derived and simulated results are presented. During simulations, molecular concentrations, encoded with messages, are simulated to change with time and distance in the environment. The RN and Rx sense the concentrations at the pre-designed sampling time, and determine messages correspondingly. The channel herein is assumed to be Memory Limited Channel (MLC) with $I = 20$. The times of the simulation trials are based on theoretical results. For example, if the theoretical BER is 10^{-7}, then 10^{11} successive bits are correspond-

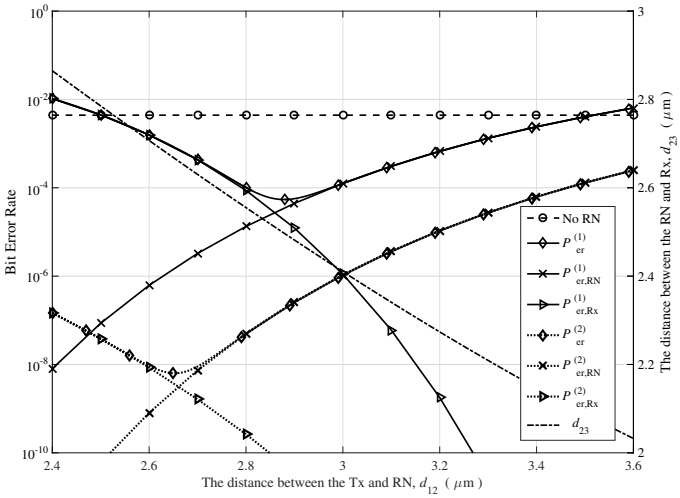

Figure 7.2: BER and d_{23} vs. d_{12} for $\theta = 20°$.

ingly simulated. All results are presented with a common set of parameters assigned in Table 7.1. These values agree with the ones used throughout the thesis and the research in [44, 55, 79].

Results in the Fig. 7.2 reveal that both of the DF relaying schemes, 'Relay-1' and 'Relay-2', can be implemented into the diffusion-based MC system. By deploying an RN between the Tx and Rx, the communication quality can be significantly improved if relative parameters are carefully designed. Especially, when two kinds of molecules are utilised (like the 'Relay-2' system), the BER can be further reduced. The main reason is that in 'Relay-2' systems, the self interference can be eliminated by using a different kind of molecules to forward messages, which helps both the RN and Rx to make better decisions when determining transmitted symbols. As a consequence, it can be deduced that $P_{\text{er,RN}}^{(2)} < P_{\text{er,RN}}^{(1)}$, $P_{\text{er,Rx}}^{(2)} < P_{\text{er,Rx}}^{(1)}$, and correspondingly $P_{\text{er}}^{(2)} < P_{\text{er}}^{(1)}$. This agrees with the results shown in the Fig. 7.2. Thus, the performance of 'Relay-2' is superior than that of 'Relay-1'.

It can also be seen that d_{12} getting larger leads to the increase of the error rate in the HOP1 and the decrease of the error rate in the HOP2. This is mainly due to the change of the distance between the corresponding two nano-machines. Another

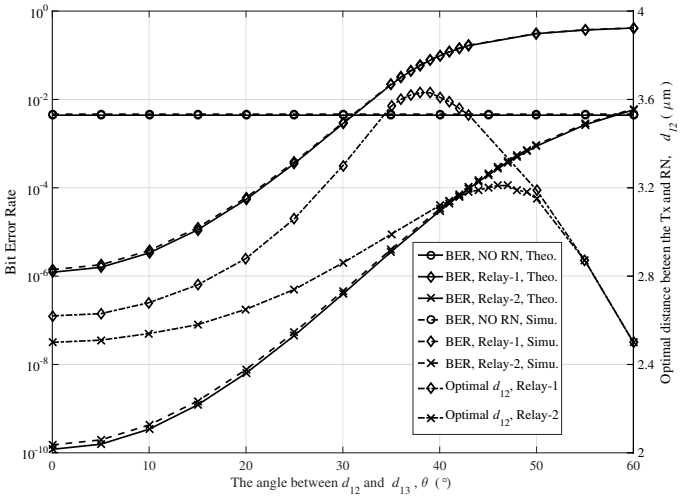

Figure 7.3: The optimal BER and corresponding for different angles θ.

important feature shown in the Fig. 7.2 is that the overall BER of the relay system is mainly determined by the larger error probability within the two Hops, which can also be proven from deviations in Section 7.3. Thus, with a rising d_{12}, if the error rate in the HOP2 is still far higher than that in the HOP1, the reduction of $P_{\text{er,Rx}}^{(1)}$ (or $P_{\text{er,Rx}}^{(2)}$) will result in a lower system BER; otherwise, the increasing $P_{\text{er,RN}}^{(1)}$ (or $P_{\text{er,RN}}^{(2)}$) will cause more errors over the system. Correspondingly, the BER of the relaying system will decrease first and increase eventually. Furthermore, if the system BER is obtained using the method described in Section 7.3.3, the difference between these two ways to calculated the system BER is only at the level of 10^{-16}, which is so tiny that can be neglected. Hence, both of these two calculation algorithms can provide a reasonable measure of the system error probability.

The Fig. 7.3 presents the minimum error probability that can be achieved for each angle θ and the corresponding locations of the RN at different angles. At each angle, the values of BER are obtained versus different values of d_{12} for both 'Relay-1' and 'Relay-2', and then the optimal distance is selected with the BER minimised for this given angle. As is clearly shown herein, the relay system tends to suffer from more errors with θ rising. This is mainly due to the increase of relative

distances from the RN to the Tx and Rx, respectively d_{12} and d_{23}. With θ getting larger, it is easy to prove the RN becomes farther away from the Tx and Rx, leading to a higher error rate. Especially, when θ is quite large (about 30° for Relay-1, and about 60° for Relay-2), the relay system may not bring in any benefit.

Results in the Fig. 7.3 also illuminates that the optimal d_{12} for both 'Relay-2' and 'Relay-1' first increases and then starts to decrease. When θ is small, the RN should be placed around the point where $d_{12} \approx d_{23}$; when θ increases to around 40°, the RN should be placed around the position where $\alpha \approx 90°$. Moreover, it is also shown that the optimal d_{12} for Relay-1 is larger than that for 'Relay-2'. For a given θ, if d_{12}=d_{23}, it can be deduced that $P_{\text{er,RN}}^{(1)} < P_{\text{er,Rx}}^{(1)}$ for 'Relay-1' and $P_{\text{er,RN}}^{(2)} = P_{\text{er,Rx}}^{(2)}$ for 'Relay-2'. Thus, the optimal position of the RN for 'Relay-1' should be closer to the Rx, which makes the optimal d_{12} of 'Relay-1' is larger than that of 'Relay-2'.

7.5 Conclusions

In this chapter, a relaying scheme is introduced in a diffusive MC system based on the enhanced transmission model. The impact of emission process has been considered and the concentration changes over time and is influenced by the channel noise and memory. Both theoretical derivations and simulations are provided to show the significantly decrease of the BER due to the implementation of the RN. Results also present that if molecules from the Tx and RN are of different species, the relay system will provide a better performance. It can be further deduced that when T_{proc} is not negligible, the superiority of the 'Relay-2' system will be more distinct. Moreover, the decoding method utilised in this chapter can mitigate the ISI as remaining concentrations of previous symbols within the ISI length have been considered when decoding messages.

Chapter 8

Conclusions and Future Work

8.1 Conclusions

Molecular Communications (MC), among all kinds of nano-communications techniques, is one of the most promising methods to enable the networking of nano-machines, where molecules are utilised as the information carrier to achieve communications between a pair of transmitter (Tx) and receiver (Rx). The aim of this Ph.D. project is to model an MC system based on molecular diffusion, to implement functional transmission schemes, and to investigate the corresponding performance by means of both theoretical derivations and simulations. Throughout all the preceding chapters, it has been presented that diffusive MC systems have be realised. Information is conveyed as a successive sequence of symbols in consecutive time slots. In each time slot, to transmit symbol '1', the Tx releases a certain amount of molecules; to transmit '0', the Tx releases nothing. These molecules will diffuse independently in the environment, and some of them can arrive at the Rx to get the message exchange accomplished. To address the propagation mechanism, relative researches have been carried out from both micro and macro angles. In the micro scope, attentions are paid to analyse the motion of each individual molecule, and the probability can be derived to describe whether a molecule will diffuse to the infinity

or be absorbed by the Rx. Consequently, the reception of these message molecules can be viewed as a Bernoulli process, and therefore the propagation mechanism in the micro level has been addressed. From the macro angle, no matter how every single molecule moves, they will form a certain concentration distribution in the environment after being sent out by the Tx. The expression of the concentration has been obtained by previous researchers. In this way, the propagation mechanism in the macro level has been settled. According to these two angles to describe the molecular propagation, two different diffusion-based MC systems models have been established.

Based on each system model, a mathematical method has been developed to evaluate the performance with regards to two channel properties, namely, the channel reliability and reliable transmission rate. The former is investigated by the system Bit Error Rate (BER), and the latter is characterised by the channel capacity. Deriving theoretical expressions of these two features provides an intuitive approach to measure the performance and to understand what impact can be brought in by choosing different values for relative parameters.

When evaluating the performance, the distance between nano-machines is found to be an essential parameter for both the Tx and Rx. Thus, there is an urgent requirement to figure out how the distance can be measured both accurately and quickly. To solve this problem, distance estimation schemes and their optimisation methods have been proposed for both system models. Compared with previous work, the accuracy has been significantly enhanced and the time consumption has been greatly reduced. By deploying these estimation schemes, nano-machines can accordingly coordinate their functionality, such as the transmission rate and the number of molecules emitted per pulse, to achieve the optimal system performance.

Furthermore, transmission technologies like Stop-and-Wait Automatic Repeat reQuest (SW-ARQ) protocols and Decode-and-Forward (DF) relaying schemes, have been proposed and implemented onto these two MC system models. Their

own properties have been investigated via both mathematical derivations and simulations. Results reveal that these transmission technologies can bring great benefits with parameters carefully designed.

Overall, the goal of the project has been accomplished by separating into 6 individual tasks, and each task has been elaborated in turn from Chapter 2 to Chapter 7. In **Chapter 2**, an MC system model, named as Model-I, is introduced, where information is expressed by the number of captured molecules. When dealing with the molecular propagation procedure, focus is concentrated onto the motion of every single molecule. In this case, the propagation mechanism is described by the capture probability, which has been derived by previous researchers. Each molecule is considered to move independently and has a probability to reach the Rx. Upon arriving at the Rx, molecules will be absorbed and removed out of the environment. By counting the number of captured molecules, the Rx is able to determine whether symbol '0' or '1' is transmitted. To evaluate the system performance, the BER and channel capacity have been analysed through both theoretical derivations and simulations. Numerical results also present the influence brought by the changing in relative parameters. Moreover, even though the Inter-Symbol Interference (ISI) has been alleviated, it will still affect the channel performance. Thus, further analysis has been carried out to investigate the impact of the ISI length. For theoretical derivations, the ISI length has been regarded as an arbitrary value to maximise the generality. For simulations, it is set to a length of 20 such that results are of as a high precision as is reasonably practical. Research described in Chapters 3 and 4 are based on the establishment of the system Model-I introduced in the Chapter 2.

In **Chapter 3**, an algorithmic scheme has been proposed to estimate the distance for the system Model-I. By periodically counting the number of captured molecules, the Rx computes the possible values of the distance, narrows down the range of these potential values over iterations, and gradually determines the estimated distance. This distance measurement scheme can be implemented under both

synchronised and unsynchronised scenarios. Simulated results show that compared with existing distance estimation schemes, the proposed scheme enjoys a desirable estimation accuracy and costs significantly less time. The performance can be further enhanced by using two optimisation methods, i.e. emitting more molecules per pulse or utilising molecules with a larger diffusion coefficient. However, either enlarging the amount of released molecules or increasing the diffusion coefficient will result in a greater energy budget and a higher requirement on both nano-machines. Hence, when deploying the distance estimation scheme and designing parameters, not only do the accuracy and time cost need to be taken into account, but also should the energy consumption and system complexity be considered.

Five SW-ARQ transmission protocols have been described in **Chapter 4** to ensure successful information transmissions over nano-networks. Two metrics of the performance have been analysed, namely, the average time cost per successful duplex transmission and the energy cost per successful duplex transmission. Numeral results illuminate that all these five methods work well, and can be beneficial depending on different application scenarios. Scheme 1 suits for adjacent communications due to its own simplicity, and Scheme 2 and 3 can be implemented for longer-range communications. Especially when the target nano-machine is far away from the source nano-machine, using Scheme 3 will significantly decrease the time and energy required for a complete successful transmission. Unlike Schemes 1 through 3 whose target application is on the pre-known channel, Schemes 4 and 5 are designed for an unknown channel or a varying channel due to the 'adaptivity'. Similar to the comparisons between Scheme 2 and Scheme 1, Scheme 5 will provide better performance than Scheme 4 with carefully designed parameters. Hence, when designing a specific diffusion-based MC system, the selection of transmission schemes should be made carefully to optimise the trade-off between the time and energy requirement.

In **Chapter 5**, a different system model, Model-II, is introduced, where messages are conveyed into molecular concentrations. From the macro angle, the

propagation procedure has been addressed via obtaining the molecular concentration distribution. The concentration is considered to change with regards to the time and distance, and the influence of the Tx releasing process is also considered. Rather than absorbing molecules like Model-I, the Rx in Model-II is a passive observer, whose capability is only to sense the concentration for decoding, but not affect the molecular distribution. Similar to the description in Chapter 2, expressions of the BER and channel capacity have been derived and simulation results are provided. The impact of the ISI length, as well as other parameters, is also illustrated. The establishment of the system Model-II lays the foundation of the research explained in Chapters 6 and 7.

Similar to the situation in Model-I, the distance is also essential to Model-II. Consequently, two distance estimation schemes have been proposed in **Chapter 6**. The Rx can sense the surrounding concentration and measure the distance by taking advantage of either the concentration peak time or the concentration energy. Simulations are conducted to compare the estimation performance of these two schemes, and to discover how it can be optimised by carefully designing parameters. Numerical results reveal that both of the schemes can provide reasonable accuracy. Using energy will enjoy a even better estimation, but the implementation is limited due to the high requirement on system complexity. Moreover, the system reliability, represented by the BER, is also evaluated for a distance-unknown channel. At the first stage, the source nano-machine estimates the distance by means of measuring the peak time, and at the second stage, starts to transmit message symbols to achieve the communications to the target. By considering the estimation deviation, the system error probability is derived. Comparisons between distance-pre-known systems and distance-unknown systems have been made, and results illuminate that the performance can be enhanced by three methods, that is, sending out more molecules, emitting as fast as possible, and mitigating the influence of the ISI.

In **Chapter 7**, on the basis of the system Model-II, a DF relaying node

(RN) has been deployed to improve the channel reliability between remote nano-machines. When forwarding information, the RN can either release the same kind of molecules as the Tx does, denoted as 'Relay-1', or send out a different kind of molecules, denoted as 'Relay-2'. A mathematical approach has been developed to derive formulations of the BER. Simulations are also designed to verify the accuracy of these expressions and to figure out the optimal positions of the RN according to different initial conditions. It is easy to find that the implementation of the RN can significantly decrease the channel error probability, and the 'Relay-2' is a superior choice due to the avoidance of the self interference by using two kinds of molecules.

8.2 Future work

Throughout the thesis, it can be noticed that all the tasks in the Ph.D. project are with regards to two different system models, namely, Model-I and Model-II. According to two scopes of angles to address the molecular propagation mechanism, Model-I and Model-II are respectively established with information expressed by either the number of captured molecules or the molecular concentration. Both of the system models can be further enhanced in future researches.

As to the Model-I, it is assumed that the reception of molecules in different time slots is viewed to be independent of each other. This assumption is not sufficiently accurate if compared with the practical situations, which can be a target for the future analysis with respect to the channel model. Under that circumstance, when dealing with molecules emitted in the same time slot, the capture numbers in the current slot and the next successive ones are no longer independent. In this way, the system can be more accurately modelled, which is therefore closer to practical situations.

Another potential enhancement that can be made on the Model-I is to discover a proper way to define the channel noise. In diffusion-based MC systems, the

molecular movement can be affected by various factors, such as the temperature, the pH level, and other properties of the surrounding fluid. However, there is no available literature offering a decent description of the channel noise, which makes this challenge to be a possible goal in the future work. Re-defining the channel noise will provide a better method to illuminate the motion of every single molecule. As a consequence, this system model can be improved.

Moreover, the system Model-I can be expanded into a multiple-receiver communication network. By implementing more than one receiver, the capture probability of each single molecule is changed, and meanwhile, the capture probability for each Rx differs according to different locations of deployed nano-machines. Even this problem seems too complicated especially when the number of receivers increases, it is achievable to address the propagation mechanism with only two receivers existing. This lays the foundation to the establishment of relaying systems, which has been proven to be a desirable method to improve the system performance of long-range communications. Future work can be carried out to get this accomplished.

As to the Model-II, the impact of the Rx on the concentration can be further investigated. In the current work, it is assumed that the Rx is a passive observer that will not affect the concentration distribution, and molecules can pass through the Rx freely. However, in reality, even if the Rx may not absorb molecules, the existence of the Rx will still have influence on the molecular distribution because there is no way for molecules to get in and out of the Rx without any restrictions. By taking this influence into consideration, the propagation mechanism can be more accurately described, and the system model can be enhanced consequently, which can be a task for future researchers.

Further improvement of the system Model-II that can be brought in is to figure out a better method to analyse the channel noise. In the current system model, the noise is viewed as an additive normal distribution. As a consequence, there exists a small probability that the value of sensed concentration is negative,

which needs to be avoided by re-defining the noise expression. In other relative work, the Poisson distribution has been utilised to solve the problem. However, the determination of the only parameter λ still remains an open challenge. Thus, it can be a possible objective in future researches.

Apart from the aforementioned future work, efforts can also be put on the transmission schemes like the ones explained in Chapter 4 and Chapter 7. Regarding to the ARQ transmission protocols, further researches can be conducted to investigate the implementation of the Go-Back-N ARQ scheme, the Selective Repeat ARQ scheme, or even the Hybrid ARQ by combining with the Forward Error Correction techniques; while for the relaying scheme, current investigation can be expanded into the establishment and performance evaluation of multi-hop systems.

In summery, the Ph.D. project, described allover the thesis, is only the first step towards the study on diffusive MC systems. Approaches of both mathematical derivations and simulations have been developed and presented to analyse diffusion-based MC systems, which has laid a solid foundation to further relative researches. Other than the preceding aspects, there are plenty of potential objects that need to be addressed in the future, which still remains as a challenge to all the researchers interested in the molecular communications.

Bibliography

[1] I. F. Akyildiz, F. Brunetti, and C. Blazquez, "Nanonetworks: A new communication paradigm," *Elsevier Comput. Networks*, vol. 52, no. 12, pp. 2260–2279, Aug. 2008.

[2] R. P. Feynman, "Theres plenty of room at the bottom," *Eng. and Science*, vol. 23, no. 5, pp. 22–36, 1960.

[3] K. E. Drexler, *Nanosystems: Molecular Machinery, Manufacturing, and Computation*. John Wiley and Sons Inc., 1992.

[4] T. Suda, M. Moore, T. Nakano, R. Egashira, and A. Enomoto, "Exploratory research on molecular communication between nanomachines," in *Int. Conf. on Genetic and Evol. Computation (GECCO)*, Jun. 2005.

[5] A. Tseng, K. Chen, C. Chen, and K. Ma, "Electron beam lithography in nanoscale fabrication: recent development," *IEEE Trans. on Electron. Packaging Manufacturing*, vol. 26, pp. 141–149, Apr. 2003.

[6] H. H. Lee, E. Menard, J. Tassi, and G. B. Blanchet, "Large area microcontact printing presses for plastic electronics," *Materials Research Society Bulletin*, vol. 846, pp. 731–736, 2005.

[7] H. Goldstein, "The race to the bottom," *IEEE Spectrum*, pp. 243–246, Mar. 2005.

[8] M. Meyyappan, J. Li, J. Li, and A. Cassell, "Nanotechnology: An overview and integration with mems," in *IEEE Int. Conf. on Micro Electro Mech. Syst. (MEMS)*, Jan. 2006, pp. 1–3.

[9] C. Peterson, "Taking technology to the molecular level," *IEEE Comput.*, vol. 33, pp. 46–53, Jan. 2000.

[10] R. Ballardini, V. Balzani, A. Credi, M. Gandolfi, and M. Venturi, "Artificial molecular-level machines: which energy to make them work?" *Accounts of Chemical Research*, pp. 445–455, May 2001.

[11] V. Balzani, A. Credi, S. Silvi, and M. Venturi, "Artificial nanomachines based on interlocked molecular species: recent advances," *Chemical Society Reviews*, pp. 1135–1149, Sept. 2006.

[12] P. K. Soong, G. D. Bachand, H. P. Neves, A. G. Olkhovets, H. G. Craighead, and C. D. Montemagno, "Powering an inorganic nanodevice with a biomolecular motor," *Science*, vol. 24, pp. 1555–1558, Nov. 2000.

[13] G. M. Whitesides, "The once and future nanomachine," *Scientific American*, pp. 78–83, Sept. 2001.

[14] B. Behkam and M. Sitti, "Bacterial flagella-based propulsion and on/off motion control of microscale objects," *Appl. Physics Lett.*, Jan. 2007.

[15] I. F. Akyildiz and J. M. Jornet, "Electromagnetic wireless nanosensor networks," *Elsevier Nano Commun. Networks*, vol. 1, pp. 3–19, Mar. 2010.

[16] R. A. Freitas, *Nanomedicine, Volume I: Basic Capabilities.* Landes Bioscience, 1999.

[17] G. Hanson, "Fundamental transmitting properties of carbon nanotube antennas," *IEEE Trans. on Antennas Propag.*, vol. 53, no. 11, pp. 3426–3435, Nov. 2005.

[18] B. Alberts, A. Johnson, J. Lewis, M. Raff, K. Roberts, and P. Walter, *Molecular Biology of the Cell*. Garland Science, 2007.

[19] W. C. Agosta, *Chemical Communication: The Language of Pheromones*. Scientific American, 1992.

[20] T. Nakano, A. W. Eckfork, and T. Haraguchi, *Molecular communication*. Cambridge University Press, 2013.

[21] I. F. Akyildiz, J. M. Jornet, and M. Pierobon, "Nanonetworks: A new frontier in communications," *ACM Commun.*, vol. 54, pp. 84–89, Nov. 2011.

[22] B. Atakan, *Molecular Communications and Nanonetworks: From Nature To Practical Systems*. Springer, 2014.

[23] T. Nakano, T. Suda, T. Koujin, T. Haraguchi, and Y. Hiraoka, "Molecular communication through gap junction channels: System design, experiments and modeling," in *IEEE Conf. on Bio-Inspired Models of Network, Inform. and Comput. Syst.*, Dec. 2007, pp. 139–146.

[24] T. Nakano, Y.-H. Hsu, W. C. Tang, T. Suda, D. Lin, T. Koujin, T. Haraguchi, and Y. Hiraoka, "Microplatform for intercellular communication," in *IEEE Int. Conf. on Nano/Micro Engineered and Molecular Syst.*, Jan. 2008, pp. 476–479.

[25] M. Moore, A. Enomoto, T. Nakano, R. Egashira, T. Suda, A. Kayasuga, H. Kojima, H. Sakakibara, and K. Oiwa, "A design of a molecular communication system for nanomachines using molecular motors," in *IEEE Int. Conf. on Pervasive Computing and Commun. Workshops*, Mar. 2006, pp. 554–559.

[26] N. Farsad, A. Eckford, S. Hiyama, and Y. Moritani, "On-chip molecular communication: Analysis and design," *IEEE Trans. on NanoBioscience*, vol. 11, no. 3, pp. 304–314, Sept. 2012.

[27] M. Gregori and I. F. Akyildiz, "A new nanonetwork architecture using flagellated bacteria and catalytic nanomotors," *IEEE J. on Select. Areas in Commun.*, vol. 28, no. 4, pp. 612–619, May 2010.

[28] L. C. Cobo and I. F. Akyildiz, "Bacteria-based communication in nanonetworks," *Elsevier Nano Commun. Networkser Nano Commun. Networks*, vol. 1, pp. 244–256, Dec. 2010.

[29] A. Guney, B. Atakan, and O. B. Akan, "Mobile ad hoc nanonetworks with collision-based molecular communication," *IEEE Trans. on Mobile Computing*, vol. 11, no. 3, pp. 353–366, Mar. 2012.

[30] T. Nakano, T. Suda, Y. Okaie, M. Moore, and A. V. Vasilakos, "Molecular communication among biological nanomachines: A layered architecture and research issues," *IEEE Trans. on NanoBioscience*, vol. 13, no. 3, pp. 169–197, Sep. 2014.

[31] P. Cuatrecasas, "Membrane receptors," *Annu Review of Biochemistry*, vol. 43, pp. 169–214, Jul. 1974.

[32] I. A. Khalil, K. Kogure, H. Akita, and H. Harashima, "Uptake pathways and subsequent intracellular trafficking in nonviral gene delivery," *Pharmacological Reviews*, vol. 1, pp. 32–45, Mar. 2006.

[33] J. D. Scott and T. Pawson, "Cell communication: The inside story," *Scientific American*, vol. 62, pp. 72–79, Jun. 2000.

[34] L. P. Gine and I. F. Akyildiz, "Molecular communication options for long range nanonetworks," *Elsevier Comput. Networks*, vol. 53, pp. 2753–2766, Nov. 2009.

[35] P.-C. Yeh, K.-C. Chen, Y.-C. Lee, L.-S. Meng, P.-J. Shih, P.-Y. Ko, W.-A. Lin, and C.-H. Lee, "A new frontier of wireless communication theory: diffusion-

based molecular communications," *IEEE Wireless Commun.*, vol. 19, no. 5, pp. 28–35, Oct. 2012.

[36] T. Nakano, M. Moore, F. Wei, A. V. Vasilakos, and J. W. Shuai, "Molecular communication and networking: opportunities and challenges," *IEEE Trans. on NanoBioscience*, vol. 11, pp. 135–148, Jun. 2012.

[37] M. Moore, T. Suda, and K. Oiwa, "Molecular communication: Modeling noise effects on information rate," *IEEE Trans. on NanoBioscience*, vol. 8, no. 2, pp. 169–180, Jun. 2009.

[38] B. Atakan and O. B. Akan, "Deterministic capacity of information flow in molecular nanonetworks," *Elsevier Nano Commun. Networks*, vol. 1, no. 1, pp. 31–42, Mar. 2010.

[39] M. Pierobon and I. F. Akyildiz, "Diffusion-based noise analysis for molecular communication in nanonetworks," *IEEE Trans. on Signal Process.*, vol. 59, no. 6, pp. 2532–2547, Jun. 2011.

[40] A. Einolghozati, M. Sardari, A. Beirami, and F. Fekri, "Capacity of discrete molecular diffusion channels," in *IEEE Int. Symp. on Inform. Theory (ISIT)*, Jul. 2011, pp. 723–727.

[41] M. Pierobon and I. F. Akyildiz, "Noise analysis in ligand-binding reception for molecular communication in nanonetworks," *IEEE Trans. on Signal Process.*, vol. 59, no. 9, pp. 4168–4182, Sept. 2011.

[42] A. Einolghozati, M. Sardari, and F. Fekri, "Capacity of diffusion-based molecular communication with ligand receptors," in *IEEE Inform. Theory Workshop (ITW)*, Oct. 2011, pp. 85–89.

[43] K. V. Srinivas, A. W. Eckford, and R. S. Adve, "Molecular communication

in fluid media: The additive inverse gaussian noise channel," *IEEE Trans. on Inform. Theory*, vol. 58, no. 7, pp. 4678–4692, Jul. 2012.

[44] M. Pierobon and I. F. Akyildiz, "Capacity of a diffusion-based molecular communication system with channel memory and molecular noise," *IEEE Trans. on Inform. Theory*, vol. 59, no. 2, pp. 942–954, Feb. 2013.

[45] A. Noel, K. C. Cheung, and R. Schober, "Optimal receiver design for diffusive molecular communication with flow and additive noise," *IEEE Trans. on NanoBioscience*, vol. 13, no. 3, pp. 350–362, Sept. 2014.

[46] N. Farsad, N.-R. Kim, A. W. Eckford, and C.-B. Chae, "Channel and noise models for nonlinear molecular communication systems," *IEEE J. on Select. Areas in Commun.*, vol. 32, no. 12, pp. 2392–2401, Dec. 2014.

[47] H. Li, S. M. Moser, and D. Guo, "Capacity of the memoryless additive inverse gaussian noise channel," *IEEE J. on Select. Areas in Commun.*, vol. 32, no. 12, pp. 2315–2329, Dec. 2014.

[48] H. Arjmandi, A. Gohari, M. N. Kenari, and F. Bateni, "Diffusion-based nanonetworking: A new modulation technique and performance analysis," *IEEE Commun. Lett.*, vol. 17, no. 4, pp. 645–648, Apr. 2013.

[49] B. Tepekule, A. E. Pusane, H. B. Yilmaz, and T. Tugcu, "Energy efficient ISI mitigation for communication via diffusion," in *IEEE Int. Black Sea Conf. on Commun. and Networking (BlackSeaCom)*, May 2014, pp. 33–37.

[50] M. S. Kuran, H. B. Yilmaz, T. Tugcu, and I. F. Akyildiz, "Modulation techniques for communication via diffusion in nanonetworks," in *IEEE Int. Conf. on Commun. (ICC)*, Jun. 2011, pp. 1–5.

[51] S. K. Mehmet, T. Yilmaz, H. B.and Tugcu, and I. F. Akyildiz, "Interference

effects on modulation techniques in diffusion based nanonetworks," *Elsevier Nano Commun. Networks*, vol. 3, no. 1, pp. 65–73, Mar. 2012.

[52] N.-R. Kim and C.-B. Chae, "Novel modulation techniques using isomers as messenger molecules for nano communication networks via diffusion," *IEEE J. on Select. Areas in Commun.*, vol. 31, no. 12, pp. 847–856, Dec. 2013.

[53] X. Wang, M. D. Higgins, and M. S. Leeson, "Relay analysis in molecular communications with time-dependent concentration," *IEEE Commun. Lett.*, vol. 19, no. 11, pp. 1977–1980, Nov. 2015.

[54] M. V. Eyuboglu, "Detection of coded modulation signals on linear, severely distorted channels using decision-feedback noise prediction with interleaving," *IEEE Trans. on Commun.*, vol. 36, no. 4, pp. 401–409, Apr. 1988.

[55] H. ShahMohammadian, G. G. Messier, and S. Magierowski, "Optimum receiver for molecule shift keying modulation in diffusion-based molecular communication channels," *Elsevier Nano Commun. Networks*, vol. 3, no. 3, pp. 183–195, Sept. 2012.

[56] M. U. Mahfuz, D. Makrakis, and H. T. Mouftah, "Sampling based optimum signal detection in concentration-encoded molecular communication: Receiver architecture and performance," in *Int. Conf. on Bio-inspired Syst. and Signal Process. (BIOSIGNALS)*, Feb. 2013, pp. 372–376.

[57] M. S. Leeson and M. D. Higgins, "Error correction coding for molecular communications," in *IEEE Int. Conf. on Commun. (ICC)*, Jun. 2012, pp. 6172–6176.

[58] Y. Lu, M. D. Higgins, and M. S. Leeson, "Comparison of channel coding schemes for molecular communications systems," *IEEE Trans. on Commun.*, vol. 63, no. 11, pp. 3991–4001, Nov. 2015.

[59] S. Hiyama, Y. Moritani, T. Suda, R. Egashira, A. Enomoto, M. Moore, and T. Nakano, "Molecular communication," in *NSTI Nanotechnology Conf.*, May 2005, pp. 391–394.

[60] R. Lentini, S. P. Santero, F. Chizzolini, D. Cecchi, J. Fontana, M. Marchioretto, C. D. Bianco, J. L. Terrell, A. C. Spencer, L. Martini, M. Forlin, M. Assfalg, M. D. Serra, W. E. Bentley, and S. S. Mansy, "Integrating artificial with natural cells to translate chemical messages that direct e. coli behaviour," *Nature Commun.*, vol. 5, May 2014.

[61] N.-R. Kim, N. Farsad, C.-B. Chae, and A. W. Eckford, "A universal channel model for molecular communication systems with metal-oxide detectors," in *IEEE Int. Conf. on Commun. (ICC)*, Jun. 2015, pp. 1054–1059.

[62] B. Atakan and O. B. Akan, "An information theoretical approach for molecular communication," in *IEEE Int. Conf. on Bio-Inspired Models of Network, Inform. and Computing Syst.*, Dec. 2007, pp. 33–40.

[63] D. Arifler, "Capacity analysis of a diffusion-based short-range molecular nanocommunication channel," *Elsevier Nano Commun. Networks*, vol. 55, no. 6, pp. 1426–1434, Apr. 2011.

[64] T. Nakano, Y. Okaie, and J.-Q. Liu, "Channel model and capacity analysis of molecular communication with brownian motion," *IEEE Commun. Lett.*, vol. 16, no. 6, pp. 797–800, Jun. 2012.

[65] B. Atakan, "Optimal transmission probability in binary molecular communication," *IEEE Commun. Lett.*, vol. 17, no. 6, pp. 1152–1155, Jun. 2013.

[66] M. Pierobon and I. F. Akyildiz, "A physical end-to-end model for molecular communication in nanonetworks," *IEEE J. on Select. Areas in Commun.*, vol. 28, no. 4, pp. 602–611, May 2010.

[67] X. Wang, M. D. Higgins, and M. S. Leeson, "Simulating the performance of SW-ARQ schemes within molecular communications," *Elsevier Simulation Modelling Practice and Theory*, vol. 42, pp. 178–188, Mar. 2014.

[68] L. Felicetti, M. Femminella, G. Reali, T. Nakano, and A. V. Vasilakos, "TCP-like molecular communications," *IEEE J. on Select. Areas in Commun.*, vol. 32, no. 12, pp. 2354–2367, Dec. 2014.

[69] B. Atakan and O. B. Akan, "On molecular multiple-access, broadcast, and relay channels in nanonetworks," in *Int. Conf. on Bio-Inspired Models Network Inform. Comput. Syst.*, Nov. 2008, pp. 16:1–16:8.

[70] A. Ahmadzadeh, A. Noel, and R. Schober, "Analysis and design of multi-hop diffusion-based molecular communication networks," *IEEE Trans. on Molecular, Biological and Multi-Scale Commun.*, no. 99, 2015.

[71] F. Walsh, S. Balasubramaniam, D. Botvich, T. Suda, T. Nakano, S. F. Bush, and M. O. Foghlu, "Hybrid DNA and enzyme based computing for address encoding, link switching and error correction in molecular communication," in *Int Conf. on Nano-Networks and Workshops*, Sept. 2008, pp. 28–38.

[72] A. Noel, K. C. Cheung, and R. Schober, "Improving receiver performance of diffusive molecular communication with enzymes," *IEEE Trans. on NanoBioscience*, vol. 13, no. 1, pp. 31–43, Mar. 2014.

[73] A. Akkaya, G. Genc, and T. Tugcu, "HLA based architecture for molecular communication simulation," *Elsevier Simulation Modelling Practice and Theory*, vol. 42, pp. 163–177, Mar. 2014.

[74] E. Gul, B. Atakan, and O. B. Akan, "Nanons: A nanoscale network simulator framework for molecular communications," *Elsevier Nano Commun. Networks*, vol. 1, no. 2, pp. 138–156, Mar. 2010.

[75] I. Llatser, D. Demiray, C.-A. Albert, T. D. Altilar, and E. Alarcon, "N3sim: Simulation framework for diffusion-based molecular communication nanonetworks," *Elsevier Simulation Modelling Practice and Theory*, vol. 42, pp. 210–222, Mar. 2014.

[76] L. Felicetti, M. Femminella, and G. Reali, "A simulation tool for nanoscale biological networks," *Elsevier Nano Commun. Networks*, vol. 3, no. 1, pp. 2–18, Mar. 2012.

[77] H. B. Yilmaz and C.-B. Chae, "Simulation study of molecular communication systems with an absorbing receiver: Modulation and {ISI} mitigation techniques," *Elsevier Simulation Modelling Practice and Theory*, vol. 49, pp. 136–150, Dec. 2014.

[78] B. Atakan and O. B. Akan, "On channel capacity and error compensation in molecular communication," in *Trans. on Computational Systems Biology X*, ser. Lecture Notes in Computer Science. Springer Berlin Heidelberg, 2008, vol. 5410, pp. 59–80.

[79] R. Mosayebi, H. Arjmandi, A. Gohari, M. Nasiri-Kenari, and U. Mitra, "Receivers for diffusion-based molecular communication: Exploiting memory and sampling rate," *IEEE J. on Select. Areas in Commun.*, vol. 32, no. 12, pp. 2368–2380, Dec. 2014.

[80] A. Singhal, R. K. Mallik, and B. Lall, "Molecular communication with brownian motion and a positive drift: performance analysis of amplitude modulation schemes," *IET Commun.*, vol. 8, no. 14, pp. 2413–2422, Sept. 2014.

[81] ——, "Effect of molecular noise in diffusion-based molecular communication," *IEEE Wireless Commun. Lett.*, vol. 3, no. 5, pp. 489–492, Oct. 2014.

[82] Y. Chahibi and I. F. Akyildiz, "Molecular communication noise and capacity

analysis for particulate drug delivery systems," *IEEE Trans. on Commun.*, vol. 62, no. 11, pp. 3891–3903, Nov. 2014.

[83] Z. R. M., S. N. Majumdar, and A. Comtet, "Capture of particles undergoing discrete random walks," *J. of Chemial Physics*, vol. 130:204104, p. 5, 2009.

[84] M. S. Leeson and M. D. Higgins, "Forward error correction for molecular communications," *Elsevier Nano Commun. Networks*, vol. 3, pp. 161–167, Sept. 2012.

[85] H. B. Yilmaz, A. C. Heren, T. Tugcu, and B. Chae, "Three-dimensional channel characteristics for molecular communications with an absorbing receiver," *IEEE Commun. Lett.*, vol. 18, no. 6, pp. 929–932, Jun. 2014.

[86] G. Aminian, H. Arjmandi, A. Gohari, M. N. Kenari, and U. Mitra, "Capacity of LTI-poisson channel for diffusion based molecular communication," in *IEEE Int. Conf. on Commun. (ICC)*, Jun. 2015, pp. 1060–1065.

[87] M. S. Kuran, H. B. Yilmaz, T. Tugcu, and B. Ozerman, "Energy model for communication via diffusion in nanonetworks," *Elsevier Nano Commun. Networks*, vol. 1, pp. 86–95, Jun. 2010.

[88] D. Kilinc and O. B. Akan, "Receiver design for molecular communication," *IEEE J. on Select. Areas in Commun.*, vol. 31, no. 12, pp. 705–714, Dec. 2013.

[89] S. Verdu and T. S. Han, "A general formula for channel capacity," *IEEE Trans. on Inform. Theory*, vol. 40, no. 4, pp. 1147–1157, Jul. 1994.

[90] A. W. Eckford, "Achievable information rates for molecular communication with distinct molecules," in *IEEE Int. Conf. on Bio-Inspired Models of Network, Inform. and Computing Syst.*, Dec. 2007, pp. 313–315.

[91] T. Nakano, Y. Okaie, and A. V. Vasilakos, "Transmission rate control for

molecular communication among biological nanomachines," *IEEE J. on Select. Areas in Commun.*, vol. 31, no. 12, pp. 835–846, Dec. 2013.

[92] I. F. Akyildiz, F. Fekri, R. Sivakumar, C. R. Forest, and B. K. Hammer, "Monaco: fundamentals of molecular nano-communication networks," *IEEE Wireless Commun.*, vol. 19, no. 5, pp. 12–18, Oct. 2012.

[93] M. Moore and T. Nakano, "Addressing by beacon distances using molecular communication," *Elsevier Nano Commun. Networks*, vol. 2, pp. 161–173, Jun. 2011.

[94] M. Moore, T. Nakano, A. Enomoto, and T. Suda, "Measuring distance with molecular communication feedback protocols," in *IEEE Int. Conf. on Bio-Inspired Models of Network, Inform. and Computing Syst.*, Dec. 2010.

[95] M. J. Moore and T. Nakano, "Comparing transmission, propagation, and receiving options for nanomachines to measure distance by molecular communication," in *IEEE Int. Conf. on Commun. (ICC)*, Jun. 2012, pp. 6132–6136.

[96] M. J. Moore, T. Nakano, A. Enomoto, and T. Suda, "Measuring distance from single spike feedback signals in molecular communication," *IEEE Trans. on Signal Process.*, vol. 60, no. 7, pp. 3576–3587, Jul. 2012.

[97] J.-T. Huang, H.-Y. Lai, Y.-C. Lee, C.-H. Lee, and P.-C. Yeh, "Distance estimation in concentration-based molecular communications," in *IEEE Global Commun. Conf. (GLOBECOM)*, Dec. 2013, pp. 2587–2591.

[98] S. Abadal and I. F. Akyildiz, "Bio-inspired synchronization for nanocommunication networks," in *IEEE Global Commun. Conf. (GLOBECOM)*, 2011, pp. 1–5.

[99] S. Abadal, I. Llatser, E. Alarcon, and A. Cabellos-Aparicio, "Quorum sensing-

enabled amplification for molecular nanonetworks," in *IEEE Int. Conf. on Commun. (ICC)*, Jun. 2012, pp. 6162–6166.

[100] J. Hesselberth, M. P. Robertson, S. Jhaveri, and A. D. Ellington, "In vitro selection of nucleic acids for diagnostic applications," *Reviews in Molecular Biotechnology*, vol. 74, no. 1, pp. 15–25, Mar. 2000.

[101] E. H. Kim and J. E. Parker, "Deciphering plant-pathogen communication: fresh perspectives for molecular resistance breeding," *Current Opinion in Biotechnology*, vol. 14, no. 2, pp. 177 – 193, Apr. 2003.

[102] N. K. Navani and Y. Li, "Nucleic acid aptamers and enzymes as sensors," *Elsevier Current Opinion in Chemical Biology*, vol. 10, no. 3, pp. 272–281, Jun. 2006, combinatorial chemistry and molecular diversityScott K Silverman and Paul J Hergenrother.

[103] B. Atakan, O. B. Akan, and S. Balasubramaniam, "Body area nanonetworks with molecular communications in nanomedicine," *IEEE Commun. Mag.*, vol. 50, no. 1, pp. 28–34, January 2012.

[104] M. Moeneclaey and H. Bruneel, "Efficient ARQ scheme for high error rate channels," *IET Electron. Lett.*, vol. 20, pp. 986–987, Nov. 1984.

[105] M. D. Munnynck, A. Lootens, S. Wittevrongel, and H. Bruneel, "Transmitter buffer behaviour of stop-and-wait ARQ schemes with repeated transmissions," *IEE Proc. on Commun.*, vol. 149, pp. 13–17, Feb. 2002.

[106] B. Atakan, S. Galmes, and O. B. Akan, "Nanoscale communication with molecular arrays in nanonetworks," *IEEE Trans. on NanoBioscience*, vol. 11, no. 2, pp. 149–160, Jan. 2012.

[107] F. Walsh, S. Balasubramaniam, D. Botvich, W. Donnelly, and S. Sergeyev,

"Development of molecular based communication protocols for nanomachines," in *Int, ICST Conf. on Nano-Networks*, vol. 19, Nov. 2007, pp. 1–5.

[108] Y. Benenson and E. Shapiro, *Molecular Computing Machines.* Taylor & Francis, 2011, ch. 187, pp. 2043–2055.

[109] F. Walsh, S. Balasubramaniam, D. Botvich, T. Nakano, and T. Suda, "Simulation framework for communication protocols of molecular communication systems," in *IEEE Int. Conf. on Bio-Inspired Models of Network, Inform. and Computing Syst.*, Sept. 2008, pp. 1–2.

[110] M. Moeneclaey, H. Bruneel, I. Bruyland, and D. Y. Chung, "Throughput optimization for a generalized Stop-and-Wait ARQ scheme," *IEEE Trans. on Commun.*, vol. 34, no. 2, pp. 205–207, Feb. 1986.

[111] M. U. Mahfuz, D. Makrakis, and H. T. Mouftah, "On the characterization of binary concentration-encoded molecular communication in nanonetworks," *Elsevier Nano Commun. Networks*, vol. 1, no. 4, pp. 289–300, Dec. 2010.

[112] I. Llatser, A. Cabellos-Aparicio, M. Pierobon, and E. Alarcon, "Detection techniques for diffusion-based molecular communication," *IEEE J. on Select. Areas in Commun.*, vol. 31, no. 12, pp. 726–734, Dec. 2013.

[113] X. Wang, M. D. Higgins, and M. S. Leeson, "Distance estimation schemes for diffusion based molecular communication systems," *IEEE Commun. Lett.*, vol. 19, no. 3, pp. 399–402, Mar. 2015.

[114] A. Noel, K. C. Cheung, and R. Schober, "Bounds on distance estimation via diffusive molecular communication," in *IEEE Global Commun. Conf. (GLOBECOM)*, Apr. 2014, pp. 2813–2819.

[115] A. Einolghozati, M. Sardari, and F. Fekri, "Relaying in diffusion-based molec-

ular communication," in *IEEE Int. Symp. on Inform. Theory Proc. (ISIT)*, Jul. 2013, pp. 1844–1848.

[116] ——, "Decode and forward relaying in diffusion-based molecular communication between two populations of biological agents," in *IEEE Int. Conf. on Commun. (ICC)*, Jun. 2014, pp. 3975–3980.

[117] T. Nakano and J.-Q. Liu, "Design and analysis of molecular relay channels: An information theoretic approach," *IEEE Trans. on NanoBioscience*, vol. 9, no. 3, pp. 213–221, Sept. 2010.

[118] T. Nakano and J. Shuai, "Repeater design and modeling for molecular communication networks," in *IEEE Conf. on Comput. Commun. Workshops*, Apr. 2011, pp. 501–506.

[119] A. Ahmadzadeh, A. Noel, and R. Schober, "Analysis and design of two-hop diffusion-based molecular communication networks," in *IEEE Global Commun. Conf. (GLOBECOM)*, Dec. 2014, pp. 2820–2825.